

Team Electric Owl

Design of an Unmanned Aerial Vehicle for Martian Exploration

Final Report

Rice University
Department of Electrical and Computer Engineering
6100 Main St. MS-366
Houston, TX 77005

| | | |
|---------------------------|--------------------------------|---------------|
| Anthony Austin | Senior, Electrical Engineering | apa1@rice.edu |
| Jeffrey Bridge | Senior, Electrical Engineering | jab3@rice.edu |
| Robert Brockman II | Senior, Electrical Engineering | rtb1@rice.edu |
| Peter Hokanson | Senior, Electrical Engineering | pch1@rice.edu |

Faculty Advisor: Dr. Gary Woods, Elec. and Comp. Eng., gary.woods@rice.edu
JSC Mentor: David Fuson, ESGC Jacobs, david.fuson@escg.jacobs.com
TSGC Mentor: Dr. Hum Mandell, UT Center for Space Research, mandell@csr.utexas.edu

Spring 2011

Contents

| | | |
|----------|--|-----------|
| 1 | Introduction | 10 |
| 1.1 | Mars: The Next Frontier | 10 |
| 1.2 | Unmanned Martian Exploration | 11 |
| 1.3 | Airborne Mission Requirements | 11 |
| 1.3.1 | Flight Environment | 12 |
| 1.3.2 | Extreme Distance | 12 |
| 1.3.3 | Component Failure | 13 |
| 1.4 | The Project | 14 |
| 2 | Design Strategy | 15 |
| 2.1 | Fault-Tolerant Mars-Capable Avionics | 15 |
| 2.1.1 | Control Surface Actuation | 15 |
| 2.1.2 | Radio Communication | 16 |
| 2.1.3 | Flight-State Sensors | 17 |
| 2.1.4 | Flight Computer | 17 |
| 2.2 | Project Focus | 18 |
| 2.2.1 | Flight-Capable Hardware | 19 |
| 2.2.2 | Basic Autopilot | 19 |
| 2.2.3 | Sensor Redundancy | 19 |
| 2.2.4 | Potential for Expansion | 20 |
| 3 | Final Design | 21 |
| 3.1 | Electrical Hardware | 21 |
| 3.1.1 | Backplane | 22 |
| 3.1.2 | Servo Board | 24 |
| 3.1.3 | Radio Board | 25 |
| 3.1.4 | Sensors Board | 26 |
| 3.1.5 | General-Purpose Computer (GPC) Board | 29 |
| 3.2 | Avionics Firmware | 31 |
| 3.2.1 | General Architecture | 32 |
| 3.2.2 | Bus Firmware | 32 |
| 3.2.3 | Servo Board | 34 |
| 3.2.4 | Radio Board | 37 |
| 3.2.5 | Sensors Board | 39 |
| 3.2.6 | GPC Board (AVR) | 42 |
| 3.2.7 | GPC Board (ARM) | 43 |
| 3.2.7.1 | System Master | 43 |
| 3.2.7.2 | Custom Real-Time Kernel | 44 |
| 3.2.7.3 | Autopilot Task | 46 |
| 3.3 | Autopilot Software | 47 |
| 3.3.1 | General Structure | 47 |

| | | |
|----------|--|-----------|
| 3.3.2 | Sensor Redundancy Management | 49 |
| 3.3.3 | Flight Plan Format | 50 |
| 3.4 | "Houston" Ground Software | 52 |
| 3.4.1 | General Interface | 53 |
| 3.4.2 | Raster Data | 54 |
| 3.4.3 | Vector Data | 55 |
| 3.4.4 | UAV Support | 56 |
| 3.4.5 | Logging Format | 57 |
| 3.5 | Communications Protocols | 58 |
| 3.5.1 | Bus Protocol | 58 |
| 3.5.2 | Radio Downlink Protocol | 66 |
| 3.5.3 | Radio Uplink Protocol | 71 |
| 3.6 | Prototype Aircraft Hardware | 74 |
| 3.6.1 | Airframe | 74 |
| 3.6.2 | Power System | 76 |
| 3.6.3 | Actuators | 78 |
| 3.6.4 | Avionics Mounting | 78 |
| 3.6.5 | Non-Integrated Sensors | 79 |
| 3.7 | Future Expansion | 79 |
| 3.8 | Errata and Revision History | 81 |
| 3.8.1 | Hardware Revision I | 81 |
| 3.8.2 | Hardware Revision II | 82 |
| 3.8.3 | Hardware Revision III | 84 |
| 4 | Testing and Results | 85 |
| 4.1 | Basic Functionality Testing | 85 |
| 4.1.1 | Electrical Testing | 85 |
| 4.1.2 | Software Testing | 85 |
| 4.1.3 | Sensor Redundancy Testing | 86 |
| 4.2 | Sensors Calibration | 86 |
| 4.3 | Hardware-in-the-Loop (HITL) Simulation | 89 |
| 4.4 | Flight Tests | 90 |
| 4.4.1 | Servo Board Flight Test: 08/22/2010 | 90 |
| 4.4.2 | Three-Board Flight Test: 01/07/2011 | 91 |
| 4.4.3 | Initial Autopilot Flight Test: 03/06/2011 | 92 |
| 4.4.4 | Basic Autopilot Flight Test: 03/19/2011 | 93 |
| 4.4.5 | Redundant Sensors Flight Test I: 03/27/11 | 94 |
| 4.4.6 | Redundant Sensors Flight Test II: 04/02/2011 | 94 |
| 5 | Summary and Recommendations | 98 |
| 5.1 | Summary | 98 |
| 5.2 | Recommendations and Future Work | 99 |

| | | |
|----------|---|------------|
| 6 | Acknowledgements | 101 |
| 6.1 | Technical Advisors | 101 |
| 6.2 | Flight Testing | 102 |
| 6.3 | Funding Sources | 102 |
| 7 | References | 103 |
| A | User's and Safety Manual | 107 |
| A.1 | Flight Test Procedures | 107 |
| A.1.1 | The Day Before | 107 |
| A.1.2 | Packing Checklist | 108 |
| A.1.3 | At the Field | 110 |
| A.2 | Software Dependencies | 113 |
| A.3 | Programming the Circuit Boards | 115 |
| A.3.1 | AVR Microcontrollers | 115 |
| A.3.2 | GPC ARM Microcontroller | 117 |
| A.4 | Assigning Board IDs | 119 |
| A.5 | Hardware-in-the-Loop Testing | 121 |
| A.6 | Software Utilities | 124 |
| A.7 | Sensor Calibration Procedure | 125 |
| A.7.1 | Step 1: Data Collection | 126 |
| A.7.1.1 | Accelerometers | 126 |
| A.7.1.2 | Magnetometers | 130 |
| A.7.1.3 | Gyroscopes | 132 |
| A.7.1.4 | Differential Pressure Sensor | 137 |
| A.7.2 | Step 2: Pre-Processing | 139 |
| A.7.2.1 | Accelerometer, Magnetometer, and Differential Pressure Data | 139 |
| A.7.2.2 | Gyroscope Data | 140 |
| A.7.3 | Step 3: Model Fitting and Analysis | 141 |
| A.7.4 | Step 4: Storing Values in EEPROM | 144 |
| A.8 | Compiling the ARM Development Toolchain | 146 |
| A.9 | Compiling Open OCD | 150 |
| A.10 | Safety Precautions | 151 |
| A.10.1 | Lithium-Polymer Batteries | 151 |
| A.10.2 | R/C Flying | 151 |
| A.10.3 | Construction | 152 |
| A.11 | Legal Requirements | 152 |
| A.11.1 | FCC Radio Frequency Regulations | 152 |
| A.11.2 | FAA Flight Regulations | 152 |
| B | Schematics and CAD Drawings | 153 |

| | | |
|----------|--|------------|
| C | Assembly Instructions and Bill of Materials | 188 |
| C.1 | Aircraft Hardware | 188 |
| C.2 | Avionics Package | 189 |
| C.2.1 | Backplane, revision 03 | 193 |
| C.2.2 | Servo Board, revision 03 | 193 |
| C.2.3 | Radio Board, revision 03 | 198 |
| C.2.4 | Sensors Board, revision 03 | 200 |
| C.2.5 | GPC Board, revision 02 | 204 |
| C.3 | Additional Tools | 208 |
| C.3.1 | Airframe Construction | 208 |
| C.3.2 | Software Development | 209 |
| C.3.3 | Testing Supplies | 209 |
| D | Budget | 210 |
| D.1 | Revenue | 210 |
| D.2 | Expenses | 210 |

List of Figures

| | | |
|------|--|-----|
| 2.1 | System block diagram of some of the features that might be needed for a Mars-capable system. | 16 |
| 3.1 | Photograph showing all four types of boards plugged into the backplane. | 21 |
| 3.2 | Data flow in the autopilot | 47 |
| 3.3 | Byte structure of a bus packet. | 59 |
| 3.4 | Byte structure of a downlink packet. | 67 |
| 3.5 | Byte structure of an uplink packet. | 72 |
| 4.1 | Heading-lock telemetry from second flight on 04/02/2011. The blue line indicates the plane's actual heading. The gray regions indicate parts of the flight for which the autopilot was active, and the orange lines indicate the plane's desired heading during those times. | 95 |
| 4.2 | Plot of plane's trajectory during the second flight test on 04/02/2011. The red lines indicate parts during which the autopilot was active. Arrows on the line segment indicate the plane's direction of travel. | 97 |
| B.1 | Backplane revision 03 circuit schematic (1/4) | 154 |
| B.2 | Backplane revision 03 circuit schematic (2/4) | 155 |
| B.3 | Backplane revision 03 circuit schematic (3/4) | 156 |
| B.4 | Backplane revision 03 circuit schematic (4/4) | 157 |
| B.5 | Servo board revision 03 circuit schematic (1/8) | 158 |
| B.6 | Servo board revision 03 circuit schematic (2/8) | 159 |
| B.7 | Servo board revision 03 circuit schematic (3/8) | 160 |
| B.8 | Servo board revision 03 circuit schematic (4/8) | 161 |
| B.9 | Servo board revision 03 circuit schematic (5/8) | 162 |
| B.10 | Servo board revision 03 circuit schematic (6/8) | 163 |
| B.11 | Servo board revision 03 circuit schematic (7/8) | 164 |
| B.12 | Servo board revision 03 circuit schematic (8/8) | 165 |
| B.13 | Radio board revision 03 circuit schematic (1/5) | 166 |
| B.14 | Radio board revision 03 circuit schematic (2/5) | 167 |
| B.15 | Radio board revision 03 circuit schematic (3/5) | 168 |
| B.16 | Radio board revision 03 circuit schematic (4/5) | 169 |
| B.17 | Radio board revision 03 circuit schematic (5/5) | 170 |
| B.18 | Sensors board revision 03 circuit schematic (1/8) | 171 |
| B.19 | Sensors board revision 03 circuit schematic (2/8) | 172 |
| B.20 | Sensors board revision 03 circuit schematic (3/8) | 173 |
| B.21 | Sensors board revision 03 circuit schematic (4/8) | 174 |
| B.22 | Sensors board revision 03 circuit schematic (5/8) | 175 |
| B.23 | Sensors board revision 03 circuit schematic (6/8) | 176 |
| B.24 | Sensors board revision 03 circuit schematic (7/8) | 177 |

B.25 Sensors board revision 03 circuit schematic (8/8) 178
B.26 GPC board revision 02 circuit schematic (1/9) 179
B.27 GPC board revision 02 circuit schematic (2/9) 180
B.28 GPC board revision 02 circuit schematic (3/9) 181
B.29 GPC board revision 02 circuit schematic (4/9) 182
B.30 GPC board revision 02 circuit schematic (5/9) 183
B.31 GPC board revision 02 circuit schematic (6/9) 184
B.32 GPC board revision 02 circuit schematic (7/9) 185
B.33 GPC board revision 02 circuit schematic (8/9) 186
B.34 GPC board revision 02 circuit schematic (9/9) 187

C.1 Front assembly diagram for Backplane Rev 03 190
C.2 Front assembly diagram for Servo Board Rev 03 191
C.3 Front assembly diagram for Radio Board Rev 03 191
C.4 Front assembly diagram for Sensors Board Rev 03 192
C.5 Front assembly diagram for GPC Board Rev 02 192

List of Tables

| | | |
|------|---|-----|
| 3.1 | Microcontroller ADC pin assignments on Sensors Board, Rev 03. | 28 |
| 3.2 | Special bytes and escape sequences. | 59 |
| 3.3 | Bus command types and corresponding identification bytes. | 61 |
| 3.4 | Data register codes used with BCMD_TELEM_FETCH and BCMD_TELEM_REPLY packets. | 62 |
| 3.5 | Layout of the data field for BCMD_SENSORS_REPLAY_HIRATE packets. Note that the sensor values are stored in little-endian order. | 64 |
| 3.6 | Layout of the data field for BCMD_SENSORS_REPLAY_LORATE packets. Taken from the Garmin Device Interface Specification [1]. | 65 |
| 3.7 | Layout of the data field for BCMD_SERVO_SETSERVOS packets. Note that the values must be sent in little-endian order. | 65 |
| 3.8 | Layout of the data field for BCMD_SENSORS_REPLY_AHPRS packets. | 66 |
| 3.9 | Downlink packet types and corresponding identification bytes. | 67 |
| 3.10 | Telemetry channel types and corresponding marker bytes. | 68 |
| 3.10 | Telemetry channel types and corresponding marker bytes. | 69 |
| 3.10 | Telemetry channel types and corresponding marker bytes. | 70 |
| 3.11 | Downlink packet types and corresponding identification bytes. | 73 |
| 3.12 | Layout of the data field for UL_CMD_JOYSTICK packets. | 74 |
| A.1 | Software dependencies required for Electric Owl development. | 114 |
| C.1 | Bill of Materials for Test Airframe | 188 |
| C.2 | Bill of Materials for Backplane Rev 03 | 193 |
| C.3 | Bill of Materials for Servo Board Rev 03 | 193 |
| C.3 | Bill of Materials for Servo Board Rev 03 | 194 |
| C.3 | Bill of Materials for Servo Board Rev 03 | 195 |
| C.3 | Bill of Materials for Servo Board Rev 03 | 196 |
| C.3 | Bill of Materials for Servo Board Rev 03 | 197 |
| C.4 | Bill of Materials for Radio Board Rev 03 | 198 |
| C.4 | Bill of Materials for Radio Board Rev 03 | 199 |
| C.5 | Bill of Materials for Sensors Board Rev 03 | 200 |
| C.5 | Bill of Materials for Sensors Board Rev 03 | 201 |
| C.5 | Bill of Materials for Sensors Board Rev 03 | 202 |
| C.5 | Bill of Materials for Sensors Board Rev 03 | 203 |
| C.6 | Bill of Materials for GPC Board Rev 02 | 204 |
| C.6 | Bill of Materials for GPC Board Rev 02 | 205 |
| C.6 | Bill of Materials for GPC Board Rev 02 | 206 |
| C.6 | Bill of Materials for GPC Board Rev 02 | 207 |
| C.7 | List of development tools | 209 |
| C.8 | List of development tools | 209 |

D.1 Expenses for the 2010-2011 School Year 210

1 Introduction

1.1 Mars: The Next Frontier

From the dawn of time, human beings have held a special fascination with the universe and its objects. Be it the early Greeks, astronomers from the Middle Ages, or scientists of the modern age, humanity has always looked up at the night sky with wonder and amazement at what lies beyond the borders of Earth's atmosphere.

On July 20, 1969, mankind made "one giant leap" towards turning that vast enigmatic expanse known as "outer space" into familiar territory. Since then, many other manned missions have been conducted and dozens of space exploration probes deployed; however, none of these efforts, useful and enlightening though they have proved, has been as successful at capturing the hearts and minds of the citizens of the world as the first lunar landing that occurred over 40 years ago. It time for humanity to take its next "giant leap" out into the universe, and there could be no better objective for this leap than to have a human being set foot on Earth's next nearest neighbor in the solar system: the planet Mars.

But before one can even think about sending humans to Mars, one first has to get the lay of the land. In order to further this objective, Team Electric Owl is interested in the development of a fully autonomous unmanned aerial vehicle (UAV) to perform efficient exploration of Mars. Such a probe would be able to fly quickly over the planet's landscape and survey large swaths of territory with great detail, thus helping prepare the way for eventual human landing and colonization.

1.2 Unmanned Martian Exploration

Current unmanned Mars exploration strategies have significant limitations. In the 1970s, NASA sent the *Viking* series of probes, which were the first successful Mars landers. While the images and data acquired from these units were invaluable, they were very limited in scope because the landers were stationary, and could not move to explore the terrain.

More recently, space exploration agencies from around the globe – specifically NASA, the European Space Agency, and Russia – have placed satellites into orbit around the Red Planet. While many of these are still successfully operating, the resolution of data they can gather is severely limited by their distance from the surface and rapid rate of travel, although they are capable of exploring almost the entire planet.

Most recently, several robotic rovers, such as *Sojourner*, *Spirit*, and *Opportunity*, have been deployed to roam the planet's surface. These, too, have been quite successful; however, their effective range of exploration is limited to at most a few tens of kilometers due to the devices' extremely slow rate of movement.

Recently, NASA's ARES project [2] has suggested that using an unmanned aircraft as an alternative to these more traditional technologies could easily provide enough data to rewrite all of human knowledge of the Red Planet with only an hour of operation [3]. An unmanned probe like this would be able to strike a balance between offering high-resolution data like landers and rovers while remaining highly mobile like the orbital probes.

1.3 Airborne Mission Requirements

For an unmanned aerial mission to be successful, there are several technical hurdles to overcome. The thin atmosphere, harsh radiation, and the fact that the extreme distance makes manual intervention impossible pose some of the serious concerns that must be addressed

before airborne exploration of Mars can be attempted.

1.3.1 Flight Environment

Martian Atmosphere The most immediate concern in designing a Mars aircraft is the thin Martian atmosphere. The air pressure at the surface of Mars is approximately equivalent to that at 100,000 feet on Earth. The thin atmosphere makes it difficult for an aircraft to generate the lift forces required to keep itself in the air. This places severe constraints on the design of the airframe, especially in terms of propulsive power and total aircraft weight.

Energy Gathering Because Mars lacks the infrastructure for any sort of chemical refueling, energy for propulsion is likely limited to electrical energy gathered with photovoltaic cells and stored in chemical batteries. Propelling the aircraft would have to be accomplished with an electric motor. Although the technology for all of these has improved substantially in the past few decades, gathering sufficient energy to ensure continued flight will be a stringent design constraint.

1.3.2 Extreme Distance

Interplanetary Transit In order to get to Mars, any probe must be designed and built on Earth. The aircraft would almost certainly need to be folded and compressed to fit into a rocket which would launch it to Mars. Traditional low-cost orbital transit routes to Mars typically take several months in cold interplanetary space. This environment can freeze components and irradiate electronic memory. Once on Mars, the probe must survive atmospheric re-entry. The aircraft would then need to unfurl and launch from midair [2].

Light Propagation Delay The extreme distance between Mars and Earth causes one-way a delay in any radio signal of between 10 and 20 minutes. This delay is too extreme to al-

low any sort of manual control of the probe in flight: the aircraft is almost certain to have impacted the terrain before notification even reaches a terrestrial operator. Because of this, fully autonomous flight is a necessity for an aerial Mars mission [3].

Flight Infrastructure Mars lacks many of the amenities available to terrestrial aviation. The constellation of satellites that enable GPS on Earth are not yet available on the Red Planet. Furthermore, there are no runways or refueling installations for the plane to return to when its internal power is exhausted.

1.3.3 Component Failure

High-Radiation Environment The thin atmosphere of Mars does not have sufficient depth to shield the planet from space radiation. Any Mars probe would need to be designed to function in this environment as well as to be able to survive the long journey in interplanetary space, which features further radiation hazards. Radiation can adversely affect the operation of electronics by causing memory errors and erroneous state changes. Although radiation-hardened chips exist, they do not fully prevent these problems.

Component Failures In the harsh environment of space, component failures must be anticipated. Failure of propulsion motors, control surfaces and flight avionics should be considered likely. NASA's unmanned probes typically sport redundant systems, particularly in the electronics; however, a failure of the primary computer leaves the system in an "unsafe" state if the level of redundancy is insufficient, as has been seen in the *Mars Reconnaissance Orbiter* [4] [5] [6].

1.4 The Project

In order to explore some of the issues that that would need to be considered in the design of a Mars UAV, the members of Team Electric Owl decided to use their capstone senior design project to design, build, and test a set of UAV flight control electronics (avionics) subject to some of the constraints faced by an actual Mars UAV. Specifically, the team aimed to produce a lightweight avionics package for a fixed-wing aircraft that could accommodate redundancy in the various system components to improve the system's overall fault-tolerance.

2 Design Strategy

2.1 Fault-Tolerant Mars-Capable Avionics

In order to better define the project, Team Electric Owl considered some of the details of the fault-tolerance that would be required for an actual Mars mission. The canonical approach for improving fault-tolerance is to eliminate single points of system failure by using redundant components. This design technique is currently used in nearly every piece of space exploration technology, from unmanned probes to the Space Shuttle. Because of the unique requirements of extra-terrestrial flight, system failure must be accounted for—and recovered from—very quickly. Thus, any fault-tolerant design must employ an automated failover scheme whereby the system immediately switches over to redundant backup components in the event of failure. A high-level block diagram of the team’s proposed solution to the design problem is shown in Figure 2.1.

2.1.1 Control Surface Actuation

Because mechanical systems are prone to failure, especially in harsh extra-terrestrial environments, duplicating at least minimal control function to ensure that a single stuck actuator would not cause catastrophic failure is needed. On the Space Shuttle, this is done using mechanical redundancy with multiple actuators[7]: a frangible pin will shear off a faulty actuator, disconnecting it from the control surface. It seems reasonable that any Mars UAV would need to have a similar system for dealing with faulty mechanical actuators.

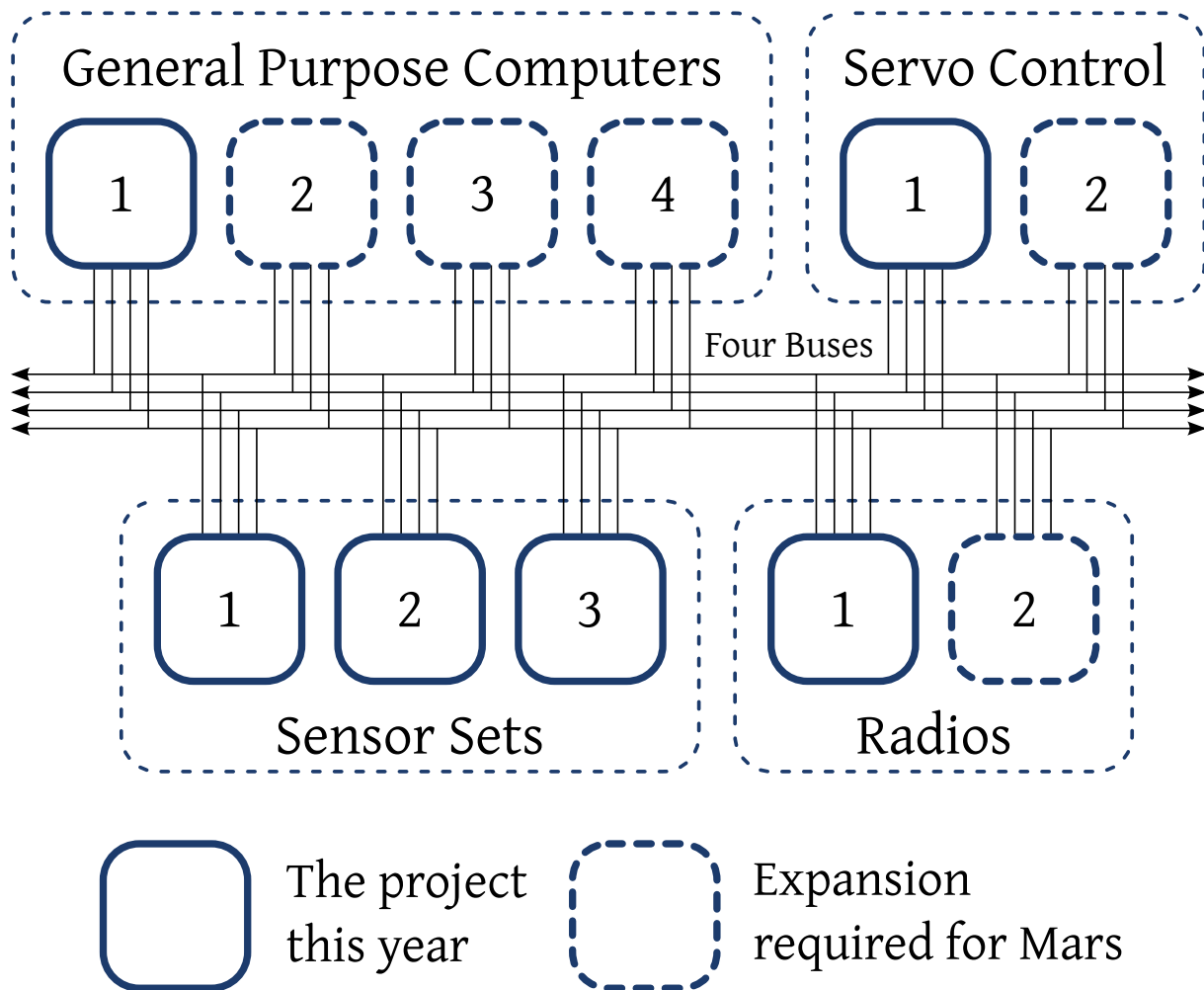


Figure 2.1: System block diagram of some of the features that might be needed for a Mars-capable system.

2.1.2 Radio Communication

The current Mars rovers avoid high-power radio requirements by relaying data to the orbiting Mars Odyssey and Mars Global Surveyor, which in turn transmit to NASA's Deep Space Network[8]. Because the Martian atmosphere and dust on ground-based solar panels significantly attenuate power from the Sun, these satellites have a much larger power budget they can use for interplanetary communication.

A Mars UAV would also be able to make use of this infrastructure; however, if the link to

these satellites is lost, even if the UAV remains airborne, then the mission is effectively terminated because it is unable to relay any gathered scientific data back to Earth. Because of this, redundancy in the radio links is a reasonable design criterion. For this component, a simple primary-plus-backup redundancy scheme (as opposed to multi-way redundancy) appears a reasonable solution, because communications failures are easily detectable, and the power required for sending transmissions to Earth is large.

2.1.3 Flight-State Sensors

In order to function, the UAV's autopilot must be capable of measuring the state of the aircraft. An inertial navigation system (INS) can be supplemented with barometric, laser or radar altimeters for above-ground-level measurement and pitot tubes to detect relative air speed. Each sensor plays an important role in determining the flight state of the aircraft and, to prevent mission failure, should be duplicated.

2.1.4 Flight Computer

NASA's unmanned probes typically sport at least a full backup computer. In at least once case [5], this has prevented a computer error from prematurely terminating a mission; however, the use of dual-redundant systems severely limits the opportunities for automatic error correction.

In contrast, The Space Shuttle employs four redundant flight computers which simultaneously execute identical programs [9] along with a fifth computer executing independently-developed code to mitigate the risk of mission failure due to software errors. If one computer suffers an error, its output will disagree with that of the other flight control computers. The system can take a majority vote and disable the failed system automatically. With four computers, a single failure leaves the system with three correctly functioning computers, a safe configuration that can still detect another error. A second error fails the system back to an operational

mode, though detection of further errors is severely hindered. During his investigations of the Space Shuttle design as part of the Rogers Commission [10] following the tragic loss of Space Shuttle *Challenger*, noted physicist Richard Feynman remarked that the Shuttle's flight computer system was very well-designed [11]. In Shuttle's first approach-and-landing test, this redundancy was inadvertently tested when one of the computers suffered an electrical short when the shuttle disconnected from the 747 that carried it to altitude [12].

Because of the unique requirements that a Mars-capable UAV must meet, the team decided that using quadruply redundant computers like the Space Shuttle would be an appropriate method for improving the fault-tolerance of the device's computing resources. Specifically, the round-trip light propagation delay between Earth and Mars requires the ability for rapid automated failover in the event of a system error, and only a system like that of the Space Shuttle allows this to happen in a manner that is at once fail-safe and fail-operational. Furthermore, the additional weight and power requirements imposed by adding the redundancy would be minimal if the system were designed using modern microcontrollers and other electronics.

2.2 Project Focus

To limit the scope of the investigation to a feasible senior capstone project, the team decided to focus on developing first flight-capable hardware with basic autopilot functionality. Once this had been done, the team focused on implementing redundant sensor capabilities in order to demonstrate the system's ability to accommodate redundancy. Though this was the only form of redundancy the team actually implemented, the team designed the hardware and the rest of the system to be capable of future expansion to provide the redundancy shown in Figure 2.1.

2.2.1 Flight-Capable Hardware

In order to demonstrate that the avionics system works, it was necessary to test it under real flight conditions. The team aimed to deliver hardware and firmware that have demonstrated their ability to control a test airframe in flight.

2.2.2 Basic Autopilot

Because any UAV operating on Mars must be capable of autonomous flight, the team developed a basic autopilot algorithm that can run on an onboard microcontroller. The team demonstrated the ability of the algorithm to fly the aircraft in a stable manner without any ground input. The autopilot is capable of waypoint-based navigation, and the team tested this extensively using hardware-in-the-loop simulation, though time did not permit a flight test of this feature.

A Mars UAV would require significantly more complex control system tuned to the characteristics of the final airframe to achieve high performance. Such considerations were deemed outside the scope of the project.

2.2.3 Sensor Redundancy

The team also implemented sensor redundancy, with the flight computer able to accept between an arbitrary number of sensor inputs from up to three modular sensor boards. (Scaling up to accept data from more sets of sensors is straightforward to do.) The software can handle situations in which data from one or more of the boards is absent and is also capable of identifying and rejecting wildly outlying data, as might be produced by a faulty sensor. Because of the way that this functionality has been implemented, the sensor boards may be added and removed while the autopilot is active, and the system will seamlessly transition to using the new configuration.

2.2.4 Potential for Expansion

The system hardware was designed with the potential for further expansion in mind, especially in the form of computer redundancy. Specifically, four flight computer boards can each master one of the four system buses, allowing for a fault-tolerant arrangement similar to that used on the Space Shuttle.

3 Final Design

3.1 Electrical Hardware

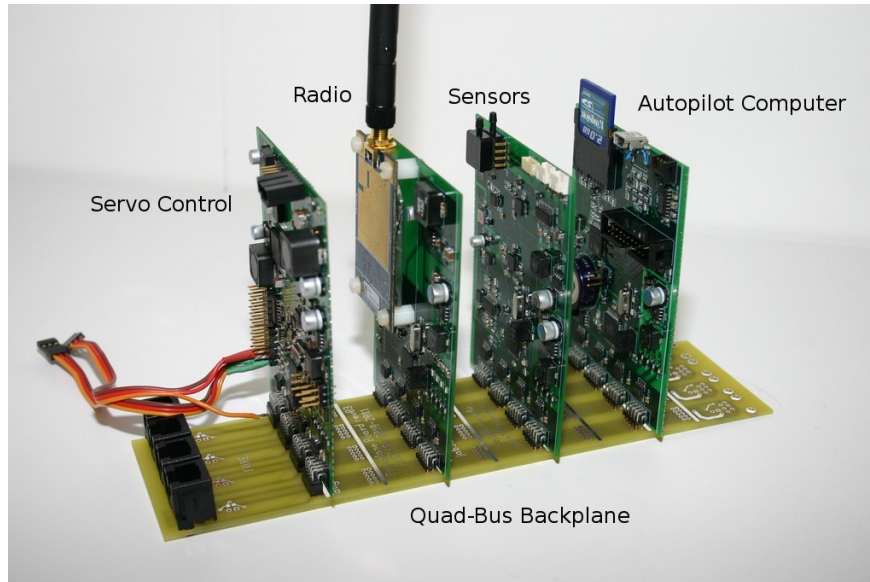


Figure 3.1: Photograph showing all four types of boards plugged into the backplane.

In order to provide satisfactory redundancy, it was decided early in the project to provide redundant electrical connections between the modular circuit boards. It was reasoned that the quadruple computer redundancy on the Space Shuttle flight computer [9] was a good starting point. In order to implement quadruple flight computers without additional failure due to bus shorts or latchups, four buses were deemed necessary. The four buses largely dictated the design of the backplane.

To reduce complexity with designing the remaining boards, it was chosen to design them around a common microcontroller and bus interface. To minimize the performance impact of communicating with multiple hardware buses, the team sought a microcontroller with both adequate computational performance and sufficient hardware serial interfaces. Atmel's AVR line of microcontrollers includes the ATxMEGA32A4, which offers 5 hardware serial ports in a

package with only 44 pins to reduce the complexity of manufacturing the avionics components. This chip was also found to have sufficient analog inputs and other peripherals, and so the team chose the ATxMEGA32A4 as the basis of all four varieties of boards.

After choosing RS-485 for the bus physical layer, TI's SN65HVD12 was chosen as the bus interface chip. The same hardware bus interface was used on all of the boards to reduce headaches due to incompatibilities and additional parts. From the four power lines, high-current diodes are used to draw power from all four without any single failure pulling the other power lines low.

The standard hardware on each board also includes National Semiconductor switch-mode power regulators to supply local 5 V and 3.3 V power rails. This choice of power supply is capable of driving all of the necessary components on all four boards. Because of the choice of components for the board power supplies, the functional voltage on the power supply rail can range from 10 V to 15 V.

3.1.1 Backplane

A front-view assembly diagram of the backplane is shown in Figure C.1. This board serves to connect the other types of boards both with each other and with various debugging tools, including a DC shore power supply and bus debugging terminals. Although the backplane contains no active components, its design heavily dictates that of the other boards. A full list of these components is listed in C.2.

Electrical connection The five lines of each bus contain two ground lines on the outside pair, with a 12-volt power supply line in the middle. The inner pair of lines carries differential power and data. This arrangement of the pins was chosen to minimize potential damage to the boards from improper connections. In particular, if the boards are inserted backwards, only the polarity of the data pins is swapped, which prevents proper functionality, but avoids

catastrophic failure. Distinctive unconnected traces are used to indicate the proper orientation of the boards.

The bus physical layer uses the RS-458 standard, which bears some similarity to the military avionics data bus standard MIL-STD-1553. RS-485 is a three-wire bus, with differential data and ground, but specifies neither a cable nor a connector. Integrated circuits such as the TI SN65HVD12 are commercially available for integrating this protocol with a variety of microcontrollers, and a variety of debugging terminals are available for interfacing with a desktop computer.

Hardware connection Up to eight boards are each physically attached to the backplane with four 3M 10-pin, 2mm header connectors, one to each of the electrical buses. These connectors provide a redundant electrical link between the boards, as well as a fairly stable mechanical linkage. Although the newest revision of the other boards features mounting holes for a more rigid mechanical connection, this has not proven to be a pressing requirement. Indeed, in one flight test that led to uncontrolled impact with terrain (see section 4.4.2), the boards separated from the backplane without significant damage, harmlessly bouncing off the grassy field rather than shattering.

External connections The complete backplane includes four RJ-45 jacks at each end that expose the bus pins. These can be used to daisy-chain multiple backplanes together to connect more than eight circuit boards, or to provide shore power and debugging interfaces. Eight modules has proven sufficient for redundant sensors measurement, but expansion may be required if the other modules are made redundant in the future.

At the ends of each bus, there are pad for terminating resistors R1 and R2 near each external header. This exists to allow proper termination of the buses by matching impedances. This reduces signal reflections in the line, at the cost of a constant current through the low-valued resistor. Testing to date has not shown a need for this component, although if boards

are connected together, it is a potential issue of which to be aware. Reflection issues should ideally be resolved by a terminating resistor on each end of each bus in a serially-connected arrangement.

3.1.2 Servo Board

The servo board uses the standard ATxMEGA32A4 AVR microcontroller found in all of the boards. This board interfaces with the R/C controller and the control servomotors uses the main and backup batteries to provide 12-volt power for the avionics system bus. A front-view assembly diagram of the third-revision servo board is shown in Figure C.2, for the parts enumerated in Table C.3.

Analog servomotors commonly seen in R/C aviation use a three-wire interface: 5 V power, ground, and a pulse-width modulated position value. The servo is a closed-loop motor control system with position feedback from a potentiometer. The motor is heavily geared down to provide large amounts of torque, although this reduces the maximum possible rotation rate.

Standard Hobbyist R/C Input Standard servo wires connect the servo board with a standard six-channel RC aircraft controller. Each of the six channels is voltage divided to a safe input level for the microcontroller, and then treated as a digital input. Software is then able to either pass-through the R/C input to the output or to use the onboard control system to set the control surfaces.

Servomotor Control A TI CD4017BM96 decade counter is used to send control outputs to the servos. Each servo is assigned to a one of the counter's ten outputs, allowing control of up to ten servomotors at once with only two control signal lines from the servo board's AVR microcontroller. Two TI TXB0101 level shifter ICs are used to convert the 3.3 V the control signals from the AVR to the 5 V levels needed to manipulate the servos.

For more information on how the servo board controls the servos, see section 3.2.3.

Battery Interface In addition to the two regulators for the local power supplies, the servo board also has connectors for the high-voltage (15 V to 35 V) and low-voltage (4.5 V to 9 V) batteries onboard the aircraft. The distinction between these two is that the larger high-voltage battery is connected through the motor controller to drive the propeller, while the backup low-voltage battery exclusively powers the avionics, so that flight control may be maintained even after the drive power fails. Both supplies feature current-sensing resistors, so that the discharge rate and voltage of the battery can be measured in flight.

The power rail outputs on the servo board are connected through fuses, to prevent a bus short from eliminating power to all of the buses.

3.1.3 Radio Board

The primary function of the radio board is to provide an interface to the on-board the XTend 900 1W RPSMA radio used to provide air-to-ground digital data communication. The standard AVR arrangement is used to provide bus connectivity, and the standard power supply is capable of powering the radio module. A front assembly diagram is shown in Figure C.3, along with the full bill of materials in Table C.4.

XTend 900 1W RPSMA The XTend 900 1W RPSMA radio is an OEM module that is bolted onto the radio board, and connected with a header. The radio module interfaces with the microcontroller over a serial protocol and features a few additional control pins. This module has a nominal range of 40 miles line-of-sight at the full 1 W transmit power. This radio uses the 900 MHz ISM band that is unlicensed in the United States and uses frequency-hopping to avoid interference.

The ground computer station uses a similar radio from the same vendor that connects to

the computer with a USB cable.

Bus Voltage Monitoring Aside from the radio module, the radio board also features hardware for monitoring the voltages of each of the four system buses. This consists of a set of simple voltage dividers connected between each bus and ground together with some capacitors for filtering out oscillations in the voltage due to traffic traveling on the bus. The center points of each voltage divider are connected to ADC pins on the radio board's AVR for reading.

3.1.4 Sensors Board

The sensors board gives the avionics system the ability to determine flight state. The sensors mounted on the board are capable of measuring the following aircraft states:

1. Relative airspeed
2. Three-axis acceleration
3. Three-axis rotation
4. Three-axis magnetic direction
5. Absolute air pressure

External connections allow the sensors board to interface with a serial GPS unit, and allow expansion to include an ultrasonic altimeter and motor telemetry input.

A front assembly diagram of the sensors board is shown in Figure C.4, with the relevant parts enumerated in Table C.5.

Analog Sensors A three-axis analog MEMS accelerometer, the ADXL335 from Analog Devices, is used to provide acceleration measurements. These are numerically integrated to estimate absolute velocity in all three axes. The raw analog measurements from the accelerom-

eter are fed through precision, micro-power op-amps from TI to condition them before they are measured in three separate channels of the internal 12-bit ADC on the AVR microcontroller.

All three axes of gyroscope measurements are also performed with the AVR ADC. Because all three axes are not currently available in a single convenient package, the gyroscope functionality is divided between two separate parts from ST Microelectronics, with an X-Y gyroscope (the LPR530AL) and a separate yaw gyroscope (the LY530ALH). The third revision of the board replaced a digital I2C yaw gyroscope with the equivalent analog part from the same vendor due to availability issues. Each of these provides a reference voltage output that must also be measured, using a total of five ADC channels.

The final analog component is the MPXV7002DP differential pressure sensor. This sensor is attached to the pitot-static tubes of the aircraft for measuring relative airspeed. The part was selected to account for a airspeed range up to approximately 50 mph. This signal is conditioned by a TI OPA335AID op-amp to bring it to the input range for the AVR ADC.

Table 3.1 shows the pin assignments on the microcontroller. The ATxMEGA32A4 uses multiplexed inputs to the four ADC channels, which can map any input pin into each ADC channel. The ADC itself is pipelined, such that conversions can be performed almost simultaneously, improving the sampling rate. A documented erratum of the ATxMEGA32A4 forces the firmware to flush the ADC pipeline for 16 reads every time one of the multiplexed inputs is changed before the reading becomes stable.

I2C Sensors The Honeywell HMC5843 is a digital I2C three-axis magnetometer. This sensor has the correct sensitivity to detect the Earth's magnetic field. The direction of the field in all three axes is used to determine the aircraft's heading, and its absolute orientation relative to the Earth. This has the 8-bit I2C address 3C and 3D, depending on whether the master is sending or receiving from the sensor. The firmware on the AVR is responsible for reading all of the registers on the chip regularly.

| Signal | Channel | Part | Description |
|-------------|---------|-------------|--------------------------------|
| GyroX | ADC1 | LPR530AL | X-axis gyroscope |
| GyroXY_VRef | ADC2 | LPR530AL | XY-gyroscope reference |
| GyroY | ADC3 | LPR530AL | Y-axis gyroscope |
| P_AIRSPPEED | ADC4 | MPXV70002DP | Differential pressure airspeed |
| GyroZ | ADC5 | LY530ALH | Z-axis gyroscope |
| GyroZ_VRef | ADC6 | LY530ALH | Z-gyroscope reference |
| AccelX | ADC8 | ADXL335 | X-axis acceleration |
| AccelY | ADC9 | ADXL335 | Y-axis acceleration |
| AccelZ | ADC10 | ADXL335 | Z-axis acceleration |

Table 3.1: Microcontroller ADC pin assignments on Sensors Board, Rev 03.

The BMP085 is a digital I2C absolute pressure sensor from Bosch. The absolute pressure in the aircraft decays exponentially with altitude. Using this external part allows for a 19-bit resolution of the pressure measurement, which ideally corresponds to sub-meter altitude resolution, and also makes available the ambient temperature measurement used for calibration; however, atmospheric pressure also varies substantially with weather patterns, and so the measurements may not be sufficient to safely land the aircraft.

The newest revision of the board features unpopulated zero-ohm resistor pads on the I2C data and clock lines to each chip, so that they can be cut and reestablished for testing, if necessary.

Serial GPS Interface An OEM Garmin GPS unit intended for serial operation is included in the standard complement of sensors onboard. This sensor has low precision, even with a 3D fix on the satellites. The accuracy is improved slightly by the addition of the FAA's WAAS system for differential measurement; however, even with these features, the margin of error of the GPS is at least 3 m, and only has a sample rate of 1 Hz. Data from this sensor is input to a rudimentary Kalman filter, meant to combine this with the inertial measurements to improve

accuracy.

The GPS is operated in Garmin's proprietary binary mode, rather than the standard NMEA data. This choice avoids the necessity of writing a parser for the text-based NMEA format, and instead allows the direct importation of binary C structures. This also exposes additional data that may be useful in future expansion.

Serial Sonar Interface In the fall, the possibility of using an external ultrasonic rangefinder to measure altitude above ground level was investigated for use during automated landing, where precision of the altitude measurement is critical for glide-slope computations. Although automated landing was not enumerated as a goal for this project, the hardware was created with the ability to easily add this sensor if time permits.

Motor Data Interface During the fall semester, a prototype motor tachometer board was produced for a separate course, capable of measuring the rotation rate of the propeller. This used a Hall effect sensor to measure the six poles of the motor as they rotated past the fixed tachometer. Because the autopilot was able to fly the aircraft without this input, it was tabled. Additionally, there was trouble mounting the tachometer close enough to the motor to measure the rotation rate and rigidly enough to avoid contact with the motor in the turbulent wake of the propeller blades, and no investigation into the drag penalty this board introduced, because it was never tested in flight.

3.1.5 General-Purpose Computer (GPC) Board

The general-purpose computer (GPC) board acts as the system master, controlling the other boards and querying them for data over the bus. It gathers data on the plane's state from the sensors board and then feeds this data into the autopilot algorithm to decide how the plane should act to meet its next objective. It then sends commands to the servo board to make the

appropriate manipulations of the plane's control surfaces.

A front-view assembly diagram of the GPC board is shown in Figure C.5. A full list of the components is given in C.6.

Atmel AT91SAM7S256 ARM Microprocessor When selecting a chip for the system's main computer, the team had three requirements. First, the device needed to be highly integrated with a substantial amount of built-in flash memory and facilities such as direct memory access (DMA) and serial controllers. Second, it needed to be capable of running the autopilot algorithm fast enough to control the plane. Simple estimates showed that this would require roughly ten thousand floating-point operations per second. Finally, the chip needed to have a set of readily available software development tools.

Based on these considerations, the team selected the 32-bit Atmel AT91SAM7S ARM microprocessor as the system's centerpiece. This chip features software-emulated floating-point arithmetic and runs at a 50 MHz clock rate, which is more than sufficient to run the autopilot control loop at the required update rate of 25 Hz. Furthermore, the chip has 256 KB of internal flash, which easily holds all of the firmware code. It has two integrated serial ports and has excellent DMA support with two DMA channels for each peripheral controller: one for transmitting and one for receiving. The chip is programmable using a standard JTAG interface. A software development toolchain based on the GNU Compiler Collection's (GCC) ARM compiler [13] and the Open On-Chip Debugger (OpenOCD) [14] is available for Linux.

Bus Interface Hardware Like the other circuit boards, the GPC board is equipped with an Atmel ATxMEGA32A4 AVR microcontroller for interfacing to the system bus. Unlike the AVRs on the other boards, the GPC AVR *only* handles bus traffic and does not communicate with any on-board devices other than the bus transceivers and the ARM. The AT91SAM7S ARM microprocessor does not have enough serial ports to listen to traffic on all four buses at once, so the board's AVR serves as a go-between, sending received bus traffic upstream to the ARM

and forwarding packets constructed by the ARM that are intended for other boards onto the bus. Communication between the ARM and the GPC AVR is accomplished using a serial link.

Serial Debug Console The GPC board has a connector that provides direct access to one of the ARM's serial ports for a software debug console to assist with development.

SD Card Interface The GPC board has an SD/MMC connector that can hold a single SD card for storing data on-board, such as system logs. The team has developed some firmware to read from an attached SD card, but the firmware for writing to one has not yet been written.

Real-Time Clock The GPC board features a DS1302 real-time clock (RTC) IC with an accompanying 1 Farad memory back-up supercapacitor to prevent the clock from losing the time when the system is unpowered. The team has not yet written any firmware to interact with the RTC but provisioned for it in the hardware design because it would be useful in providing timestamps for system logs.

USB Interface A mini-USB connector has been provided to allow for easy interaction with the system “in the field” using a laptop and a USB cable. The team has not yet written any firmware to use the USB interface but included it in the hardware design because of the improved ease-of-use that such an interface would provide.

3.2 Avionics Firmware

This section describes the firmware that runs on each of the AVRs on the different types of circuit boards and on the GPC board's ARM processor.

3.2.1 General Architecture

Event Loop Upon boot, each board's AVR firmware performs some initialization routines (e.g., sets up the system clock, activates the serial ports attached to the buses, etc.) and then enters a main event loop. The system sits in the event loop, polling a number different condition flags, waiting for an event to happen. When one of the conditions becomes true, the AVR immediately executes an event handler to process the event and then returns to the polling loop. The events listened for differ from board to board, but the software on all boards adheres to this same basic pattern.

This description applies only to the programs running on each board's AVR microcontroller. The software running on the GPC's ARM microprocessor has a completely different architecture and is described in section 3.2.7.

Board ID Number Each board has a unique ID number written into the EEPROM of its AVR microcontroller. This ID is read out of EEPROM by the AVR on startup and is used to identify the board in the address fields of bus packets (see section 3.5.1): a board will ignore any packets with a destination ID other than its own.

3.2.2 Bus Firmware

Each board's AVR microcontroller implements the system bus protocol (see section 3.5.1). To reduce the likelihood of missing incoming bytes due to time spent processing other tasks, receipt of bytes is handled by the AVR's direct memory access (DMA) controller. The DMA controller stores bytes in a receive buffer as they arrive with no intervention from the processor. Each AVR has four DMA channels, and there are four system buses, so each bus is assigned its own DMA controller and receive buffer.

All AVR's poll for new bytes added to the DMA receive buffers for each bus as part of the

main event loop. When a new byte is added, it is copied into a packet construction buffer, and then control returns to the event loop. Frame delimiters are not added to the packet buffer, and escaped bytes are unescaped before they are added to the packet buffer. The computation of the packet's CRC checksum is advanced as each byte arrives for maximum efficiency. When a packet is complete, a packet handler routine is called to verify the packet's CRC and process it before polling continues.

This firmware required several re-writes before satisfactory performance was achieved. Early attempts used interrupt handlers to receive bytes off of the bus, but both the context-switching overhead associated with entering and leaving the interrupt service routines and the length of the routines themselves proved too large for the system to handle and still run at the full 921600 bps bus speed.

This was the main driving force behind the decision to use an event-driven software architecture on all of the AVRs. By splitting each board's tasks into the smallest possible parts and polling for when each part is complete, time spent in task handlers is kept to minimum. This prevents any one piece of code from blocking up the system and ensures that all tasks get handled roughly in parallel. As such, the code on each AVR has been written to eschew interrupts entirely except on the servo board, where they are unavoidable but kept to a minimum in terms of execution time.

Transmission to each bus is handled using DMA. A bus packet is first assembled in a buffer, complete with frame delimiters and escape sequences. The DMA channel for the transmit bus is then switched from receive mode to transmit mode, and the buffer is handed to the DMA unit to be written out to the bus. This prevents the system from using any CPU time transmitting bytes, allowing the microcontroller to continue processing other events while transmissions are occurring.

3.2.3 Servo Board

Bus Interface The servo board listens for the following bus commands (see section 3.5.1):

- `BCMD_TELEM_FETCH` – The board will reply with a `BCMD_TELEM_REPLY` packet containing the voltages and currents for both the high-voltage and low-voltage batteries, the outputs being sent to every servo, and whether or not the plane is currently being flown under manual override.
- `BCMD_SERVO_SETSERVOS` – The board will set the servos to the values specified in the packet. These are used when controlling the plane via autopilot.

Servo Outputs The primary job of the servo board firmware is to ensure the correct setting of the servo outputs. In particular, this entails ensuring that the servos are supplied with voltage pulses of the appropriate width at a regular rate. This is accomplished by manipulating the board's 4017 decade counter (see section 3.1.2). Each output of the decade counter is connected to a different servo. When it is time to send a voltage pulse to one of the servos, its output on the decade counter is pulled high and held there for an amount of time equal to the desired pulse duration. When pulse length is reached, the decade counter is advanced, and the system proceeds to the next servo output. The system cycles through setting outputs to the different servos by stepping through the states of the decade counter.

Because this procedure requires precise timing to ensure that the control pulses last exactly as long as they need to, one of the AVR's built-in timer-counter units is used to measure the amount of time to be taken between steps of the decade counter. When the decade counter is stepped and a new control pulse begins, the timer is set with a period equal to the pulse duration and begins counting. When the timer expires, an interrupt is triggered that steps the decade counter to the next servo in the cycle and resets the timer period to the duration of the next servo's pulse. The interrupt routine is written to take as few cycles as possible so that the

servo board can return to polling in the main event loop as quickly as possible.

The use of interrupts introduces one additional minor complication in the servo firmware: operations that are not atomic must be protected by disabling interrupts before beginning them and reenabling them after they are complete. In particular, since the AVR is an 8-bit microcontroller, this includes any operation that reads a 16-bit value from memory.

Servo Inputs (From GPC Autopilot) The servo board accepts input values from the GPC board running the autopilot via bus packets of the type `BCMD_SERVO_SETSERVOS`. These packets contain values that are used in setting the period of the output pulse width control timer for each servo (see “Servo Outputs”, above). The servo board will use values sent to it over the bus to control the servos unless it is also receiving commands from a manual RC transmitter, which are given priority (see “Servo Inputs (From RC Transmitter)”, below).

In the future, this facility may be enlarged to accept commands from multiple GPC boards connected in a redundant configuration. The servo firmware would be expanded to arbitrate between the different sets of received values and use them to determine the final set of servo outputs.

Servo Inputs (From RC Transmitter) The servo board is also capable of accepting commands from a standard six-channel hobbyist RC transmitter for manual backup control. The inputs from the receiver come in as servo control pulses. The servo firmware uses AVR’s timer/counter units and AtXMEGA32A4 compare-and-capture events to precisely time the durations of these pulses, which are then stored in memory to be used to set the period of the pulse width control timer for each servo (see “Servo Outputs”, above).

More precisely, a rise in the voltage on one of the lines for the RC input channels triggers a timer capture event, causing the timer value to be recorded in a special compare-and-capture register. An interrupt is then triggered, which reads this value and sets up a timer capture event to occur when the RC input line voltage falls. When the RC input line is pulled low, the

timer is stamped once again, and another interrupt is triggered that takes this value and uses it in conjunction with the rise timestamp to determine the duration of the pulse.

One of the RC servo input lines is used to determine if RC manual control is active. When the user wants to engage manual control, a switch is flipped on the RC transmitter that causes the manual override input line to be pulled high. The servo board AVR checks for this to occur and sets the servos to use the manual control inputs when it does.

It is important to note that even when manual control is engaged, the servo board continues to listen for and store servo values from autopilot control packets received over the bus. This ensures that the transition to autopilot control is as smooth as possible should manual override be deactivated at the transmitter or should the transmitter go out of range.

Emergency Mode The servo firmware is programmed to disable the throttle and set all control surfaces (rudder, elevator, and ailerons) to their neutral positions in the event that the board both stops receiving servo commands from the autopilot and is not receiving any commands from a manual RC transmitter. This should cause the aircraft to enter a gentle glide and reduce the risk of damage both to the plane and to objects on the ground should the plane eventually crash.

The status of the manual transmitter is assessed using the value of the manual control input line (see "Servo Inputs (From RC Transmitter)", above). The autopilot is deemed to have stopped responding if the board goes more than 200 ms without receiving a bus packet containing servo values.

Battery Monitoring As mentioned in section 3.1.2, the servo board features hardware for monitoring voltages and currents of both the high-voltage and low-voltage batteries. Once every second, the servo board AVR sets its ADC unit to begin conversions on the pins connected to this hardware. The AVR then polls for these conversions to finish inside the main event loop, and when they do, it scales the values to have units of millivolts (for voltages) or milliamperes

(for currents) and then stores them in memory. The GPC board can request the latest set of battery monitoring data by sending a `BCMD_TELEM_FETCH` command to the servo board.

3.2.4 Radio Board

Bus Interface The radio board listens for the following bus commands (see section 3.5.1):

- `BCMD_TELEM_FETCH` – The board will reply with a `BCMD_TELEM_REPLY` packet containing the voltage level on each bus.
- `BCMD_SEND_DLPACKET` – The board will send the radio downlink packet attached to the bus packet via the radio.
- `BCMD_MAILBOX_PEEK` – The board will reply with a `BCMD_MAILBOX_CONTENTS` packet containing the contents of the uplink packet at the front of the uplink mailbox queue.
- `BCMD_MAILBOX_POP` – The board will remove the uplink packet at the front of the uplink mailbox queue if the uplink packet’s mailbox sequence number matches that sent in the pop request packet.

XTend Radio Module Interface In addition to interfacing to the system bus, the radio board also communicates with the on-board XTend radio module using a serial line. The communications are structured according to the XTend API mode 2 protocol, described in the XTend datasheet [15], which forms an additional protocol layer on top of the downlink (see section 3.5.2) and uplink (see section 3.5.3) protocols.

Since the AVR only has four DMA controllers, and since these are all allocated to handling bus communications (see section 3.2.2), receiving from the XTend module is accomplished by polling the radio’s assigned USART receive register for new bytes inside the main event loop. Because the serial link to the radio runs at the relatively slow speed of 230400 bps (compared,

e.g., to the 921600 bps system bus), the likelihood of the polling loop missing radio bytes is reasonably small.

When a new byte arrives from the radio, it is copied into a radio packet construction buffer. XTend protocol headers and frame delimiters are processed and stripped as they arrive, and XTend escape bytes are unescaped before being added to the buffer. Computation of the XTend protocol checksum is advanced as each byte arrives. When a complete packet is received, its XTend checksum is verified, and if the checksum passes, the packet is assigned a mailbox sequence number and is placed in the uplink packet mailbox queue (see “Uplink Packet Mailboxing”, below).

Transmission to the XTend radio is also handled in the main event loop. When a packet is ready to be sent to the radio, the AVR adds it to a radio packet transmit queue. In the event loop, the AVR checks to see if the radio transmit queue is nonempty. If it is, and if no packet is currently being sent to the radio, the AVR takes a packet from the radio transmit queue and sends a byte by byte. It polls in the event loop, waiting for the byte to finish sending, and then transmits the next and so on until the entire packet is sent.

Uplink Packet Mailboxing As uplink packets are received, they are stored in the uplink mailboxing queue, where they await retrieval by the GPC. When the radio board receives a `BCMD_RADIO_MAILBOX_PEEK` request from the GPC, it copies the contents of the packet at the front of the queue (i.e., the oldest uplink packet in the mailbox) into a bus packet and then sends this bus packet to the GPC.

Each uplink packet is assigned a mailbox sequence number (this is not the same as the uplink protocol sequence number; see section 3.5.3) that identifies its position in the mailbox queue. A packet is removed from the mailbox queue only when the radio board receives a `BCMD_RADIO_MAILBOX_POP` command carrying that packet’s sequence number in the data field. The reason for this is so that the GPC can request retransmission of an uplink packet

over the bus by sending another `BCMD_RADIO_MAILBOX_PEEK`, e.g., in the event that a bus error caused the original transmission to fail its CRC check.

Bus Voltage Monitoring The radio board is equipped with hardware for monitoring the voltages of each of the four system buses. Inside the event loop, the radio board AVR periodically sets the ADC channels attached to the voltage monitoring hardware to begin a conversion. It polls the ADC conversion flags for each channel, and when a conversion is complete, it converts the ADC value into a voltage value and saves the result.

The radio board will send the most recent values of the bus voltages in response to a `BCMD_TELEM_FETCH` packet by the GPC.

3.2.5 Sensors Board

Bus Interface The sensors board listens for the following bus commands (see section 3.5.1):

- `BCMD_SENSORS_FETCH_HIRATE` – The board will reply with a `BCMD_SENSORS_REPLY_HIRATE` packet containing a set of high-rate sensor data, including measurements from the accelerometers, magnetometers, gyroscopes, airspeed sensor, static pressure sensor, and temperature sensor.
- `BCMD_SENSORS_FETCH_LORATE` – The board will reply with a `BCMD_SENSORS_FETCH_LORATE` packet containing the latest set of GPS data.

Analog Sensors Interface The accelerometers, gyroscopes, and differential pressure sensor are all analog sensors (see section 3.1.4). The sensors board reads values from these sensors using the AVR's built-in ADC unit.

There are seven analog sensors (three accelerometer axes, three gyroscope axes, and the airspeed sensor), but the ADC unit on the AVR has only four channels, so the AVR's ADC multiplexer is used to alternate channel assignments between the different sensors. A

software state machine is used to control the order in which the sensors are read. When the state machine is advanced, a set of ADC conversions are initiated on the set of sensors being read. The ADC conversion complete flags are polled inside the firmware's main event loop. When the conversions are complete, the state machine is advanced, enabling the next set of sensors to be read.

Unfortunately, due to a hardware erratum in the revision of the AVR being used on all the system boards, switching the ADC multiplexer to accept input from a different bank of sensors causes the ADC to report bogus conversion values for several conversion cycles after the switch is complete. To get around this problem, the sensors board performs sixteen "dummy" conversions in between states of the analog sensors state machine to flush the ADCs before beginning the conversions used to read the sensors.

I2C Sensors Interface Two of the sensors on the sensors board communicate using the I2C protocol: the HMC5843 magnetometer chip from Honeywell and the Bosch BMP085 static pressure and temperature sensor (see section 3.1.4). The sensors board uses the AVR's built-in I2C interface capabilities to manage the low-level aspects of communicating with these sensors. The I2C bus on the sensors board runs at a rate of 100 kHz. The I2C sequence begins with several initialization transactions carried out upon boot that set the gain and update rates of the magnetometers and read calibration values from the BMP085. Then, the I2C system enters a cycle of transactions that repeatedly read values from each of the I2C sensors.

The firmware for querying the I2C sensors is built around two software state machines: a high-level state machine that dictates the order in which the different sensors are read and a low-level state machine that manages the sending and receiving of individual bytes over the I2C bus. When the I2C system is ready to handle the next transaction (i.e., process the next state in the high-level state machine), the low-level state machine is set to an idle state. This condition is detected when the state of the I2C system is next polled in the sensors board's

main event loop, causing a function to be called that re-initializes the low-level state machine for the next transaction. In particular, it sets up a buffer containing the bytes that comprise the I2C command to be sent and prepares a second buffer for receiving the response.

The low-level state machine then manipulates the AVR's I2C hardware to send the command and retrieve the reply. At each pass of the event loop, the I2C hardware is polled to see if it is ready for the next action, and if so, it is carried out. When the full reply has been received, it is processed, the low-level state machine is set to an idle state, and the high-level state machine is advanced, causing the system to proceed to the next I2C transaction.

Garmin GPS Interface The sensors board receives GPS positioning information from the off-board Garmin GPS unit over a standard serial link using the Garmin proprietary binary format described in [1]. The GPS emits a packet with a new position record once every second.

Since the AVR only has four DMA controllers, and since these are all allocated to handling bus communications (see section 3.2.2), receiving from the GPS is accomplished by polling the GPS's assigned USART receive register for new bytes inside the main event loop. Because the GPS serial link runs at only 9600 bps (compared, e.g., to the 921600 bps system bus), the likelihood of the polling loop missing GPS bytes is reasonably small. Failure here will result in the loss of a single GPS packet, which seems acceptable.

A state machine is used to process the Garmin binary protocol for GPS data, which is a thin wrapper around raw C structures that are transmitted as binary. When a new, data byte arrives from the GPS, it is copied into a GPS packet construction buffer. Garmin protocol headers and frame delimiters are processed and stripped as they arrive, and Garmin escape bytes are unescaped before being added to the buffer. Data packets other than the PVT location packets are ignored at present, but satellite-specific data is available. Computation of the Garmin protocol checksum is advanced as each byte arrives. When a complete packet is received, its Garmin checksum is verified, and if the checksum passes, the GPS data is saved

in memory where it awaits request by the GPC board.

Sensor Calibration Calibration values for all of the sensors are stored in the EEPROM memory unit on the sensors board AVR, except for the BMP085, which comes with factory-loaded calibration values that are read during the I2C startup sequence. The sensors firmware uses the stored calibration values to remove zero offsets and convert the sensor outputs into the units required by the autopilot algorithm. For more information on sensor calibration, see sections 4.2 and A.7.

3.2.6 GPC Board (AVR)

Bus Passthrough The sole purpose of the GPC AVR is to serve as a passthrough between each of the buses and the GPC's ARM microcontroller. As discussed in section 3.1.5, it is used to make up for the fact that the ARM does not have enough serial ports to interface with all of the buses.

Like the bus firmware on the AVRs on the other boards, the GPC AVR polls for incoming bytes on the four system buses. When a completed packet is received, it immediately begins transmitting the packet to the ARM using DMA. Unlike the bus firmware on the other AVRs, the GPC AVR does not strip frame delimiters, process escape sequences, or check the packet's CRC or destination ID, leaving those tasks to be handled by the ARM. This minimizes the likelihood that the AVR will miss an incoming byte by ensuring that it returns to the polling loop as rapidly as possible.

ARM Interface In addition to listening on the buses, the GPC AVR polls for incoming bytes sent to it by the ARM, buffering them as they enter. All traffic from the ARM to the GPC AVR is wrapped using the bus protocol. When the GPC AVR receives a complete packet from the ARM, it checks to see if it is a special packet addressed to it (see "Special Commands",

below), and if so, processes it. Otherwise, the packet is immediately transmitted to the board's assigned bus using DMA.

The GPC AVR is also responsible for forwarding all packets received from the system bus to the ARM for processing (see “Bus Passthrough”, above). Because the ARM does not use a polling event loop as the basis for its interaction with peripheral devices, the ARM must be signaled when it has been sent a complete packet. Upon the completion of transmission to the ARM, the GPC AVR toggles ones of the ARM's GPIO pins, triggering an interrupt on the ARM that is picked up and handled by the ARM kernel.

Special Commands The GPC AVR board listens for the special bus commands sent to it from the ARM (see section 3.5.1). They are called “bus commands” because they are defined as part of the bus protocol, but these commands are never sent over the system bus:

- `BCMD_GPCAVR_WHOAMI` – This is sent by the GPC's ARM microcontroller in order to ascertain its board ID, which is stored in the EEPROM of the GPC AVR. The GPC AVR replies with a `BCMD_GPCAVR_BOARDID` packet containing the board ID.

3.2.7 GPC Board (ARM)

3.2.7.1 System Master

The software running on the ARM provides master timing of all system events. By virtue of the command/response nature of the bus protocol, it is guaranteed that the GPC board will initiate all bus transmissions, and the other boards will wait until a reply is demanded of them before transmitting. In a future configuration with multiple GPC boards, it is envisioned that each GPC would be the master of a different bus, so that even without cross-GPC synchronization, there would still be no collisions.

3.2.7.2 Custom Real-Time Kernel

Overview The ARM microcontroller runs a custom written kernel named MAL. This kernel provides scheduling, timing, interprocess communication (IPC) and interrupt management features. Because the microcontroller does not have a Memory Management Unit, the kernel does not provide memory protection between different threads. Furthermore, the kernel also does *not* provide dynamic memory allocation — this eliminates the program space, runtime and memory overhead costs associated with an allocator, as well as helping the developer to ensure that the firmware remains strictly within the bounds of the available RAM resources.

Tasks and Contexts The kernel allows for an arbitrary number of user threads to be present, and provides a separate user stack, registers, and instruction pointer for each thread. The kernel uses only a single privileged-mode stack, so there is only one kernel context. This means that context switching between different user threads is performed when the kernel returns out from kernel mode to user mode, rather than switching from one kernel context to another.

The kernel provides a macro called `STATIC_TASK` which statically allocates all memory required for a thread and adds it to the scheduler. One of the arguments is a stack size for the new thread, so the developer must take care to choose a sufficiently large value. The kernel does contain some checks to help detect stack overflow.

Scheduling and Timing The scheduling algorithm is designed to accommodate the real-time requirement of the main autopilot thread, while also allowing other threads to receive CPU cycles. The scheduler is capable of waking up the autopilot thread to run a new calculation cycle every 40 milliseconds, with vanishing jitter and zero long-term systematic delay errors. Priority is handled using a system of reservations, rather than static or dynamic priority numbers. Each thread is configured with a CPU percentage, which could be from 0% to 100%.

The sum of all percentages must be less than 100%. Over the course of one 40-millisecond cycle, any thread which has not yet used up all its reservation is given priority over a thread which has already used its guaranteed time. The autopilot thread is configured with approximately a 50% reservation, which is several times the amount of CPU cycles it needs for any given 40-millisecond cycle. This way, so long as the autopilot is ready to run, the kernel will give it priority. Other threads have been given small reservations, such as 10% or 0%. A small positive number will ensure that the thread does not starve.

During one calculation cycle, the autopilot thread both communicates with other boards and runs computations. During the communication, the thread will go to sleep to wait for the bus I/O to complete. While the autopilot is sleeping, the scheduler will allow other ready threads to run, until the autopilot I/O completes and the autopilot thread wakes up again.

The kernel timer subsystem is designed to provide high granularity for timer events, without wasting lots of CPU cycles with frequent clock interrupts. One hardware timer is configured to operate in a free-running mode, and provides a reliable reference synchronized to the clock crystal with no drift. It only fires an interrupt infrequently upon overflow. A second hardware timer operates in a countdown mode, and is only switched on when there is an event pending soon. It is preloaded with the exact amount of delay needed between now and the next event. In this way, a timer interrupt only fires when a requested event is supposed to occur, and provides near-exact delay straight to the requested time.

Interprocess Communication The interprocess communication facility of the kernel was inspired by the minimalism of the L4 microkernel. The kernel does not maintain variable-length message queues, or even buffer message contents inside the kernel at all. There are only two system calls: `ipc_send` and `ipc_recv`. A valid message target identifier is simply a pointer to the target thread. If the target thread is ready to receive a message, then the message is communicated immediately, and the sending call returns. Otherwise, the sender

must wait until either the recipient is ready to receive the message, or a timeout occurs.

Similarly, when a thread attempts to receive a message, it will return immediately if another thread is currently blocked waiting to send. Otherwise, the receiver will block until either someone else sends a message to it, or a timeout is reached. Special timeout values of zero and infinity are available.

The simplicity of the IPC subsystem means that the required kernel support code is very small, and thus its correctness is relatively easy to verify. If more complicated IPC interactions are desired by user threads, they can be built on top of this single low level primitive.

Interrupt Management The kernel includes device drivers for only the two timers required to implement preemptive multitasking and other scheduling/timing events. All other device drivers are handled inside user threads. Since the ARM microcontroller has no memory protection, it is important for the programmer to ensure that only one thread attempts to use a given I/O device at a time.

Although the drivers for I/O devices are implemented outside of the kernel, the kernel does provide some support to make these drivers more efficient. Specifically, it provides a facility for a thread to sleep until a given hardware interrupt is triggered. This is done through an extension of the IPC primitive mentioned in the previous section. When an interrupt occurs which the application wishes to receive, the kernel creates a fake IPC message with a source address indicating that it is coming from an interrupt. Thus, in order to wait for an interrupt to occur, a user thread can simply call `ipc_recv` with the appropriate arguments.

3.2.7.3 Autopilot Task

The autopilot program was originally developed as a user program running on a PC, then ported into the embedded environment this year. Currently, it runs as a user thread under the custom kernel. The thread runs infinitely in a main loop which polls other circuit boards for data

over the bus, processes the data, and sends replies back out. At the end of each time through this processing cycle, the thread sleeps until the beginning of the next 40 millisecond processing window. The autopilot's computations are split into a standard guidance/navigation/control (GNC) configuration. Details on the autopilot algorithm can be found in section 3.3.

3.3 Autopilot Software

3.3.1 General Structure

The autopilot software is split into guidance, navigation, and control components. The data flow between the different components is shown in figure 3.2.

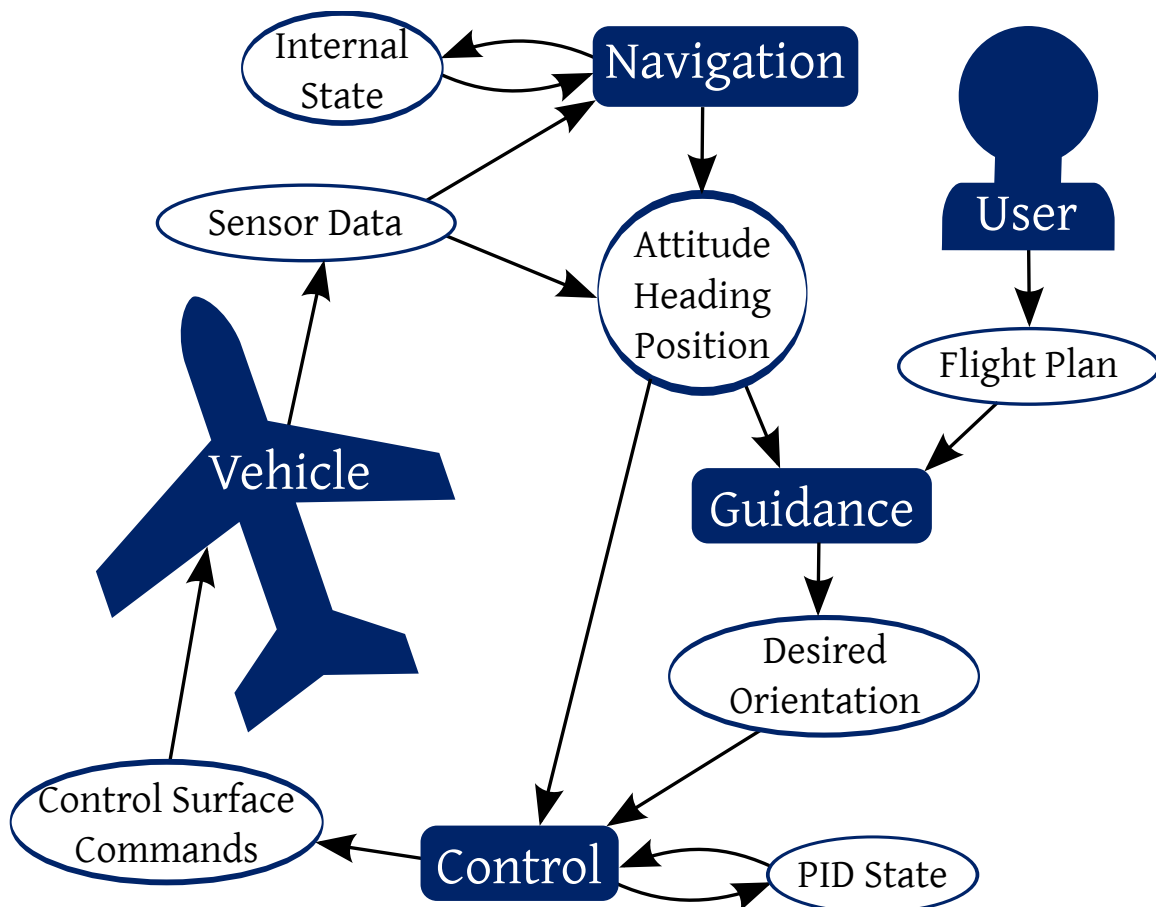


Figure 3.2: Data flow in the autopilot

Navigation The navigation component takes low-level sensor readings, such as accelerometers and gyroscopes, and integrates them into a coherent picture of the state of the vehicle. Internally, it uses quaternions to track the attitude in three dimensions, to avoid the problem of gimbal lock. From this internal state, it outputs the more traditional heading, pitch, and roll angles, which are then used by the other software components.

Guidance The guidance component is primarily concerned with interpreting the step-by-step flight plan which has been input by the user. Its job is to decide when a given flight segment has been completed, so that the plane can begin executing the next flight segment. It also has a facility to watch for various possible error conditions (altitude not sustained, wind too strong, location too far from home base, etc) and automatically switch to a contingency plan when necessary. Using the current step in the flight plan, it calculates a desired orientation to move the vehicle closer to the right position. The desired orientation is then used as input data for the control component.

Control The control component performs low-level vehicle attitude and thrust manipulations. It compares the current attitude as calculated by the navigation component to the desired attitude output by the guidance component, then decides what control surface movements will best move the vehicle toward the desired orientation. This function is performed using a set of PID controllers, one for each axis of elevators, ailerons, and throttle. There are also some cross-axis coupling terms which have been added manually. Currently, the controller gains are set at compile time; it would be a useful future extension to allow these gains to be changed at runtime.

3.3.2 Sensor Redundancy Management

The GPC ARM firmware processes redundant sensor data before supplying it to the autopilot algorithm. First, it queries all sensor boards attached to the system. Then, based on the number of replies it receives and on the type of data asked for (high-rate IMU measurements or low-rate GPS data), the GPC integrates the data it has received into a single set of sensor readings, which it then passes to the autopilot. Presently, the system is configured to handle data for up to three sensors boards; however, it can be straightforwardly extended to process data from more.

Redundant High-Rate Data Processing If only a single set of high-rate data is received, then that set is sent directly to the autopilot with no further processing. If two sets of data are received, the values for each sensor are averaged together before being sent to the autopilot. If three sets of data are received, the GPC inspects each piece of sensor data to see if one of the values deviates substantially from the other two. If so, the offending datum is labeled an outlier, and the remaining, non-outlier values are averaged together to form the final estimate which is sent to the autopilot. If no datum is judged to be an outlier, all three pieces of data are averaged together to form the final estimate. The GPC keeps track of the number of outliers rejected for each sensor and can send these down to the ground computer over the radio with the rest of the telemetry.

Outlier detection in the three-reply case is handled using the Dixon Q-test at 90% confidence [16]. While not the most robust statistical criterion in general, this test is good at handling very small sets of data and does not make any assumptions about the nature of the source distribution aside from its normality. It is also straightforward to implement.

Redundant Low-Rate Data Processing Redundant low-rate data is handled in a different manner from the high-rate data because performing averaging and outlier rejection on GPS

data is not appropriate. Rather, the GPC takes all sets of GPS data it receives and looks to see which one has the highest-quality satellite fix and sends that to the autopilot. GPS data from a unit with a 3D-WAAS fix is preferred over data from one with just a 3D fix. Data from units with no fix or only a 2D fix is discarded. If multiple units are found to have the best fix, data from them is chosen arbitrarily to be used as the input to the autopilot.

3.3.3 Flight Plan Format

The flight plan is formatted as a series of steps, where each step contains all the information needed for its own execution. Each step includes a criterion used to determine when it has been completed, so the autopilot can switch to the next step. In addition, each step can optionally contain one or more error conditions. If the criteria for an error condition is met, the guidance component will skip the normal step increment and follow a pointer to an arbitrary step. The user is responsible for writing a flight plan which includes alternate contingency steps, to be used in case of an error condition in one of the normal steps.

The autopilot software currently supports five types of steps:

- **Glide.** The motor powers off, a slight down pitch is maintained, and a given heading is maintained. During flight testing, extra code was written to grab the current heading when manual to automatic switchover occurred, and use this heading for a glide step.
- **Takeoff.** The motor is commanded to a tunable high-throttle setting, and the vehicle tries to travel straight down the centerline of the runway. The tail wheel is used for steering on the ground, while the ailerons attempt to maintain zero roll so the wingtips don't scrape the ground. The takeoff continues until a given elevation is reached, or fails to be reached.
- **Waypoint.** The airplane attempts to fly toward a specified waypoint, without regard for its ground track or wind correction. The motor and elevator are used in conjunction to

approach and maintain a desired altitude and airspeed.

- 2D Path. This is similar to the waypoint mode, except that the airplane attempts to fly a specific 2D line along the ground. In order to maintain the desired ground path, the airplane will automatically yaw to crab into the wind if required.
- Landing. This is the most complicated type of step. Similar to takeoff, the step specifies the location of a runway centerline along the ground; however, in addition, it incorporates a desired sink rate for the approach, and a targeted touchdown point along the runway. The vehicle is controlled to fly along the runway centerline in the horizontal dimension, while maintaining the correct vertical approach speed and angle. Once the vehicle is over the runway, the motor is stopped and a flare pitch comes into effect. This procedure has proven remarkably resilient to varying wind speed and direction in simulation.

There are currently five types of step completion criteria available:

- Never. This is used for testing, finishing a flight plan, or for the final step in a contingency plan.
- Point cross. This completion criteria is only valid for the Waypoint and 2D Path step types. One difficulty is that the airplane can be expected to never follow a precise trajectory arbitrarily close to the desired waypoint — there must be some definition of “close enough”. The original version of this criterion measured how quickly the angle from the airplane to the waypoint was changing to determine when the airplane had passed through a region close to the point; however, in recent testing this measure gave frequent false positives due to an unrelated packet dropout problem, which affected the timebase. It has been rewritten to work for *only* the 2D Path step, by comparing the airplane’s position to a line running through the destination waypoint perpendicular to the desired 2D ground path. This new test does not depend on time and proved reliable. This change effectively deprecates the Waypoint step type for now.

- Above/Match/Below Elevation. These three completion criteria simply measure if the plane has reached above, crossed in either direction, or fallen below a specified elevation. This is used if the planner would like the UAV to change altitude, and switch to the next phase of the plan as soon as the altitude change is finished.

There are currently four types of error conditions, each of which can be enabled or disabled for any given flight plan step:

- Altitude attainment failure. This error condition is intended to be used in conjunction with the Takeoff step type. It has data fields for an altitude and a timeout timer. If the vehicle has not reached the specified altitude in the given number of seconds, the error will trigger. The user can configure the contingency plan step to shut off the motor to terminate further movement of the vehicle.
- Orientation error. This can detect several types of errors, including the exceeding of preprogrammed pitch or roll limits, and the airplane attempting to go backwards during a Takeoff, 2D Path, or Landing step.
- Too long. This condition will trigger if the current step has been executing for longer than a given time.
- Too low. This condition will trigger if the airplane falls below a trigger altitude. This may happen if, for instance, the main propulsion battery is drained and the airplane can no longer keep itself in the air.

3.4 "Houston" Ground Software

A graphical PC application has been designed to run on a ground support laptop and provide various real-time and off-line support functions for the UAV system. The core functionality consists of a fast multithreaded Internet-enabled two-dimensional map viewer, with support for

several vector and raster geo-referenced data formats. This software base was written prior to the 2010-2011 school year. During the current school year, the application was extended to add an interface for receiving, displaying, and recording real-time telemetry from the UAV. Loading a previously-recorded telemetry file to view the two dimensional flight track is also supported.

In addition to the main graphical ground software, the team developed a number of other standalone utilities to assist with development and data processing. These are described in section A.6 of the User's Manual.

3.4.1 General Interface

Upon starting, the ground software displays a default location with several data sources enabled. Two toolbars provide controls to switch the set of data being displayed, open a new data source, zoom and pan, or measure distances. Several menus are available to open new files, change settings, configure UAV communications parameters, and switch on an active tracking mode.

The main map display shows a combination of a background raster image plus one or more layers of vector data overlaid on top. The raster images are always displayed in their original resolution — this means that the map scale and map projection are determined by the selected raster data source and resolution. All vector data is re-projected on the fly from latitude/longitude coordinates in order to match up with the raster map being displayed. Because the resolution is taken from the raster data, the available zoom levels are discrete and predetermined.

Along the left side of the main window is a list showing which data sources have been loaded. Each source can be switched on or off for viewing by clicking on a box next to its name.

3.4.2 Raster Data

The ground software currently supports two main raster image sources: Microsoft Research Maps (formerly TerraServer) aerial photos and topographic maps, and Shuttle Radar Topography Mission (SRTM) digital elevation maps. At the lowest zoom level, some SRTM-derived prerendered images are displayed.

The Microsoft Research Maps images come in resolutions ranging from 512 meters per pixel (mpp) down to 0.25 meters per pixel in some areas, and use the Universal Transverse Mercator (UTM) projection. Three image types are supported via toolbar buttons: older black-and-white aerial photos down to 1 mpp, newer color aerial photos down to 0.25 mpp in certain urban areas, and old topographic maps down to 2 mpp. The application supports automatic downloading of image tiles directly from the MSRMaps.com web server as the user scrolls around the map. The image tiles are cached locally on the hard drive to enable offline viewing later. In this way, the user can build up a local database of imagery for areas of interest, then take it on the go to a location without Internet access.

The SRTM elevation maps come in two resolutions, 1 arcsecond (approximately 30 meters per pixel) and 3 arcseconds. This data is in unprojected direct latitude/longitude coordinates, so it has a distinctive x- versus y- scale difference, which becomes greater when viewing farther away from the equator. The files store actual elevation numbers measured in feet, which are not suited for display directly as pixel colors. Instead, the application looks for the maximum and minimum elevations in the current viewing area, then automatically scales all points to a black-and-white rendering based on elevation. In this way, an individual point does not have a fixed color, but its brightness will change as the map is scrolled by the user. The source files with the elevation data are uncompressed and rather large, so the application does not support automatic downloading for this map type.

The different resolution levels available have been interleaved in order of scale. Thus,

when zooming in or out, the program automatically switches between the MSRMaps images and the SRTM images, with the geographic projection switching simultaneously. Although the map distorts in different ways in the two different projections, the geographic point at the center of the current view remains constant when the switch is made.

3.4.3 Vector Data

The ground software supports a wide range of vector data sources, both static and live-updating. The static sources include street data from the US Census Bureau, the global airport list used in the X-Plane flight simulator, G7T and GPX log files, and UAV telemetry files from this project. The live sources include a network-enabled GPS link and streaming data from the UAV.

The US Census Bureau data comes from their data product named “TIGER/line”. It includes every street in the United States and Puerto Rico, along with railroads and creek/lake outlines. The original Census Bureau data comes in an uncompressed text format with even more types of data, making it unsuited for direct use. Instead, a custom intermediate data format has been created, along with tools to reprocess the original data into the intermediate format. With this compression, the user can choose to copy around files on a county-by-county basis, or grab the whole thing. In the compressed format, an individual file ranges up to approximately 5 megabytes for a populated county such as Harris County, and the entire United States database weighs in at about 1.5 gigabytes. Individual county files are loaded and unloaded automatically on demand as the user scrolls around the map, with no further action required.

The global airport list comes as the same file used by the X-Plane flight simulator for its internal airport database. The source file has complete coordinates for individual runway locations, lengths, and widths, as well as even taxiways for a large proportion of the airports. The ground software skips over the taxiways and other auxiliary information, but loads up all

the runways and displays them as four-sided outlines overlaid on the map. The four-letter airport identifier and airport name are also displayed, depending on the zoom level. The entire world database uses around twenty megabytes of RAM when loaded, and is internally sorted using a tree data structure for efficient display of only the relevant data.

The G7T, GPX, and UAV telemetry files are all loaded and displayed in a similar manner. The application loads all geographic path traces from a file and displays them as overlaid data as the user scrolls around. Double clicking on the loaded file in the layer-tree will cause the map view to center and zoom to see the whole contents of that one file. The color of the displayed traces can be set on a file-by-file basis by right clicking on the name and going to the color selection dialog.

The GPS vector data source uses the open source `gpsd` program and library to interface to a GPS unit. This GPS can be either connected directly to the computer the ground software runs on, or remotely to another `gpsd` instance across a network. The ground software displays a small icon indicating the current position reported by the GPS, and also records the path history to display as a trace leading to the current position of the icon. There is no provision for saving this trace, as that function is easily accomplished using the tools which come with `gpsd`.

The UAV vector data source is similar to the GPS source, except that its data comes from either the telemetry downlink radio or the X-Plane flight simulator. It displays an airplane icon on the map, which rotates around as the live or simulated UAV heading changes. This vector layer does not display the track history on its own during live operations. A saved telemetry log file can instead be loaded using the UAV telemetry static vector layer.

3.4.4 UAV Support

The ground software has a number of features to support development and testing of the UAV, some of which were mentioned in the previous section. The application can connect to the

telemetry radio over USB, plug into one of the onboard communication buses using a USB-to-RS485 adapter, and connect over a network (or locally) to another PC running the X-Plane flight simulator. In addition, a joystick can be connected to provide a form of manual flight control with some differences from the R/C transmitter discussed elsewhere. All of these links can be active at once, and the communications are handled in a separate software thread to avoid delays caused by other components of the application.

There are several modes available under the UAV menu, to accommodate different testing and flight profiles. The “X-Plane” mode is used merely to fly a remote X-Plane instance using a joystick attached to the ground software. The “HITL” (Hardware-In-The-Loop) mode connects the X-Plane flight simulator to a GPC board running the autopilot algorithm, for development and testing of the autopilot. The “Live” mode receives and records telemetry using the radio link, displaying the airplane position both on the map and in X-Plane. The user can also connect to the onboard bus in live mode, to record a combined radio + bus telemetry stream. This has proved useful for debugging.

3.4.5 Logging Format

The log format output by the ground software shares some elements in common with the byte-oriented protocol used for the onboard buses. Specifically, each packet of data is encapsulated using start and stop delimiter bytes, with escaping of data bytes to avoid any ambiguity for these delimiters. This encapsulation proved to be far more robust than the first version of the log format. It has even enabled the capability to start and stop external analysis programs on the live telemetry stream without interrupting the recording, by using the Unix `tail -f` command.

Inside of each encapsulated log packet is a timestamp with microsecond-level resolution, a marker indicating what sort of payload is in the packet, and then the payload. The payload consists of either a telemetry downlink packet, a bus packet, a command uplink packet, or

a raw radio packet. The timestamp is added by the PC running the ground software. The microsecond resolution enables the user to ascertain timings even on closely-spaced bus packets.

Each time one of the UAV modes is activated, the ground software creates a new telemetry log file to record data. The file is named with the date and time it was created to ensure uniqueness and as a convenience for the user.

In addition to recording all UAV communications into a log file, the application can read in a previously recorded file and plot the aircraft's track in two dimensions, as described in section 3.4.3.

3.5 Communications Protocols

In addition to the protocols used to communicate with the various peripherals on each board, communication between the different parts of the system is accomplished using several custom-designed protocols. This section describes these custom protocols and how they operate.

3.5.1 Bus Protocol

The bus protocol defines the mechanism for communication between the different types of circuit boards over the system's 1 megabit RS-485 bus.

Delimiters and Escape Bytes The basic unit of bus traffic is the *packet* (or *frame*), which is a sequence of bytes structured in the appropriate manner for transmission over the bus (see "Packet Structure," below). The packets can be of variable length to accommodate data payloads of various sizes. To make it easy to determine packet boundaries, the bytes 0x7E and 0x81 are reserved for use as frame delimiters and may not appear anywhere inside a bus packet, including the headers. Prior to sending a packet, the byte 0x7E is sent to indicate the

start of a new frame. After the last byte of the packet’s data section is transmitted, 0x81 is sent to mark the end of the current frame.

If a board needs to send a packet containing these values, the offending bytes must be escaped prior to transmission. Escaping is accomplished by first sending the byte 0x7D followed by a second byte that depends on the value of the byte being escaped. These values are given in table 3.2. For instance, to send a data byte with value 0x7E, one must send the sequence 0x7D 0x5E instead.

| Special Byte | Function | Escape Sequence |
|--------------|--------------------------|-----------------|
| 0x7E | Start-of-frame delimiter | 0x7D 0x5E |
| 0x81 | End-of-frame delimiter | 0x7D 0x51 |
| 0x7D | Escape byte | 0x7D 0x5D |

Table 3.2: Special bytes and escape sequences.

Packet Structure Bus packets have two major parts parts: the header and the data section. The layout of a bus packet is illustrated in figure 3.3.

The packet header begins with a two-byte CRC checksum, sent in big-endian order. The next byte holds the ID of the board sending the packet and is followed by a byte with the ID of the destination board. Following these, the data length byte specifies the size of the packet’s data field prior to the addition of escape bytes (see “Delimiters and Escape Bytes,” above). Next comes the command byte, which specifies what kind of data the packet is carrying. The command byte is the last byte in the packet header. Following the command byte, there are the payload bytes, which constitute the data being sent.

| Bit Offset | 0-7 | 8-15 | 16-23 | 24-31 |
|------------|--------------|--------------|-----------|----------------|
| 0 | CRC Checksum | | Source ID | Destination ID |
| 32 | Data Length | Command Byte | Data | |
| 64+ | Data | | | |

Figure 3.3: Byte structure of a bus packet.

Validation Checksum Each packet contains a 16-bit CRC-CCITT checksum that can be used to help detect errors in packet transmission. Every byte in the packet is included in the CRC calculate except the start and end delimiters and the checksum bytes themselves. Since the checksum must be computed before escape bytes are added (in case the checksum bytes themselves need escaping), the CRC calculation is not performed on escape sequences but on the underlying bytes being escaped. For example, if a packet's data section contains the byte 0x7E, the CRC will be calculated using the byte 0x7E instead of the sequence 0x7D 0x5E.

At the receiving end, the destination board strips off the frame delimiters, de-escapes any escaped bytes in the received packet and then computes the CRC of the result. This is then compared to the checksum bytes sent in the packet header. If there is a mismatch, a transmission error has occurred, and the board can execute an error-recovery procedure to handle the bad packet.

Command Bytes The command byte field in the packet header designates what type of data the packet is carrying. The name *command byte* is derived from the idea that a packet sent by the GPC board typically contains a command for another board to execute. Possible values for the command byte are given in table 3.3. The data payload types associated to each of these values are discussed in the sections below. Since the system uses few of the available values for the command byte, it is easy to expand the system to accommodate more packet types by defining new command bytes.

Generic Data Fetch Commands The BCMD_TELEM_FETCH command is used for retrieval of data from any of the boards in the system except for sensors data, which has its own set of commands as described in the “Sensors Board Commands” section below. For instance, the GPC can issue this command to request battery voltage and current monitoring data from the servo board. The data field of a BCMD_TELEM_FETCH packet is empty: the list of data registers that are read back in a reply to a BCMD_TELEM_FETCH request is programmed into each board

| Command / Packet Type | Command Byte | Description |
|---------------------------|--------------|---------------------------------------|
| BCMD_GPCAVR_WHOAMI | 0x07 | ARM queries GPC AVR for board ID |
| BCMD_GPCAVR_BOARDID | 0x08 | Reply to ARM board ID request |
| BCMD_SEND_DLPACKET | 0x09 | Send downlink packet over radio |
| BCMD_MAILBOX_PEEK | 0x0A | Get message from radio mailbox queue |
| BCMD_MAILBOX_POP | 0x0B | Remove from radio mailbox queue |
| BCMD_MAILBOX_CONTENTS | 0x0C | Radio mailbox contents reply |
| BCMD_TELEM_FETCH | 0x14 | Generic data fetch command |
| BCMD_TELEM_REPLY | 0x15 | Generic data reply |
| BCMD_SENSORS_FETCH_HIRATE | 0x1E | Fetch high-rate sensor data |
| BCMD_SENSORS_REPLY_HIRATE | 0x1F | High-rate sensor data reply |
| BCMD_SENSORS_FETCH_LORATE | 0x20 | Fetch low-rate sensor data |
| BCMD_SENSORS_REPLY_LORATE | 0x21 | Low-rate sensor data reply |
| BCMD_SENSORS_FETCH_AHPRS | 0x22 | HITL fetch sensor data from X-Plane |
| BCMD_SENSORS_REPLY_AHPRS | 0x23 | HITL sensor data reply |
| BCMD_SERVO_SETSERVOS | 0x28 | Set servo outputs to specified values |

Table 3.3: Bus command types and corresponding identification bytes.

ahead of time. This saves both bus bandwidth and processing cycles on each board's AVR.

A `BCMD_TELEM_REPLY` command is sent to reply to a `BCMD_TELEM_FETCH` request. The data field of a `BCMD_TELEM_REPLY` packet contains a list of data register code bytes that indicate which registers were read, each followed immediately by the corresponding data. Possible values for these codes are listed in table 3.4. Multi-byte data values are sent in big-endian order. The sizes of all data values are known beforehand at both the source and destination, so no data length bytes are necessary.

As an example, suppose that the radio board is programmed to reply to `BCMD_TELEM_FETCH` requests with the voltages on buses 0 and 1. When the GPC needs this data, the GPC sends a `BCMD_TELEM_FETCH` packet addressed to the radio board. The radio board replies in the form of a `BCMD_TELEM_REPLY` packet with a data section that begins with the `RADIO_REG_BUS0_VOLTAGE` register code, followed by two bytes of voltage data for bus 0, then by the `RADIO_REG_BUS1_VOLTAGE` register code, and finishing with two bytes of voltage data for bus 1.

| Register Name | Code Byte | Description |
|------------------------|-----------|--------------------------------|
| SERVO_REG_JOYSTICK | 0x00 | Servo joystick values (unused) |
| SERVO_REG_OUTPUT0 | 0x01 | Servo output 0 |
| SERVO_REG_OUTPUT1 | 0x02 | Servo output 1 |
| SERVO_REG_OUTPUT2 | 0x03 | Servo output 2 |
| SERVO_REG_OUTPUT3 | 0x04 | Servo output 3 |
| SERVO_REG_OUTPUT4 | 0x05 | Servo output 4 |
| SERVO_REG_OUTPUT5 | 0x06 | Servo output 5 |
| SERVO_REG_OUTPUT6 | 0x07 | Servo output 6 |
| SERVO_REG_OUTPUT7 | 0x08 | Servo output 7 |
| SERVO_REG_OUTPUT8 | 0x09 | Servo output 8 |
| SERVO_REG_OUTPUT9 | 0x0A | Servo output 9 |
| SERVO_REG_LV_VOLTAGE | 0x0B | Low-voltage battery voltage |
| SERVO_REG_LV_CURRENT | 0x0C | Low-voltage battery current |
| SERVO_REG_HV_VOLTAGE | 0x0D | High-voltage battery voltage |
| SERVO_REG_HV_CURRENT | 0x0E | High-voltage battery current |
| RADIO_REG_BUS0_VOLTAGE | 0x0F | Bus 0 voltage level |
| RADIO_REG_BUS1_VOLTAGE | 0x10 | Bus 1 voltage level |
| RADIO_REG_BUS2_VOLTAGE | 0x11 | Bus 2 voltage level |
| RADIO_REG_BUS3_VOLTAGE | 0x12 | Bus 3 voltage level |
| SERVO_REG_OVERRIDE | 0x13 | Manual override status |

Table 3.4: Data register codes used with BCMD_TELEM_FETCH and BCMD_TELEM_REPLY packets.

Radio Board Commands The radio board accepts a handful of commands for handling data transmitted and received over the radio link. The BCMD_SEND_DLPACKET command is used to send a downlink packet to the radio board for transmission. The data field for packets of this type consists of a single complete downlink packet, structured according to the radio downlink protocol (see section 3.5.2).

There are three packet types for processing packets received by the radio from the ground computer. When the GPC is ready to handle an uplinked packet, it sends a BCMD_MAILBOX_PEEK command to the radio board. The data field for packets of this type is empty. The radio then replies with a BCMD_MAILBOX_CONTENTS packet. The data field of this packet begins with the mailbox sequence number byte which is immediately followed by an uplink packet as specified by the uplink protocol (see section 3.5.3). If there are no uplink packets waiting,

the sequence number field in the data section of the `BCMD_MAILBOX_CONTENTS` reply packet will have the value `0x00` and no uplink packet data will follow it. If the GPC receives the `BCMD_MAILBOX_CONTENTS` packet correctly, it can then send a `BCMD_MAILBOX_POP` command to remove the uplink packet from the mailbox queue. The data field of the `BCMD_MAILBOX_POP` command is one byte in size and consists only of the sequence number of the packet to remove.

For more information on the radio mailboxing system, see section 3.2.4.

Sensors Board Commands There are four packet types associated with the retrieval of data from the sensors board. The `BCMD_SENSORS_FETCH_HIRATE` packet type is sent by the GPC to the sensors board to retrieve high-rate sensor data, such as IMU measurements. Similarly, the `BCMD_SENSORS_FETCH_LORATE` packet type is sent to retrieve low-rate sensor data, such as GPS positioning information. The data fields for packets of these types are empty.

The sensors board replies to packets of type `BCMD_SENSORS_FETCH_HIRATE` with ones of type `BCMD_SENSORS_REPLY_HIRATE`. The layout of the data field for these packets is given in table 3.5. Sensor data values are stored in the data section in little-endian order. The units of the values were chosen to match the input expectations of the autopilot algorithm (see section 3.3) and are scaled to preserve a reasonable number of significant digits while remaining within the confines of variables of integer-type.

A `BCMD_SENSORS_REPLY_LORATE` packet is used to reply to a `BCMD_SENSORS_FETCH_LORATE` request. Since low-rate sensor data consists entirely of GPS data at this time, the layout of the data field for a `BCMD_SENSORS_REPLY_LORATE` packet is identical to that for GPS data encoded in Garmin's proprietary binary format (see section 3.1.4). For convenience, this format is presented in table 3.6, but for more detail, the user should consult the Garmin Device Interface Specification datasheet [1]. The GPS data is stored in the packet in little-endian order, exactly as it comes out of the GPS.

| Field Type | Name | Description |
|------------|----------|--|
| int16 | accelX | <i>x</i> -acceleration in cm/s ² |
| int16 | accelY | <i>y</i> -acceleration in cm/s ² |
| int16 | accelZ | <i>z</i> -acceleration in cm/s ² |
| int16 | gyroX | Pitch-up rate in mrad/s |
| int16 | gyroY | Roll-right rate in mrad/s |
| int16 | gyroZ | Yaw-right rate in mrad/s |
| int16 | magX | <i>x</i> -direction magnetometer output (unitless) |
| int16 | magY | <i>y</i> -direction magnetometer output (unitless) |
| int16 | magZ | <i>z</i> -direction magnetometer output (unitless) |
| int16 | airspeed | Pitot pressure sensor reading in dPa |
| uint24 | baro | Air pressure in cPa |
| int16 | temp | Temperature in tenths of degrees centigrade |

Table 3.5: Layout of the data field for BCMD_SENSORS_REPLAY_HIRATE packets. Note that the sensor values are stored in little-endian order.

Servo Board Commands The BCMD_SERVO_SETSERVOS command is issued by the GPC to set the servo outputs in accordance with the decisions made by the autopilot algorithm. The data field contains the exact servo values to be set, stored as four 16-bit unsigned integers in little endian order. The exact layout of the data field is shown in table 3.7.

ARM–GPC AVR Commands There are two special commands used privately between the ARM processor and AVR microcontroller on a GPC board. Since they are used between chips on the same board, packets of these types are not transmitted over the bus but are wrapped using the bus protocol headers anyway to avoid the need to design a special protocol just for these types of transactions.

The ARM uses a BCMD_GPCAVR_WHOAMI request to discover the ID number of the board it is on, which is stored in the EEPROM on the AVR. The data field for packets of this type is empty. The GPC AVR replies with a BCMD_GPCAVR_BOARDID packet, which has a one-byte data field to hold the board ID.

| Field Type | Name | Description |
|------------|-----------|----------------------------------|
| float32 | alt | Ellipsoid altitude in m |
| float32 | epe | Estimated position error in m |
| float32 | eph | Position error, horizontal in m |
| float32 | epv | Position error, vertical in m |
| uint16 | fix | Type of position fix |
| float64 | gps_tow | GPS time of week in s |
| float64 | lat | Latitude in rad |
| float64 | lon | Longitude in rad |
| float32 | lon_vel | Longitude velocity in m/s |
| float32 | lat_vel | Latitude velocity in m/s |
| float32 | alt_vel | Altitude velocity in m/s |
| float32 | msl_hght | Height above mean sea level in m |
| int16 | leap_sec | UTC leap seconds |
| uint32 | grmn_days | Garmin days (since 31 Dec 1989) |

Table 3.6: Layout of the data field for BCMD_SENSORS_REPLAY_LORATE packets. Taken from the Garmin Device Interface Specification [1].

| Field Type | Name | Description |
|------------|----------|------------------------|
| uint16 | throttle | Throttle servo setting |
| uint16 | aileron | Aileron servo setting |
| uint16 | elevator | Elevator servo setting |
| uint16 | rudder | Rudder servo setting |

Table 3.7: Layout of the data field for BCMD_SERVO_SETSERVOS packets. Note that the values must be sent in little-endian order.

HITL-Only Sensors Board Commands There are also two special packet types used for operating the system in HITL-testing mode, in which the GPC receives its sensors data from a computer running X-Plane instead of from a sensors board. The GPC requests this data with a BCMD_SENSORS_FETCH_AHPRS command. The data field for packets of this type is empty. The computer replies with a BCMD_SENSORS_REPLY_AHPRS packet, which is structured as showed in table 3.8. The data is stored in the reply packet in little-endian order.

| Field Type | Name | Description |
|------------|----------|-------------------------------------|
| float32 | Gnormal | Normal acceleration in G's |
| float32 | Gaxial | Axial acceleration in G's |
| float32 | Gside | Side acceleration in G's |
| float32 | Q | Pitch rate in rad/s |
| float32 | P | Roll rate in rad/s |
| float32 | R | Yaw rate in rad/s |
| float32 | pitch | Pitch angle in rad |
| float32 | roll | Roll angle in rad |
| float32 | hdg | Heading in rad |
| float64 | lat | Latitude in rad |
| float64 | lon | Longitude in rad |
| float32 | elev_msl | Elevation above mean sea level in m |
| float32 | hpath | Horizontal pat in rad |
| float32 | Vtrue | Velocity relative to ground in m/s |
| float32 | VVI | Vertical velocity indicator in m/s |

Table 3.8: Layout of the data field for BCMD_SENSORS_REPLY_AHPRS packets.

3.5.2 Radio Downlink Protocol

The radio downlink protocol governs communications sent by the plane down to the ground computer. In particular, it defines the structure of telemetry packets.

Packet Structure Like bus packets, downlink packets can be of variable length to handle data payloads of varying sizes. The layout of a downlink packet is illustrated in figure 3.4.

The packet header begins with a two-byte protocol signature. After the signature is a byte that specifies the size of the data section in bytes. Since this field is one byte, the data section of a downlink packet may be anywhere from 0 to 255 bytes in size. The size byte is followed by a two-byte CRC checksum, sent in big-endian order. Like the CRC checksums used in the bus protocol, the checksum is used by the ground computer to check for transmission errors in received packets. After the CRC is a byte that specifies the packet type, analogous to the command byte for bus packets. The packet type byte completes the header, and the rest of the packet consists of data.

Note that, unlike the bus protocol, the downlink protocol does not reserve any special bytes for frame delimiters, etc. These constructs are defined handled by separate protocol layer used for communication with the radio board’s XTend radio module (see sections 3.1.3 and 3.2.4). Before being sent to the radio, downlink packets are wrapped using the XTend protocol framework. At the receiving end, received packets exit the radio encased in the XTend headers, which are stripped away to expose the underlying downlink packet. For more information about the XTend protocol, see the datasheet for the XTend radio module [15].

| | | | | |
|------------|--------------------|-------------|-----------|-----------|
| Bit Offset | 0-7 | 8-15 | 16-23 | 24-31 |
| 0 | Protocol Signature | | Data Size | CRC16 MSB |
| 32 | CRC16 LSB | Packet Type | Data | |
| 64+ | Data | | | |

Figure 3.4: Byte structure of a downlink packet.

Protocol Signature Protocol signature bytes were added to the downlink header in anticipation that the downlink protocol would evolve in the future. The signature bytes encode the version of the downlink protocol being used. These bytes allow users to easily distinguish between sets of hardware using different versions of the downlink protocol.

Packet Types There are three types of downlink packets. These types and the corresponding values for the packet type field in the downlink packet header are given in table 3.9. Like for bus packets, since the system uses few of the possible values for the packet type byte, it is easy to expand the system to accommodate more packet types by defining new bytes as needed.

| Packet Type | Byte | Description |
|-------------------|------|--------------------------------------|
| DL_TYPE_TELEMETRY | 0x40 | Telemetry packet |
| DL_TYPE_STEP_READ | 0x42 | Read flight plan step from memory |
| DL_TYPE_PTR_READ | 0x44 | Currently executing flight plan step |

Table 3.9: Downlink packet types and corresponding identification bytes.

Telemetry Packets The most common type of downlink packet is the telemetry packet, indicated by a `DL_TYPE_TELEMETRY` packet type byte. The structure of the data field for a telemetry packet is similar to that for a `BCMD_TELEM_REPLY` bus packet: it consists of a list of telemetry channel codes, each immediately followed by a piece of telemetry data. Multi-byte telemetry data values are stored in the packet in big-endian order. Possible values for the telemetry channel codes are given in table 3.10. Most of these codes are currently used by the existing system, but a few, such as the `CH_MOTOR_TACH` and `CH_MOTOR_CURRENT` channels, have been added in anticipation of additional features (a motor tachometer and current monitor, in the case of the two explicitly mentioned).

As an example, a telemetry packet containing all accelerometer data would have a data field that begins with the `CH_ACCEL_AXIS1` marker, followed by two bytes of data for accelerometer axis 1, MSB first. Next would come the `CH_ACCEL_AXIS2` marker, followed by two bytes of data for accelerometer axis 2. Following this would be the `CH_ACCEL_AXIS3` marker and the data for accelerometer axis 3.

| Channel | Byte | Description |
|--------------------------------|------|------------------------------|
| <code>CH_HVBATT_VOLTAGE</code> | 0x00 | High-voltage battery voltage |
| <code>CH_LVBATT_VOLTAGE</code> | 0x01 | Low-voltage battery voltage |
| <code>CH_HVBATT_CURRENT</code> | 0x02 | High-voltage battery current |
| <code>CH_LVBATT_CURRENT</code> | 0x03 | Low-voltage battery current |
| <code>CH_ACCEL_AXIS1</code> | 0x04 | Accelerometer axis 1 |
| <code>CH_ACCEL_AXIS2</code> | 0x05 | Accelerometer axis 2 |
| <code>CH_ACCEL_AXIS3</code> | 0x06 | Accelerometer axis 3 |
| <code>CH_GYRO_AXIS1</code> | 0x07 | Gyroscope axis 1 |
| <code>CH_GYRO_AXIS2</code> | 0x08 | Gyroscope axis 2 |
| <code>CH_GYRO_AXIS3</code> | 0x09 | Gyroscope axis 3 |
| <code>CH_MAG_AXIS1</code> | 0x0A | Magnetometer axis 1 |
| <code>CH_MAG_AXIS2</code> | 0x0B | Magnetometer axis 2 |
| <code>CH_MAG_AXIS3</code> | 0x0C | Magnetometer axis 3 |
| <code>CH_AIRSPEED</code> | 0x0D | Airspeed reading |
| <code>CH_MOTOR_TACH</code> | 0x0E | Motor tachometer |

Table 3.10: Telemetry channel types and corresponding marker bytes.

| Channel | Byte | Description |
|-------------------------------|------|--|
| CH_MOTOR_CURRENT | 0x0F | Motor current draw |
| CH_SERVO_OUT0 | 0x10 | Servo output 0: Throttle |
| CH_SERVO_OUT1 | 0x11 | Servo output 1: Ailerons |
| CH_SERVO_OUT2 | 0x12 | Servo output 2: Elevator |
| CH_SERVO_OUT3 | 0x13 | Servo output 3: Rudder |
| CH_SERVO_OUT4 | 0x14 | Servo output 4: Manual Override |
| CH_SERVO_OUT5 | 0x15 | Servo output 5 |
| CH_BUS0_VOLTAGE | 0x16 | Bus 0 voltage |
| CH_BUS1_VOLTAGE | 0x17 | Bus 1 voltage |
| CH_BUS2_VOLTAGE | 0x18 | Bus 2 voltage |
| CH_BUS3_VOLTAGE | 0x19 | Bus 3 voltage |
| CH_TEMPERATURE | 0x1A | BMP085 temperature reading |
| CH_RC_CHAN1 | 0x20 | Received RC channel 1 |
| CH_RC_CHAN2 | 0x21 | Received RC channel 2 |
| CH_RC_CHAN3 | 0x22 | Received RC channel 3 |
| CH_RC_CHAN4 | 0x23 | Received RC channel 4 |
| CH_RC_CHAN5 | 0x24 | Received RC channel 5 |
| CH_RC_CHAN6 | 0x23 | Received RC channel 6 |
| CH_BUS1ERRCNT | 0x30 | Bus 1 packet error count |
| CH_BUS2ERRCNT | 0x31 | Bus 2 packet error count |
| CH_BUS3ERRCNT | 0x32 | Bus 3 packet error count |
| CH_BUS4ERRCNT | 0x33 | Bus 4 packet error count |
| CH_ERR_SERVO_TELEM_NOREPLY | 0x40 | Servo data no-reply counts |
| CH_ERR_RADIO_TELEM_NOREPLY | 0x41 | Radio data no-reply counts |
| CH_ERR_RADIO_MAILBOX_NOREPLY | 0x42 | Radio mailbox no-reply counts |
| CH_ERR_SENSORS_HIRATE_NOREPLY | 0x43 | Sensors high-rate data no-reply counts |
| CH_ERR_SENSORS_LORATE_NOREPLY | 0x44 | Sensors low-rate data no-reply counts |
| CH_ERR_SENSORS_AHPRS_NOREPLY | 0x45 | AHPRS no-reply counts (HITL only) |
| CH_RS_ACCELX_OUT | 0x50 | Count of x-accelerometer outliers |
| CH_RS_ACCELY_OUT | 0x51 | Count of y-accelerometer outliers |
| CH_RS_ACCELZ_OUT | 0x52 | Count of z-accelerometer outliers |
| CH_RS_GYROX_OUT | 0x53 | Count of x-gyroscope outliers |
| CH_RS_GYROY_OUT | 0x54 | Count of y-gyroscope outliers |
| CH_RS_GYROZ_OUT | 0x55 | Count of z-gyroscope outliers |
| CH_RS_MAGX_OUT | 0x56 | Count of x-magnetometer outliers |
| CH_RS_MAGY_OUT | 0x57 | Count of y-magnetometer outliers |
| CH_RS_MAGZ_OUT | 0x58 | Count of z-magnetometer outliers |
| CH_RS_AIRSPEED_OUT | 0x59 | Count of airspeed outliers |
| CH_RS_BARO_OUT | 0x5A | Count of barometer outliers |
| CH_RS_TEMP_OUT | 0x5B | Count of temperature outliers |

Table 3.10: Telemetry channel types and corresponding marker bytes.

| Channel | Byte | Description |
|----------------------|------|--------------------------------------|
| CH_EXT_AIR_TEMP | 0x80 | External air temperature |
| CH_GPS_FIX_STATUS | 0x81 | GPS fix status |
| CH_MANUAL_OVERRIDE | 0x82 | Manual override status, 1 = override |
| CH_FP_POINTER | 0x90 | Flight plan pointer |
| CH_RED_VOTING_MATRIX | 0x91 | Redundancy failure voting matrix |
| CH_RED_WORKING_SET | 0x92 | Redundancy working set |
| CH_PRESS_ALT | 0xC0 | Pressure altimeter |
| CH_GPS | 0xC1 | GPS sentences |
| CH_STATE_LAT | 0xD0 | State vector: latitude (degrees) |
| CH_STATE_LON | 0xD1 | State vector: longitude (degrees) |
| CH_STATE_ALT | 0xD2 | State vector: altitude (meters msl) |
| CH_STATE_HEADING | 0xD3 | State vector: heading (radians) |
| CH_STATE_PITCH | 0xD4 | State vector: pitch (radians) |
| CH_STATE_ROLL | 0xD5 | State vector: roll (radians) |
| CH_STATE_VEL_X | 0xD6 | State vector: x-velocity |
| CH_STATE_VEL_Y | 0xD7 | State vector: y-velocity |
| CH_STATE_VEL_Z | 0xD8 | State vector: z-velocity |
| CH_STATE_GNDSPD | 0xD9 | State vector: ground speed |
| CH_STATE_AIRSPD | 0xDA | State vector: air speed |
| CH_RADIO_ERRCNT | 0xE0 | Radio error count |
| CH_FP_STEP | 0xF0 | Flight plan step |
| CH_GLIDE_HDG | 0xF1 | Desired glide heading |

Table 3.10: Telemetry channel types and corresponding marker bytes.

Flight Plan Query Replies The other types of downlink packets are used as replies to queries from the ground computer about the state of the flight plan currently stored on the GPC. The DL_TYPE_PTR_READ packet type is used to reply to uplink packets of type UL_TYPE_PTR_READ (see section 3.5.3) and have a data section consisting of a single byte, which holds the number of the current step.

Similarly, the DL_TYPE_STEP_READ packet type is used to reply to uplink packets of type UL_TYPE_STEP_READ (see section 3.5.3). The data section of a DL_TYPE_STEP_READ packet consists of a flight plan step, laid out as specified by the flight plan mechanism (see section

3.3.3) followed by a single byte that is the number of the step that was read.

For more information about flight plans, see section 3.3.3.

3.5.3 Radio Uplink Protocol

The radio uplink protocol specifies the structure of communications sent from the ground computer to the UAV. Importantly, it dictates the procedure for uploading flight plans to the plane.

The chief reason for having a different protocol to govern uplink operations instead of just using the downlink protocol for bidirectional communication is security. Uplinked commands need to be received by the UAV securely and reliably in order to ensure that the plane behaves as desired and is not “hijacked” by unwanted third parties. This entails the addition of a few extra fields to the packet header, as described below. By contrast, downlink communications need as much bandwidth as possible so that telemetry may be transmitted to the ground at the fastest possible rate. Thus, for downlink packets, keeping the packet overhead to a minimum is desirable.

Packet Structure The structure of an uplink packet is depicted in figure 3.5. The uplink packet header begins with a two-byte protocol signature, followed by a 32-bit message authentication code (MAC). This is succeeded by a 32-bit sequence number, and the header is completed with a byte that identifies the type of uplink packet. The rest of the uplink packet contains data pertinent to the packet type.

Note that, unlike downlink packets, uplink packets do not have a field for specifying data size. The data fields of all uplink packet types have fixed, known sizes, and so sending a size byte along with the packet is unnecessary.

Protocol Signature Like for the downlink protocol, uplink packets have a two-byte protocol signature field that specifies the version of the uplink protocol in use. See the paragraph in

| Bit Offset | 0-7 | 8-15 | 16-23 | 24-31 |
|------------|--------------------|------|-----------------|-------|
| 0 | Protocol Signature | | MAC32 | |
| 32 | MAC32 | | Sequence Number | |
| 64 | Sequence Number | | Packet Type | Data |
| 96 | Data | | | |

Figure 3.5: Byte structure of an uplink packet.

protocol signatures in section 3.5.2 for more information.

Message Authentication Code The uplink protocol provides a mechanism for verifying the authenticity of received uplink commands in the form of a 32-bit message authentication code (MAC) attached to each uplink packet. Matching encryption keys are stored on the UAV and on the ground computer. When the ground computer sends an uplink packet, it uses its key and cryptographic hashing algorithm to produce a 32-bit digest of the contents of the uplink packet and attaches this digest to the packet as the MAC. When the plane receives an uplink packet, it uses its key and the same hashing algorithm to produce its own digest of the uplink contents, which is then compared to the MAC sent with the packet. If the values match, the packet is very likely to have come from the ground computer.

In addition to being used for authenticity verification, the MAC also plays the role of the 16-bit CRC checksum in the downlink protocol. If a transmission error occurs, the digest computed onboard the plane will very probably not match the sent MAC, enabling such errors to be detected.

Sequence Numbering Every uplink packet sent to the plane from the ground computer is given a 32-bit sequence number, analogous to sequence numbers in TCP/IP packets. The sequence number plays two roles. First, it can be used to detect lost transmissions. If the plane receives two uplink packets which do not directly follow each other in sequence (i.e., have sequence numbers that differ by more than 1), then there must have been a packet transmitted in between them that the plane did not receive. The plane can then send a packet

to the ground computer requesting re-transmission of the lost data (though this has not yet been implemented). This is especially important for ensuring the integrity of flight plan upload (see section 3.3.3), since flight plan steps must be updated in a specified order.

Second, the sequence number bolsters system security by guarding against potential packet replay attacks. If uplink packets were not numbered, an attacker could conceivably “sniff” an uplink command out of the air and then re-transmit it. This could have disastrous effects if the plane carries out the instructions contained within the re-transmitted packet, such as overwriting the current flight plan. With the sequence number, the plane can know if a packet has already been transmitted once and ignore it if so.

Packet Types Presently, there are two main categories of uplink packet: joystick packets and packet types that are used for changing the plane’s onboard flight plan. The type of an uplink packet is determined by its packet type field. Possible values for the packet type byte are given in table 3.11. Just as for bus and downlink packets, new uplink packets can be defined by specifying new values of the packet type byte.

| Packet Type | Byte | Description |
|-------------------|------|--|
| UL_CMD_JOYSTICK | 0x10 | Human-input joystick control |
| UL_CMD_STEP_WRITE | 0x20 | Write flight plan entry |
| UL_CMD_STEP_READ | 0x21 | Read back flight plan entry |
| UL_CMD_PTR_WRITE | 0x22 | Set current flight plan step |
| UL_CMD_PTR_READ | 0x23 | Read which flight plan step is currently executing |

Table 3.11: Downlink packet types and corresponding identification bytes.

Joystick Packets Joystick packets have type UL_CMD_JOYSTICK and are sent when the plane is being flown under PC joystick control from the ground computer. The data section of these packets contain servo output values to be used directly by the servo board for controlling the servos. The servo values are stored as 16-bit unsigned integers in big-endian order and are laid out as shown in table 3.12.

| Field Type | Name | Description |
|------------|----------|------------------------|
| uint16 | throttle | Throttle servo setting |
| uint16 | aileron | Aileron servo setting |
| uint16 | elevator | Elevator servo setting |
| uint16 | rudder | Rudder servo setting |

Table 3.12: Layout of the data field for UL_CMD_JOYSTICK packets.

Flight Plan Packets There are four types of packets used to for reading and changing the plane’s on-board flight plan (see section 3.3.3) from the ground computer. Packets of type UL_CMD_PTR_READ are sent to request the number of the flight plan step that the plane is currently executing. The data section for such packets is empty. Similarly, UL_CMD_PTR_WRITE packets are used to set the plane to execute a specific step in the current flight plan. The data field for packets of this type consists of a single byte: the number of the step to begin executing.

UL_CMD_STEP_READ commands are sent to read back the flight plan entry for a specific flight plan step. The data field for such packets contains one byte that holds the number of the step to read back. Likewise, UL_CMD_STEP_WRITE commands can be used to write a new entry to the onboard flight plan. The data section of UL_CMD_STEP_WRITE packets consists of a flight plan step laid out as specified by the flight plan mechanism (see section 3.3.3) followed immediately by one byte indicating the step to modify.

3.6 Prototype Aircraft Hardware

3.6.1 Airframe

In order to simplify development, a popular oversized hobby R/C aircraft was chosen to carry the avionics package. This aircraft, the *Senior Telemaster* from Hobby-Lobby, is a high-wing monoplane with a 7 foot 10 inch wingspan, conventional landing gear, and lifting tail. In the absence of the avionics package, the plane weighs about 11 pounds including motor, servos,

battery, R/C receiver, and landing gear.

Features The *Senior Telemaster* is an exceptionally stable, slow flying, and generally well behaved aircraft, and this simplified autopilot development considerably. The fuselage of the plane is very open and has significant free space for payload, thus allowing flexibility in positioning the avionics and auxiliary sensors. The plane is quite light for its size, while still remaining relatively durable.

Limitations The chosen aircraft does suffer from two limitations: high parasite drag and the conventional landing gear. The high drag is not particularly important for testing the avionics package, but renders the plane quite unsuitable for high altitude flights or flights lasting over an hour. The conventional landing gear complicates the takeoff roll because it makes the plane unstable in yaw. This effect is particularly noticeable on grass fields. The small tail wheel is also not very stable and is easily damaged, furthermore, damage to the tail wheel tends to propagate up into the tail assembly.

Revision History The first prototype, the “OWLbatross”, was built from a kit by Mr. Brockman when he was in high school. This prototype was modified to have a tricycle landing gear with a steerable nose wheel instead of a conventional landing gear. This modification increased weight and drag but greatly improved taxi and takeoff controllability. The first prototype also had only one servo for controlling both ailerons. Although this decreased drag, it required the servo to be larger and specialized, as well as decreased the volume available for payload. The first prototype also had only one elevator surface driven by one servo.

The fuselage of the “OWLbatross” was destroyed during the first test of the sensor board because the center of gravity was too far aft. Wind gusts were a contributing factor in the crash. The motor, batteries, servos, and avionics survived the crash largely unharmed. The wing was slightly damaged and was retained as a spare.

Because of the time and expense of assembling and covering the balsa airframe, a second backup prototype, the “FOWLcon”, was purchased in an almost-ready-to-fly (ARF) condition from the manufacturer. Replacement parts for the ARF prototype are quite inexpensive, with the entire fuselage costing a mere \$40. Several spare fuselages and tail assemblies, as well as one spare wing, are kept on hand in case the originals are damaged in a crash.

After the destruction of the first prototype, it was determined that modifying subsequent prototypes to have a tricycle landing gear would take too much time and would distract from the immediate focus of the project, so the second (and current) prototype retains its stock conventional landing gear.

Repairs Cyanoacrylate glue was used for the vast majority of the wood assembly and repair. The entire fuselage and wings were originally covered with an inexpensive low-temperature mylar coating from the factory. Where this has been damaged, it has been replaced with superior high-temperature “Super Monokote” from Topflite. Special care had to be taken to avoid burning the original covering at the interfaces between the original covering and the patches.

Landing Gear The stock landing gear has several inadequacies which have been addressed with varying degrees of success. The foam main wheels shipped with the kit are too easily damaged and have been replaced by DuBro rubber wheels. The tail wheel has likewise been replaced – although the current tailwheel is sturdier, it is not currently connected to the rudder and thus is not steerable, limiting low-speed taxi steering.

3.6.2 Power System

Propulsion for the plane is provided by an electric brushless motor from AXI, the 4130/20. This motor is capable of delivering over $1000W$ of power to the propeller when equipped with an

8S1P Lithium-polymer battery and the correct 14x10 propeller. The smaller 7S1P 5000mAh battery actually used decreases thrust somewhat, but the motor remains greatly overpowered, causing the plane to be able to take off in less than 15 meters with no wind and full payload.

A smaller motor, the 4120/16, was also acquired, but the lighter weight of the motor made managing the center of gravity of the plane more difficult, so its use was discontinued.

As of the time of this report, the 4130/20 motor makes a high-pitched whine when operated above 80% throttle setting. This may indicate that the motor was damaged slightly during the crash which destroyed the first prototype's fuselage.

Since the motor is AC, the DC voltage from the battery must be converted with a JETI motor controller rated for 70 amps. This motor controller is connected to the servo control board, which sees it as a normal servo, thus allowing the avionics to control the throttle.

Alternative Propulsion The chosen electric motor is less powerful and has significantly less range than the glow-fuel motor that the plane was originally designed for, a 0.60 cubic inch 2-cycle motor capable of generating 1.8 horsepower. The electric motor was chosen because it is much safer and more reliable than the glow-fuel motor. The glow-fuel mixture contains about one-third castor oil for lubrication, a considerable amount of which ends up coating the wings and tail of the plane with sludge after a flight. Starting the glow-fuel motor requires standing precariously close to the propeller, which is smaller and runs at twice the RPM of the electric motor. The glow-fuel motor's carburetor, located about an inch behind the spinning propeller, regularly requires hand adjustment while running. The glow-fuel motor also has a nasty tendency to stall while climbing if the carburetor is incorrectly adjusted; the procedure for avoiding this is to hold the plane straight up in the air and apply full power to check for proper operation.

3.6.3 Actuators

The plane has four flight controls: ailerons to control roll rate, elevators to adjust angle of attack, throttle for climb rate, and rudder for ground steering and to compensate for the adverse yaw effect caused by the ailerons. The current prototype has a separate servo for each aileron; they are wired together to form a single PCM channel for control. Throttle control is provided by the motor controller as described earlier. The rudder is controlled by a single servo, while the elevator is split into two independent sections, each connected to its own servo. Like the aileron servos, the two elevator servos are wired together to form a single PCM channel. All of the servos are of the same standard model, the Hitec HS-322HD.

The servos are connected to the appropriate flight control surface with control rods. The control rods for the ailerons are metal with plastic clevises connecting them to plastic control horns on both ends. Small sections of fuel tubing have been used to secure the plastic clevises. The elevator control rods are carbon fiber, while the rudder control rod has been replaced with steel to prevent flutter. Both elevator and rudder control rods are connected to plastic control horns on both ends with metal clevises secured with metal locking clips.

The stock radio control receiver used for manual override is the 2.4 GHz Spektrum AR6200. Because of limited servo cable length and the need for the servo board to be between the manual override receiver and the servos, the receiver is located right next to the servo board. The receiver has a remote which is located in the tail assembly and is oriented at right angles to the main receiver to improve reception.

3.6.4 Avionics Mounting

The avionics suite has been mounted in the plane in a crude but effective manner. The main backplane has been glued to square balsa dowels which have in turn been glued to the bottom of the main compartment. The rest of the modules plug into the backplane, while two notched

balsa sticks glued to the sides of main compartment serve to prevent the modules, especially the sensors boards, from moving. The modules are not at present held in place from the top, since the connectors to the backplane seem to be stiff enough.

The servo board is installed in the slot closest to the front of the plane to allow space for the large number of servo and receiver wires, as well as to shorten the wires running to the primary and secondary batteries in the battery compartment. The positioning of the other modules is somewhat arbitrary, although keeping the telemetry radio antenna connection far from the servo board and servo wires helps decrease servo jitter from EMI.

3.6.5 Non-Integrated Sensors

In the present configuration, the plane has two Garmin 18x LVC OEM GPS units for navigation. One of these is integrated into the wing, while the other is located above the main battery in the battery compartment behind the motor. The GPS units are intentionally kept far apart to avoid oscillator interference. The units are secured from moving with double-stick foam tape.

The pitot-static tubes extend from holes drilled in each wing about half-way to the wing tips. This positioning keeps them out of the propeller wash which would impair accuracy. The pitot-static tubes are glued into the wings and are each connected to two lengths of medical tubing. This flexible tubing runs along the inside of the wing and emerges from the wing in the center where it can be connected directly to the sensors board.

3.7 Future Expansion

When considering the modular architecture used for this project, thought was given to implementing full redundancy, even though this is outside the scope of the project for this year. After considering the design of current NASA space systems, including manned vehicles like the Space Shuttle [9] [17] and autonomous probes like the Mars Reconnaissance Orbiter [4] [5]

[6]. Other inspiration came from the redundant systems used on commercial airliners [18]. This plan calls for redundant placement of all of the boards, rather than only the sensors. This system would resemble the one shown in 2.1.

Servo Boards With the design of the servo board, it should be possible to drop in multiple boards, although this requires redundant external control surfaces, which significantly adds to the weight of the airframe. Multiple power supplies should be supported transparently.

Radio Boards If the code for the bus master is changed somewhat, it should be possible to add a second radio board in a failover capacity, where only one functions until failure is reported. With the radio board, loss of signal can be interpreted as a failure, and the backup system can be activated.

GPC Boards With significant software upgrades, up to four GPC boards could be expected to work together in lockstep operation, based on the design of the Space Shuttle [9] flight computer architecture. In this situation, each of the GPC boards controls a bus, and operation proceeds with a single bus until the non-primary boards detect an error, and then disable the faulty GPC.

Four GPC boards were selected to provide failsafe, fail-operational behavior. Specifically, the first failure is easily detected as a difference between one computer and the other three. Note that two pairs of computers reaching two separate conclusions is extremely unlikely because it depends on at least two computers failing in identical ways. After one GPC has been marked inoperative, the remaining three boards still form a voting set, and can correctly detect errors. After a second failure, the system is reduced to two working boards, and is forced to depend on heuristics to determine which board is faulty if the two differ.

3.8 Errata and Revision History

The electrical hardware within the aircraft has undergone three major revisions.

3.8.1 Hardware Revision I

The first revision of the hardware was ordered in July 2010. Only the servo board was ordered and populated. This allowed the team to produce initial firmware, implementing the manual override, and allowed initial flight testing.

The following is a complete list of known errata for Servo Rev 01:

- All Schottky diode silkscreens (D40, D50, D60, D70) show the line at the wrong end of the diode.
- The SOT23-6 footprints (U30, U31) do not have any orientation marker.
- The power jumper section could be improved by adding labels to indicate which side is LV_BUS and which HV_BUS.
- The servo wire holes (S_IN1 thru S_IN6, LV_BATT) are too small for the 22 gauge stranded wires to easily fit in. Also, putting the wires straight in like that may lead to early stress breaking.
- The ground plane vias near U40 and U60 should probably be filled-in style, instead of thermal relief style.
- The HV battery connector should have reverse polarity protection in the form of either a crowbar diode and fuse, crowbar zener diode and fuse, or forward bias Schottky diode.
- Current sense outputs have no low-pass filtering.

- There is no good reason not to add more bypass capacitors to the input of U21 and the outputs of U21 and U22.
- To increase safety, a different connector should be used for HV_BATT which has more physical spacing between the pins.
- **Board fails to power up with just the HV battery.** This problem only manifests if you try to transition from fully off (no LV battery, no external power on buses 0-3) to connecting the HV battery input. The HV_Shutdown line is held low by the Vcc static protection diodes on the ATxmega32A4. As a workaround, cut the HV_Shutdown trace between the XMEGA and the LM2676S-12 (not yet tested). In the future, this straight wire will be replaced with a MOSFET and a gate pull-down resistor.
- LED missing.

3.8.2 Hardware Revision II

The second revision of the hardware reduced the height of all of the boards to ease fitting them into the aircraft. All of these boards were built and tested. An improper option in one of the software packages resulted in several mis-labelings of components on the silkscreen.

It was discovered that the yaw gyro on the sensor board was ordered incorrectly, and the desired part was no longer available, which required the creation of the third revision. The remainder of this section documents known errata with this series of boards.

Backplane 02

- Mounting holes in bottom (try not to expand total area).
- Missing board revision text.
- Additional timing lines (2) would be useful for synchronization.

Servo 02

- Silkscreen labels for R87 and R89 are swapped in location.

Sensors 02

- Silkscreen for C4A sucks.
- R81, R82, R83, and R84 should be moved right near U5 to reduce EMI pickup concerns.
- Silkscreen for R54 and C55 are reversed. (Accelerometer channel Y)
- ATXMEGA32A4 errata number 7 applies to the ADC: several ADC samples must be junked after switching the input MUX.
- An analog output version of the LY530AL chip is available as the LY530ALH, which could be used with the other analog inputs on the AVR.
- U41 (LY530AL) has CS pin 10 connected to ground instead of Vdd_IO. This forces the chip into SPI mode, when it should be in I2C mode.
- C81 needs to be low-ESR.
- GPS PPS line should be accessible (ideally through backplane timing lines).

GPC 01

- The USB connector is placed backwards on the board.
- The mounting holes on the USB connector are too small.
- Silkscreen labels for R34, R30, and R35 are obscured by vias.
- TST line is not accessible via jumper.

- Need to allocate a pin on the ARM for the AVR to use to trigger an interrupt upon complete receipt of a bus packet.

3.8.3 Hardware Revision III

The third revision of the hardware adds mounting holes to the circuit boards, and fixes the yaw gyro issue in the servo board by replacing it with the analog sensor that was mistakenly ordered.

Backplane 03

- Labels should be added to the bus connectors to simplify use.

Sensors 03

- The EOC pin on the Bosch BMP085 pressure sensor is not connected to anything. Hooking up to a pin on the AVR would save the need to use a timer/counter to delay for 25.5 ms while waiting for the sensor to complete a conversion.

GPC 02

- The numbering of GPC boards is confusing. This originated because the second revision of the hardware was the first to include the GPC board. In the future, the numbers should be aligned.

4 Testing and Results

4.1 Basic Functionality Testing

4.1.1 Electrical Testing

The electrical connectivity of each circuit board was thoroughly checked after assembly with a digital multimeter (DMM) before the board was ever powered up for the first time. This allowed the team to detect electrical problems due to open or shorted traces before they could damage any of the sensitive chips.

Once a board passed its check for opens and shorts, it was attached to a backplane and powered up. The DMM was again used to verify the voltage levels at the output of each board's power regulators were correct. If they were, then the team would attempt to program the board's AVR microcontroller with its assigned board ID (see section 3.2) and then with the main set of firmware. If the programming was successful, the board was then checked to ensure that all features of the current version of the firmware worked properly.

4.1.2 Software Testing

The team performed basic testing of the software functionality on an ad-hoc basis, vetting out each new feature as it was added. This was typically accomplished by having each board being tested print debug text to an unused system bus and using the serial terminal program `minicom` to read it out on the PC.

Once the bus protocol was developed, the need arose to test the ability of the boards to reply correctly to bus packets addressed to them. Before the development of the GPC firmware, this was usually accomplished using some simple test programs written for the PC that would inject packets onto the system bus. The board's reply would then be captured using

`minicom` or the `busmonitor` or `busmonitor2` programs (see section A.6). Once the basic GPC firmware was written and the logging features of the Houston ground software were developed, these programs were set aside in favor of using the GPC board to send packets and Houston to monitor the replies.

4.1.3 Sensor Redundancy Testing

Ground testing of the sensor redundancy was performed by using the GPC's debug console to continuously print information about the sensor data it had received and how it was processing it. The debug stream was then carefully checked to make sure that the results of its processing conformed to the desired behavior outlined in section 3.3.2. In particular, the team was able to confirm the correct operation of the outlier rejection procedure by watching the GPC identify and set aside wild values from one of the noisier pitch gyroscopes on one of the sensors boards.

The team also performed tests in which all three redundant sensors boards were loaded into the airplane and the GPC was programmed to maintain a fixed pitch. Tilting the airframe off-pitch would cause the GPC to respond by moving the plane's elevator to compensate. The team then yanked the sensors boards out of the airframe one-by-one to confirm that the plane could react to the loss of sensor data on the fly and still respond correctly when tilted.

Finally, the team also tested the ability of the system to process redundant sensor data in a real flight environment. The results of the flight test are described in section 4.4.6.

4.2 Sensors Calibration

Before the sensors could be used to determine the plane's orientation, they first had to be calibrated to remove zero-offsets and scale their outputs into the ranges expected by the autopilot algorithm. This section describes the team's general approach to sensor calibration.

For specific step-by-step calibration procedures using the programs and scripts developed, see section A.7.

Accelerometers Each axis of the three-axis accelerometer is calibrated individually. First, the sensors board is oriented such that the axis to be calibrated is aligned pointing directly at the ground. Several measurements are taken with the accelerometer in this configuration and then averaged together (to curtail noise) to form an estimate for the sensor's value with the axis aligned with the direction of gravity, i.e., for an acceleration of 1 G. Next, the board is rotated such that the axis to be calibrated is aligned pointing directly upward. Again, several measurements are taken and averaged together, this time to get an estimate of the sensor's value with the axis antiparallel to the direction of gravity, i.e., for an acceleration of -1 G.

These two points lie on a line. The slope and vertical intercept of this line can be used to correct for any zero-offsets and to scale the axis output into the same range as that of the other axes.

This calibration procedure cannot correct for cross-axis correlations due to non-orthogonality of the axes; however, practice has found these effects to be negligible and the above procedure to be adequate.

Magnetometers Ideally, the magnetometers could be calibrated in the same way as the accelerometers, one axis at a time, using the Earth's native magnetic field as a reference the same way that the Earth's gravitational field serves as a reference for the accelerometers. Unfortunately, while the Earth's magnetic field is locally of approximately constant strength and uniform direction (when away from buildings and large metal objects) as desired, it is difficult to precisely determine the field direction. Knowing the field direction is important because it gives the direction along which the magnetometers should register their largest values. Knowing this maximum is critical for choosing scaling constants that make the magnetometer values range as large as possible for maximum sensitivity while keeping it confined to the range

representable using a 16-bit integer type. Thus, a slightly different calibration technique had to be developed.

The procedure the team came up with is as follows. The Earth's magnetic field is still used as a reference, but instead of trying to take measurements along each axis separately, a large number of measurements from all three axes are taken simultaneously with the magnetometer oriented in a variety of different directions. These measurements are then plotted as points in three-dimensional space (one coordinate dimension for each axis of the magnetometer), where they form an ellipsoidal point cloud. By taking a large number of measurements with the sensor oriented in many different directions, the equation of this ellipsoid can be determined. The coordinates of the centroid of this ellipsoid gives the zero-offsets for each of the magnetometer axes, and the lengths of the ellipsoid axes can be used to adjust the relative scaling of the magnetometer axes.

To do the curve fitting, the team cast the problem as a non-linear least squares optimization problem in six dimensions (three for the coordinates of the centroid, three for the axis lengths) and used MATLAB's `lsqnonlin` routine to solve for the optimal set of parameters. `lsqnonlin` uses a trust region method to perform optimization. For more information, see the MATLAB manual page for `lsqnonlin` and the papers [19] and [20].

Gyroscopes Calibration of the gyroscopes requires a source of constant angular rotation. The team procured a standard $33\frac{1}{3}$ RPM record player for this purpose, measured its rate of rotation, and took gyroscope measurements with the boards placed on the rotating platform. To avoid the need to hook cables up to the rotating assembly to tap into the bus, the measurements were sent wirelessly to a PC using the radio link.

Two measurements were taken for each gyroscope axis: one with the system rotating about the axis at the turntable speed and one with the boards in a stationary, non-rotating configuration. The team used these data to generate a linear model for the behavior of the

gyroscopes.

Relative Airspeed To calibrate the differential pressure sensor used for measuring the plane's indicated airspeed, the team connected one of the pitot tubes that had been purchased for use with airspeed measurement to the sensor's input ports and mounted the tube inside a wind tunnel. Several pressure measurements were taken with the wind tunnel set to produce airstreams with a variety of flow rates between 10 and 30 mph. At the same time, the team recorded the readings of the wind tunnel's own pitot-static pressure measurement system and used these to compute a linear model for the behavior of the pressure sensor.

4.3 Hardware-in-the-Loop (HITL) Simulation

To enable ground development and testing of the autopilot algorithm, the team created a hardware-in-the-loop (HITL) test framework centered around the commercially available flight simulator X-Plane [21]. The term hardware-in-the-loop refers to the fact that the autopilot algorithm is running on the actual GPC hardware during the test (as opposed to a software-in-the-loop test, in which the algorithm would be running inside a software emulator for the GPC ARM).

To perform HITL testing, the only change to the firmware that must be made is that the GPC board must be programmed to handle sensor data from X-Plane instead of from a sensors board. During each pass of the main system loop, the GPC requests data from X-Plane by sending a `BCMD_SENSORS_FETCH_AHPRS` request packet out on the system bus (see section 3.5.1). This is picked up by the Houston ground software, which is listening to traffic on the bus as part of its HITL testing mode (see section 3.4). Houston then retrieves airplane state data from X-Plane, wraps it in a `BCMD_SENSORS_REPLY_AHPRS` packet, and sends it on to the GPC. The GPC takes the data it has received and inputs it into the autopilot algorithm, which decides how to manipulate the control surfaces to best adhere to the programmed flight plan. The GPC

then sends these manipulations out over the bus in the form of a `BCMD_SERVO_SETSERVOS` packet. Houston picks this up and forwards the data to X-Plane, which uses this information and its internal flight model to update the state of the simulated aircraft.

The team made extensive use of the HITL test framework for trying out changes to the autopilot prior to actual flight tests and for tuning autopilot control loop constants to improve the dynamic behavior of the aircraft. This required the team to construct a simple X-Plane model of the prototype *Senior Telemaster* used as the test airframe.

Most importantly, the team used the HITL framework to demonstrate the ability of the autopilot to successfully follow a series of waypoints. For instance, in one particular test, the GPC was programmed to fly repeatedly in a box-like pattern through a series of waypoints whose coordinates form the four corners of a rectangle. The plane exhibited some position overshoot as it turned when proceeding from one waypoint to the next but otherwise tracked the expected path reasonably well.

4.4 Flight Tests

In order to demonstrate the functionality of the system in a real flight environment, the team conducted a series of flight tests over the course of the year. Each flight test was performed with the aim of demonstrating a specific feature. This section catalogues all the flight tests that the team carried out, their purposes, and their results.

4.4.1 Servo Board Flight Test: 08/22/2010

The purpose of this flight test, which was conducted at the end of the summer, just prior to the start of the Fall, 2011 term, had two goals. First, At this point in time, the team had just finished writing the first version of the firmware for the servo control board and wanted to verify that the manual override feature worked properly. In this test, the team was able to successfully fly the

plane under manual control with only the servo board installed, operating in manual override mode. This confirmed the ability of the servo board to take correctly receive and process input from the manual RC receiver and also to provide control pulses to each of the servos with the appropriate timing and duration.

The second goal of this test was to verify the operation of the power supplies on the servo board (which would eventually be used to power the complete avionics package; see section 3.1.2) under real flight conditions. The team was concerned that the high current draw from the plane's powerful electric motor might cause microcontroller resets, which would necessitate a hardware revision with re-designed power supplies. Fortunately, these were not observed, and the system appeared to operate correctly.

4.4.2 Three-Board Flight Test: 01/07/2011

Over the course of the Fall, 2011 term and the winter recess, the team worked on developing the bus protocol, wrote the firmware for the radio board, and wrote a first draft of the GPC firmware that was not based on the MAL kernel, which was still being developed. In particular, the basic facilities for command uplink and telemetry downlink had been established.

The goal of the three-board flight test was to try out these facilities and see what needed to be improved. The test was dubbed the "three-board" flight test is because the test involved three of the four types of circuit boards: the GPC board, the radio board, and the servo board. The GPC was programmed to retrieve bus and battery voltages and battery currents from the servo and radio boards and downlink them over the radio, where they would be picked up by the ground software. The team had also developed some code for flying the plane using a PC joystick and planned to use this to test the ability of the plane to receive uplinked commands.

Unfortunately, the flight test ended too quickly for any of these facilities to really be exercised. Due to what was later determined (using video analysis) to be a misbalanced center of gravity, the plane crashed after about five seconds of flight, shattering the front end of the

airframe and causing the electronics to become ejected from their mounted positions. On the other hand, the team was able to successfully collect a handful of telemetry frames, demonstrating that the telemetry downlink worked. The team's experience with decoding the down-linked packets also led the team to re-design the telemetry logging capabilities of the ground software and spurred the development of the logging protocol (see section 3.4.5), in particular.

4.4.3 Initial Autopilot Flight Test: 03/06/2011

The next flight test the team conducted was aimed at demonstrating basic autopilot functionality by having the plane maintain a fixed horizontal path. By this time, the team had written firmware for all of the different boards, calibrated all of the sensors except for the airspeed sensor, and integrated the autopilot code into the GPC firmware.

In order to avoid the problem with the plane's center of gravity that caused the previous flight test to end prematurely, the team had some of the experienced RC pilots at the flying field help check to ensure that the plane was properly balanced. Additionally, since the team's experience flying RC aircraft is relatively limited, the team enlisted the help of one of the pilots, Mr. Keith Klix, in flying the aircraft under manual control to reduce the risk of damaging the airframe during takeoff and landing.

Mr. Klix flew the plane up to a reasonable altitude and then turned control over to the autopilot by engaging the manual override switch on the RC transmitter. The plane was programmed to fly in a straight line, adhering to the horizontal path it was last on before the autopilot was engaged. While the plane appeared to try and maintain this path as programmed, it exhibited substantial undesirable oscillations in its heading. At the end of the test, Mr. Klix landed the plane perfectly, leaving the hardware in good condition for future testing.

Though the autopilot did not perform quite as well as the team had hoped, this test was valuable because it was the first test of the fully integrated system in a real flight environment. The team successfully collected a full stream of telemetry data from the flight, including sensor

values and the autopilot's estimates of the plane's state for every flight frame. This gave strong confirmation of the correct operation of the radio downlink and gave the team some data to analyze to improve the autopilot for the next flight.

4.4.4 Basic Autopilot Flight Test: 03/19/2011

After the previous test, the team made some modifications to the autopilot to try and fix the oscillating behavior that had been observed. Specifically, the autopilot code was altered to try and maintain a fixed heading for the aircraft instead of a fixed horizontal path as was done previously. After performing a successful short flight test at a nearby location to see if the changes looked like they would work, the team traveled out to Dick Scobee Field on March 19, 2011 try a longer flight test and gather more data. Additionally, the team had finished calibrating the airspeed sensors and installing a pitot tube in the plane's wing, so the team hoped to use this flight test to collect airspeed data for the first time.

As in the flight test that was conducted on March 6, the team had one of the experienced pilots at the field fly the plane to a reasonable altitude and engage the autopilot. The plane was programmed to try and maintain its last heading just prior to the transition to autopilot. The autopilot performed well, and the magnitude of the oscillation in the plane's heading while under automatic control appeared to have been reduced substantially from the previous flight test. With some advice from the pilot about the plane's handling, the team adjusted some of the control constants in the autopilot feedback loop and conducted a second flight. With these improvements, the autopilot performed even better, maintaining its heading with even less oscillation than before.

As with the previous flight test, the team collected a full stream of telemetry data and used this to gauge the autopilot's performance and find ways to improve it for the next test.

4.4.5 Redundant Sensors Flight Test I: 03/27/11

The goal of this flight test was the same as the previous one: to demonstrate basic functionality of the autopilot in the form of the ability of the plane to maintain a fixed heading; however, this flight test also added the extra element of sensor redundancy. By the time of this flight test, the team had constructed two additional copies of the sensors board, calibrated them, and had written the sensor redundancy management code for the GPC. This flight test would try out these new features in a real flight environment.

As with the previous two flight tests, the team had one of the experienced pilots at Dick Scobee Field take the plane off under manual control. While the pilot was in the process of bringing the plane up to altitude, the plane suddenly began performing a series of successive rapid vertical loops, all under manual control. Despite the pilot's best efforts to bring the aircraft out of this pattern, the plane continued to perform loops for just under two minutes before crashing into a tree.

Thankfully, the damage to the airframe was minimal. A post-mortem analysis of the telemetry gathered during the flight (which included the commands the plane was sending to the servos) with the assistance of the team's NASA mentor David Fuson suggested that the repeated loops may have been inadvertently induced by the pilot while he was trying to save the plane. Though the team was unable to gather any data on the performance of the autopilot, the sensor telemetry gathered during the flight seemed to suggest that the system was correctly processing the data from the redundant sensors boards.

4.4.6 Redundant Sensors Flight Test II: 04/02/2011

Since the team did not get the information it wanted during the flight test on March 27, the team conducted a second flight test on April 2 with the same objective: to demonstrate the autopilot's ability to maintain a fixed heading while handling data from redundant sensors inputs. As in

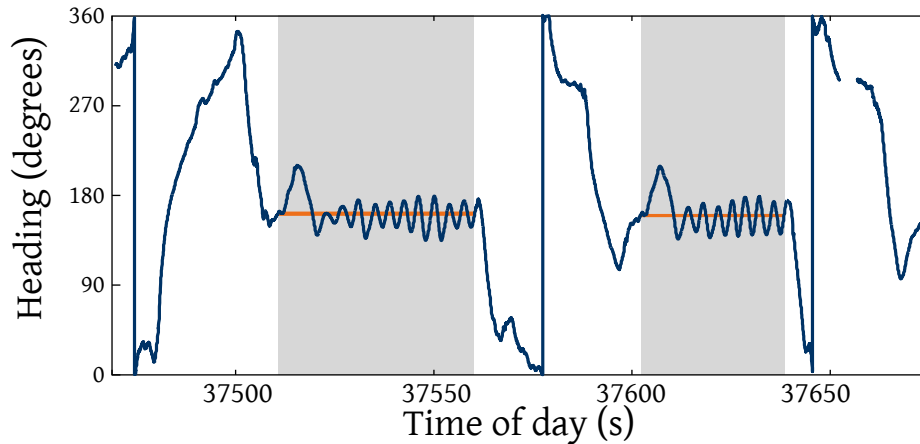


Figure 4.1: Heading-lock telemetry from second flight on 04/02/2011. The blue line indicates the plane's actual heading. The gray regions indicate parts of the flight for which the autopilot was active, and the orange lines indicate the plane's desired heading during those times.

the flight test on March 19, the plane was programmed to try and maintain its last heading just prior to the transition to autopilot.

Once again, the team enlisted the services of Mr. Keith Klix for help with flying the plane. Mr. Klix flew the plane up to a reasonable altitude and then engaged the autopilot. The plane did an excellent job maintaining the desired heading with fairly low levels of oscillation. After Mr. Klix landed the plane, the team made a some adjustments to the plane's pitch and had Mr. Klix take it up for a second flight. The plane's flight characteristics showed a minor improvement.

Telemetry data from the second of these flight tests is illustrated in figure 4.1. The blue line plots the plane's heading versus time. The regions of the graph shaded in gray indicate portions of the flight during which the autopilot was engaged, and the orange lines mark the heading which the plane was trying to maintain. As the plot shows, after a short start-up transient following the transition to autopilot, the plane does a reasonably good job maintaining the desired heading, though it oscillates a bit.

Figure 4.2 displays the plane's flight trajectory during the second flight test, overlaid on top

of a satellite image of Dick Scobee Field and the surrounding area. The red lines indicate portions of the flight for which the autopilot was active. The arrows on the path indicate the plane's direction of flight. The telemetry data in figure 4.1 comes from the two long autopilot flight segments in the lower part of the image. In agreement with the numerical data of the previous figure, the trajectory plot shows that, barring an initial transient, the plane successfully maintained its heading over an extended distance with some mild oscillations.

Having accomplished the main objective, the team decided to try a third flight test, this time with the autopilot programmed to maintain a fixed horizontal path, like it had been during the flight test on March 6. The hope was that the improvements that had been made to the autopilot over the weeks since the March 6 test might have fixed the problems the team had observed then. Unfortunately, the autopilot showed similar oscillatory behavior. In the weeks since this flight test, the team has conducted extensive tuning of the autopilot using HITL simulation in an attempt to improve this behavior and hopes to try out the modifications along with a fully waypointed version of the autopilot (which has also been verified to operate correctly in HITL simulation; see section 4.3) in another flight test soon.



Figure 4.2: Plot of plane's trajectory during the second flight test on 04/02/2011. The red lines indicate parts during which the autopilot was active. Arrows on the line segment indicate the plane's direction of travel.

5 Summary and Recommendations

5.1 Summary

The team successfully designed and fabricated a complete set of avionics hardware for a fixed-wing UAV from scratch. The hardware was designed in a modular manner, separating the different pieces of system functionality onto four different types of circuit boards so as to make the system easily extensible to accommodate redundancy of the various components for the sake of improving the system's overall fault-tolerance. In particular, the team focused on implementing redundancy in the system's sensors but designed the system so that other types of component redundancy can be easily added in the future.

The team wrote and tested a complete set of firmware for each of the circuit boards, including a basic autopilot algorithm and a custom real-time kernel for the general-purpose computer board. The system is capable of sensing the plane's current state and using this information to manipulate the plane's control surfaces to get the aircraft to follow a stored, on-board flight plan. It also continuously transmits telemetry about the plane's status to a computer on the ground using an on-board radio link. The team developed a PC ground software application for real-time UAV monitoring, telemetry analysis, and system simulation and testing.

The team successfully demonstrated the basic functionality of the system operating with a triply redundant set of sensors in a real flight environment with the avionics package installed in a standard, off-the-shelf RC airframe. The plane successfully processed data from each of the redundant sets of sensors and used this data with a simple version of the autopilot to get the plane to maintain a fixed heading. The team also performed successful hardware-in-the-loop simulation testing of a more complete version of the autopilot that features waypoint-based navigation and is ready to test it in actual flight at the next available moment.

5.2 Recommendations and Future Work

There are many possible directions in which the project could be extended, spanning a wide range of disciplines, including electrical engineering, computer science, mechanical engineering, and applied mathematics.

- **Additional Redundancy** – Although sensor redundancy was implemented this year, developing the software needed to support redundancy in the main computers would improve reliability. Adding software support for redundancy in the servos and control surfaces would be useful as well. Hardware support for these features is already built-in to the design.
- **Sensors Payloads** – A design team could work on developing payload suites of sensors other than those required to fly the actual plane, e.g., a camera for live video downlink.
- **Improved Autopilot** – The autopilot algorithm could be changed to be more robust and to support additional features, including completely autonomous (i.e., non-waypoint-based) navigation and terrain avoidance.
- **Alternate Power Sources** – The existing plane has an electric motor powered off of a lithium-polymer battery. Existing battery technology makes flights of longer than an hour impractical without the addition of solar panels. A design team could enhance the existing power management system to use solar panels to recharge the batteries and run the motor.
- **Improved Airframe** – A team of mechanical engineers could design an airframe capable of flying at very high Earth altitudes, where the consistency of the atmosphere is similar to that on Mars. The UAV could then carry sensors payloads up to such altitudes

and collect data. Such an improved airframe would allow live testing of the avionics in extreme conditions more similar to those found on Mars.

6 Acknowledgements

6.1 Technical Advisors

The team would like to thank numerous mentors and advisors for their role in the success of this project:

David Fuson of ESCG Jacobs has been an invaluable resource for the team, providing practical engineering experience and project management advice. He has also provided feedback on presentation practices and slides.

Dr. Humboldt Mandel was team's TSGC mentor. He provided the team with insight into what it takes to make a Mars-capable space probe and supported the team at both the spring and fall TSGC Design Showcase presentations.

Within the ECE department, Dr. Woods and Dr. Wise have both provided practical advice concerning technical issues ranging from reducing EMI issues to fixing mismatched PCB components.

Joe Gesenhues and the Mechanical Engineering Department graciously provided access to and assistance with operating the department wind tunnel, which was used to calibrate the airspeed sensor.

Michael Dye, Joe Gesenhues, and Carlos Amaro provided assistance in ordering parts. They also provided assistance with solving several issues, including finding mounting standoffs for the radio board, and locating an acceptable pitot tube.

Bob Ziegenhals and Cullen Newsom provided the team with some advice about selecting and mounting pitot tubes.

6.2 Flight Testing

Team Electric Owl would like to thank the Bayou City Flyers for access to Dick Scobee Field. Other model aviators at the field provided invaluable advice during flight testing with respect to flight dynamics, equipment selection, and RC flying.

Team Electric Owl owes a great debt to the members of the Bayou City Flyers that volunteered to fly the test aircraft manually. Although the team members are all licensed AMA members, and can fly the aircraft, an experienced hand was often necessary to ensure success in flight testing. Keith Klix, among others, has offered significant assistance.

6.3 Funding Sources

Funding for this project has been provided through Rice University's Department of Electrical and Computer Engineering, as part of the capstone design sequence, and through the Texas Space Grant Consortium, which funds educational NASA-related projects.

7 References

- [1] Garmin International, Inc., “Garmin Device Interface Specification.” http://eukles.googlecode.com/svn-history/r2/trunk/doc/spec/spec_garmin_interface.pdf, last checked 2011-05-03.
- [2] R. D. Braun, H. S. Wright, M. A. Croom, J. S. Levine, and D. A. Spencer, “Design of the ARES Mars Airplane and Mission Architecture,” 2006.
- [3] H. S. Wright, J. S. Levine, M. A. Croom, W. C. Edwards, G. D. Qualls, and J. F. Gasbarre, “Measurements from an Aerial Vehicle: A New Tool for Planetary Exploration,” 2004.
- [4] NASA, “Mission News - Preventative Care Continues, Science on Hold,” September 04 2009. http://www.nasa.gov/mission_pages/MRO/news/mro-20090904.html, last checked 2010-10-08.
- [5] NASA, “Mission News - Spacecraft out of Safe Mode,” December 08 2009. http://www.nasa.gov/mission_pages/MRO/news/mro-20091208.html, last checked 2010-10-08.
- [6] NASA, “Mission News - NASA’s Mars Reconnaissance Orbiter Resumes Observations,” December 16 2009. http://www.nasa.gov/mission_pages/MRO/news/mro20091216.html, last checked 2010-10-08.
- [7] “Space Shuttle news reference,” tech. rep., NASA, 1981.
- [8] “Telecommunications Innovations for the Mars Exploration Rover Mission,” tech. rep., NASA Jet Propulsion Laboratory.
- [9] J. F. Hanaway and R. W. Moorehead, *Space Shuttle Avionics System*, 1989. NASA Publication SP-504.
- [10] “Report of the presidential commission on the space shuttle challenger accident,” tech. rep., Presidential Commission on the Space Shuttle Challenger Accident, 1986. <http://science.ksc.nasa.gov/shuttle/missions/51-1/docs/rogers-commission/table-of-contents.html>, last checked 20101007.
- [11] “Appendix F - Personal observations on the reliability of the Shuttle,” tech. rep., Presidential Commission on the Space Shuttle Challenger Accident, 1986. <http://science.ksc.nasa.gov/shuttle/missions/51-1/docs/rogers-commission/Appendix-F.txt>, last checked 2010-10-09.
- [12] “Shuttle ALT Free Flight 1: GPC 2 Failure,” tech. rep., NASA Office of Logic Design. http://klabs.org/DEI/Processor/shuttle/alt_gpc2/index.htm, last checked 2010-10-07.
- [13] T. G. Team, “GCC, the GNU Compiler Collection.” <http://gcc.gnu.org/>, last checked 2011-05-03.

- [14] D. Rath, "Open On-Chip Debugger." <http://openocd.berlios.de/web/>, last checked 2011-05-03.
- [15] Digi International, Inc., "XTend RF Module." http://ftpl.digi.com/support/documentation/90000958_C.pdf, last checked 2011-05-03.
- [16] R. Dean and W. Dixon, "Simplified statistics for small numbers of observations," *Analytical Chemistry*, vol. 23, no. 4, pp. 636–638, 1951. Accessed Online: ACS Publications, 05/03/2011.
- [17] G. D. Carlow, "Architecture of the space shuttle primary avionics software system," *Commun. ACM*, vol. 27, no. 9, pp. 926–936, 1984.
- [18] Y. Yeh, "Safety critical avionics for the 777 primary flight controls system," in *Digital Avionics Systems, 2001. DASC. The 20th Conference*, vol. 1, pp. 1C2/1–1C2/11 vol.1, 2001.
- [19] T. Coleman and Y. Li, "An Interior, Trust Region Approach for Nonlinear Minimization Subject to Bounds," *Siam Journal on Optimization*, vol. 6, pp. 418–445, 1996.
- [20] T. Coleman and Y. Li, "On the Convergence of Reflective Newton Methods for Large-Scale Nonlinear Minimization Subject to Bounds," *Mathematical Programming*, vol. 67, no. 2, pp. 189–224, 1994.
- [21] Laminar Research, "X-Plane." <http://www.x-plane.com/>, last checked 2011-05-05.
- [22] R. P. G. Collinson, *Introduction to Avionics Systems*. Kluwer Academic Publishers, second ed., 2003.
- [23] D. McRuer, I. Ashkenas, and D. Graham, *Aircraft dynamics and automatic control*. Princeton University Press, July 1990.
- [24] C. K. Chui and G. Chen, *Kalman filtering: with real-time applications*. Springer, 2009.
- [25] R. Langton, *Stability and control of aircraft systems: introduction to classical feedback control*. John Wiley and Sons, Oct. 2006.
- [26] *Code of Federal Regulations, Title 47, Telecommunication, Pt. 0-19, Revised as of October 1, 2009*. Government Printing Office, 2010.
- [27] "Model Aircraft Operating Standards," Advisory Circular 91-57, Federal Aviation Administration, June 1981.
- [28] "Unmanned Aircraft Operations in the National Airspace System," notice of policy, Federal Aviation Administration, February 2007. Federal Register Document E7-2402.
- [29] P. L. Walter, "The History of the Accelerometer: 1920s-1996," January 2007. http://findarticles.com/p/articles/mi_qa4075/is_200701/ai_n18705234/pg_16/, last checked 20090726.

-
- [30] “An Introduction to AC Propulsion’s Split Phase Drives for Brushless Motors,” tech. rep., AC Propulsion, 2003.
- [31] R. Miura, M. Maruyama, M. Suzuki, H. Tsuji, M. Oodo, and Y. Nishi, “Experiment of tele-com/broadcasting mission using a high-altitude solar-powered aerial vehicle Pathfinder Plus,” in *The 5th International Symposium on Wireless Personal Multimedia Communications*, vol. 2, pp. 469–473, October 2002.
- [32] ““AC Propulsion SoLong UAV Flies for 48 Hours on Sunlight Two Nights Aloft Opens New Era of Sustainable Flight”,” press release, AC Propulsion, June 2005.
- [33] “SkySite Network & SkySite Telemetry Services Overview,” tech. rep., Space Data Corporation, December 2005.
- [34] “RAD750 MRQW 2002,” tech. rep., BAE Systems, December 2002.
- [35] AeroVironment, “Online poll on where small unmanned aircraft systems can offer the greatest benefit outside the military,” July 2009. http://www.avinc.com/poll_results/, last checked 20090726.
- [36] “NASA Solar Aircraft Sets Altitude Record and Communications and Environmental Breakthroughs Expected,” press release, NASA Dryden Flight Research Center, August 2001.
- [37] “Space Shuttle General Purpose Computers,” fact sheet, NASA Spaceflight, April 2002.
- [38] ““QinetiQ’s Zephyr UAV exceeds official world record for longest duration unmanned flight”,” press release, QinetiQ, September 2007.
- [39] ““The Unveiling of the Solar Impulse HB-SIA”,” press release, Solar Impulse, June 2009.
- [40] ““X-29 Fact Sheet”,” fact sheet, NASA Dryden Flight Research Center, December 2009.
- [41] “2009 Official AMA National Model Aircraft Safety Code,” Document 105, Academy of Model Aeronautics, January 2006.
- [42] “First Person View Operations,” Document 550, Academy of Model Aeronautics.
- [43] “ARRL Band Plans,” web page, American Radio Relay League. <http://www.arrl.org/FandES/field/regulations/bandplan.html>, last checked 20090726.
- [44] “Frequency Chart for Model Operation,” web page, Academy of Model Aeronautics. <http://www.modelaircraft.org/events/frequencies.aspx>, last checked 20090726.
- [45] “Experimental certificates,” Regulation 14 CFR 21.191, Federal Aviation Administration.
- [46] “Experimental certificates: general,” Regulation 14 CFR 21.193, Federal Aviation Administration.

- [47] “Experimental certificates: Aircraft to be used for market surveys, sales demonstrations, and customer crew training,” Regulation 14 CFR 21.195, Federal Aviation Administration.
- [48] B. Clinton, “Statement By The President Regarding The United States’ Decision To Stop Degrading Global Positioning System Accuracy,” press release, The White House, May 2000.
- [49] “WAAS Fact Sheet,” GNSS Library, Federal Aviation Administration. http://www.faa.gov/about/office_org/headquarters_offices/ato/service_units/techops/navservices/gnss/library/factsheets/#q2, last checked 20090727.
- [50] ““AC Propulsion’s Solar Electric Powered SoLong UAV”,” Fact Sheet, AC Propulsion, June 2005.
- [51] “Understanding Radio Language for RC Airplanes,” web page, Hooked-On-RC-Airplanes.com. <http://www.hooked-on-rc-airplanes.com/radio-language.html>, last checked 20090727.
- [52] “Cis-Lunar MK5 Closed-Cycle PLSS,” technical description, Stone Aerospace. <http://www.stoneaerospace.com/products-pages/products-cis-lunar-mk5.php>, last checked 20090727.
- [53] tech. rep. <http://www.technologyreview.com/blog/deltav/23917/>, last checked 20090803.
- [54] RADA Electronic Industries, Ltd., “MAVINS: Modular Avionics and INS/GPS for UAV,” tech. rep. <http://www.rada.com/solutions/mavins.html>, last checked 2010-10-07.
- [55] “Zephyr unmanned aerial vehicle,” tech. rep., QinetiQ.
- [56] C. Anderson, “ArduPilot - DIY Drones.” <http://diydrone.com/notes/ArduPilot>, last checked 2010-10-08.
- [57] MicroPilot, “MP2028 Series Autopilots.” <http://www.micropilot.com/products-mp2028-autopilots.htm>, last checked 2010-10-08.
- [58] Rotomotion, LLC, “UAV Helicopter Controller.” http://www.rotomotion.com/prd_UAV_CTLR.html, last checked 2010-10-08.
- [59] AeroVironment, Inc., “Small Unmanned Aircraft Systems - Puma AE.” http://www.avinc.com/uas/small_uas/puma/, last checked 2010-10-08.
- [60] Real Time Engineers, Ltd., “The FreeRTOS Project.” <http://www.freertos.org/>.

A User's and Safety Manual

This User's and Safety Manual contains procedures for performing the most common tasks required during development and testing of the team's project and guidelines for safe operation of the aircraft. Procedures for performing tasks on the computer are written assuming a Linux-based operating environment with all of the project's software dependencies installed (see section A.2). If a different environment is used, then the procedures will need to be changed accordingly.

A.1 Flight Test Procedures

This section summarizes the team's recommended procedures for carrying out a flight test. In particular, section A.1.2 contains a checklist of items that should be brought to the test site.

A.1.1 The Day Before

The day before the flight test, be sure to do the following:

- Check the weather forecast. In particular, be sure to check wind speeds and plan to test during periods of low wind activity. The team has found that in Houston, the best times to fly are in the early morning between 7:00 A.M. and 11:00 A.M.
- Check that all of the circuit boards have been programmed with the appropriate version of the code.
- Perform a ground test of the functionality that is to be tested.
- Check the airframe for flight readiness. In particular,
 - Patch any holes in the surface with mylar.

- Verify the polarity of the drive motor.
- Verify the polarity of the plane's control surfaces.
- Charge all the batteries, including the following:
 1. Main propulsion battery (22.2V 6S1P LiPo)
 2. Avionics 4-cell NiCd backup battery
 3. 6-channel RC transmitter battery
- Announce to interested parties that a flight test will be conducted, e.g., by posting a notification message to the `uav-test-announce` listserv. As a courtesy to individuals who may need more advance notice to plan their schedules, it is best to do this as early as the flight test can be confirmed, perhaps even earlier than on the day immediately before the flight test.

A.1.2 Packing Checklist

1. Airframe
 - Wings and fuselage
 - Battery compartment hatch
 - Rubber bands (for attaching the wings)
 - Avionics package and 900 MHz radio antenna (mounted in the plane)
 - Batteries: lithium-polymer main propulsion battery and NiCd backup battery
 - Motor controller
 - Plane-mounted flight camera
2. Ground Control

- Extension cord and power strip
- Digi 900 MHz radio module and cables
- Laptop computer with all project development tools installed and which is capable of running the Houston ground software
- Laptop computer with X-Plane installed (for live 3-D visualization of the plane's trajectory)
- 6-channel Spektrum RC transmitter for manual control

3. Development Tools Box

- AVR programmer
- ARM programmer
- RS-485 transceiver
- Shore power cable

4. Repair Kit

- Spare propellers
- Wrench and prop axle coring tool
- Extra mylar to patch holes
- Mylar application iron
- Superglue
- Balsa sticks
- Hacksaw
- X-Acto knives
- Hex wrench set

- Multitool
- Digital multimeter
- Spare fuses

5. Battery Charger

- Battery charge power supply
- Main charging unit
- LiPo and NiCd battery adapters
- Metal battery storage box for charging

6. Miscellaneous

- AMA Memberships for all pilots
- Video camera and camera operator for photographing and filming the flight from the ground
- Sunscreen, hats, sunglasses
- Water and snacks
- Cellular telephones
- First aid kit
- Safety glasses

A.1.3 At the Field

This section is written assuming that the test is being conducted at Dick Scobee Field in George Bush Park out in west Houston. Other flying fields may have their own distinct set of procedures that will need to be followed.

1. Upon Arrival

- (a) Set up a workspace on one of the provided work tables.
- (b) Reserve transmitter frequency (2.4 GHz for the 6-channel Spektrum transmitter) by placing the one pilot's AMA ID in an appropriate slot at the frequency registration station and taking the corresponding frequency tag.
- (c) If no member of the team is a competent RC pilot and the plane will need to be flown under manual control for at least part of the flight test, negotiate with the pilots at the field and see if one would be willing to assist the team with flying the plane manually. If one agrees, instruct him or her in how to operate the team's hardware; in particular, give the procedure for manually activating and deactivating the autopilot.

2. Transmitter Range Check – Use the following procedure to check the range on the RC transmitter.

- (a) Ensure that the plane is unpowered.
- (b) Have one member of the team take the RC transmitter out to the range check point. At Dick Scobee Field, this is marked by a large pole in the ground on the west side of the flight field.
- (c) Have a member of the team power the plane's control surfaces by flipping the NiCd battery switch to the "on" position.
- (d) Have the team member out at the range point test movement of all control surfaces using the RC transmitter. Be sure to check the functioning of the autopilot/manual-override toggle switch as well.
- (e) If everything worked, remove power from the plane by flipping the NiCd battery switch to the "off" position and have the team member with the transmitter return

from the range checkpoint.

3. Pre-Flight Assembly and Testing – Follow these steps to get the plane ready for flight. The ground control computer(s) should be set up while this is occurring for maximum efficiency.
 - (a) Attach wings to plane using rubber bands looped around the wooden pegs on the top of the airplane. The wings should be attached with several rubber bands connected in each of the following three configurations:
 - Fore-to-aft, parallel to body
 - Fore-to-aft, diagonal across body
 - Left-to-right, parallel to wings / transverse to body
 - (b) Inspect the propeller for damage and replace it if needed.
 - (c) Ensure that the NiCd battery switch is flipped to the “off” position.
 - (d) Install the main lithium-polymer propulsion battery in the plane, but *do not connect it yet*.
 - (e) Perform a weight and balance check. Make sure that the plane’s center-of-gravity is in an acceptable position. If necessary, try to enlist one of the experienced RC pilots to assist with this task.
 - (f) Turn on the 6-channel RC transmitter.
 - (g) Flip the manual override switch to the “on” position (towards the operator).
 - (h) Flip the NiCd battery switch to the “on” position.
 - (i) Use the RC transmitter to check that at least one of the control surfaces moves correctly.
 - (j) Move the plane manually out to the motor testing area. At Dick Scobee Field, this is just in front of the runway.

- (k) Connect the main lithium-polymer battery and wait for the motor controller to finish its start-up sequence.
- (l) Use the RC transmitter to make sure that the main motor spins correctly.
- (m) Check the control surface polarity one more time.
- (n) Check functionality of the manual override switch one more time.
- (o) Use the telemetry downlink to ensure to that the plane's GPS has acquired a suitable fix.
- (p) At this point, the plane is ready for flight, and the test can begin. Be sure to invoke all necessary deities and request a safe and successful test prior to takeoff.

A.2 Software Dependencies

Certain packages must be installed on the development workstation to successfully build the firmware and ground control software and program the microcontrollers. A list of these is shown in Table A.1. The listed packages are for a Linux-based operating environment.

| Package | Version | Description |
|-----------------|----------------|---|
| arm-dev | 20100728 | Team-compiled ARM cross-compiler toolchain |
| avr-dev | 20100709 | Team-compiled AVR cross-compiler toolchain |
| dev-extralibs32 | 20100728 | Team-compiled 32-bit compatibility libraries |
| geda-gaf | 1.6.1 | gEDA electronics design suite, including gschem |
| pcb | 20091103 | gEDA PCB layout software |
| openocd | 0.4.0 | The Open On-Chip Debugger |
| wxGTK | 2.8.11 | wxWidgets GUI library for GTK |
| git | 1.7.1 | Git version control software |

| | | |
|-------------------|--------|---|
| <code>gcc</code> | 4.4.4 | GNU compiler collection |
| <code>make</code> | 3.81 | GNU make utility to maintain groups of programs |
| <code>perl</code> | 5.10.1 | The Practical Extraction and Report Language |

Table A.1: Software dependencies required for Electric Owl development.

The `arm-dev`, `avr-dev`, and `dev-extralibs32` packages have been specially compiled by the team for work on this project and are provided in binary form as bzip2-compressed tar archives on the team's internal website. To install them, download the corresponding archive and unpack it in the system's root directory. For example, to install the ARM cross-compilation toolchain, use the following command sequence:

```
$ su
# cd /
# mv /path/to/arm-dev-20100728.tar.bz2 .
# bunzip2 -cd arm-dev-20100728.tar.bz2 | tar -xv
# rm arm-dev-20100728.tar.bz2
```

It is highly recommended that the developer use the team's provided binary packages for these toolchains and libraries, but if this is not possible, they can be built from source. Instructions for building the `arm-dev` package from source are given in section A.8. `avr-dev` and `dev-extralibs32` are more straightforward to compile.

The remaining packages in Table A.1 can either be built from source by the user or obtained as standard binary packages shipped with most Linux distributions. Only Open OCD should require a special build procedure; this is outlined in section A.9. Note that some of these packages have dependencies not listed in Table A.1 that will also need to be installed, e.g., Open OCD requires `libFTDI` and `libconfuse` to run.

Aside from the packages listed in Table A.1, `LATEX` and `doxygen` are required to build some of the project documentation. Any of the binary packages provided for most Linux distributions should suffice to satisfy these dependencies.

A.3 Programming the Circuit Boards

This section gives the procedures for writing programs into the flash memory of the microcontrollers on the circuit boards.

A.3.1 AVR Microcontrollers

Programming the AVR microcontrollers on each board requires the following:

- The target board to be programmed
- The program to be flashed, in the form of a `*.hex` file. (This should be produced automatically when the program is built using the project `make` scripts.)
- One backplane board with at least one RS-485 connector and at least one row of circuit board connection headers.
- One AVR programmer.
- One shore power cable.
- One PC with all necessary software dependencies installed, a copy of the project Git repository, and at least one USB port.

To program one of the AVRs, use the following procedure:

- (a) Take the backplane board and insert the target board to be programmed into an available row of circuit board connection headers.

- (b) Power the backplane by plugging the wall-adaptor end of the shore power cable into an available wall socket and the other end into one of the RS-485 jacks on the backplane.
- (c) Take the AVR programmer and attach the PDI programming header to the appropriate site on the target board. Note that the connector is keyed and will only attach to the target site in one way. Plug the USB end of the AVR programmer into an available USB port on the PC. Check that the status light on the AVR programmer is green. If it is red, double-check that the system is powered.
- (d) Change to the `software/majortom` directory and use the `avr-program.sh` script to do the programming. As an example, if the program to be loaded is located in the `software/majortom/build-avr/` directory and is called `prog.hex`, then the following command sequence will carry out the programming:

```
$ ./avr-program.sh build-avr/prog.hex
```

The status light on the AVR programmer will blink as the program is written into memory. When it is finished, a line like the following will be displayed:

```
avrdude: verifying ...
avrdude: 11298 bytes of flash verified

avrdude: safemode: Fuses OK

avrdude done. Thank you.
```

The program will automatically begin execution.

NB: This step may require root permissions if the account of the user doing the programming does not have access rights to the system's USB hardware.

A.3.2 GPC ARM Microcontroller

The procedure for programming the GPC ARM microcontroller is only slightly more complicated than that for programming the AVR's. Programming the ARM requires the following:

- The target board to be programmed
- The program to be flashed, in the form of a *.elf file. (This should be produced automatically when the program is built using the project make scripts.)
- One backplane board with at least one RS-485 connector and at least one row of circuit board connection headers.
- One ARM-USB-OCD programmer.
- One shore power cable.
- One PC with all necessary software dependencies installed, a copy of the project Git repository, and at least one USB port.

To program the ARM, follow these steps:

- (a) Take the backplane board and insert the target GPC board to be programmed into an available row of circuit board connection headers.
- (b) Power the backplane by plugging the wall-adaptor end of the shore power cable into an available wall socket and the other end into one of the RS-485 jacks on the backplane.
- (c) Take the ARM-USB-OCD programmer and attach the programming header to the appropriate site on the target board. Note that the connector is keyed and will only attach to the target site in one way. Plug the USB end of the programmer into an available USB port on the PC.

(d) Inside the `software/majortom/`, start up Open OCD by typing `openocd` at a command prompt. This *must* be run inside `software/majortom/`, since this is where the project's Open OCD configuration file resides.

(e) Again inside `software/majortom/`, fire up GDB on the program to be loaded. For example, if it is located in `software/majortom/build-arm/` and is called `prog.elf`, running

```
$ arm-elf-gdb build-arm/prog.elf
```

will do the trick.

(f) Open OCD runs a GDB local server on port 3333. Connect to it by issuing

```
(gdb) target remote localhost:3333
```

at the GDB prompt.

(g) Run the following sequence of GDB commands:

```
(gdb) monitor halt
```

```
(gdb) monitor reset
```

```
(gdb) monitor flash erase_sector 0 0 15
```

```
(gdb) load
```

The first two commands halt the ARM and reset it into a known state. The third erases the flash memory in preparation for loading the new program. Finally, the fourth command writes the program into memory.

(h) Due to certain issues with the interaction between GDB and Open OCD, the first attempt to load a program onto the ARM almost always fails in spite of the fact that GDB displays text indicating that the program has been successfully loaded. To get around this, quit out of GDB by typing `quit` at the GDB prompt. Then, repeat steps 3e-3g again to load the program a second time.

(i) Have the ARM resume program execution by running

```
(gdb) jump _vec_reset
```

```
(gdb) continue
```

at the GDB prompt. The first command sets the ARM to begin executing starting at its reset vector, and the second actually runs the program.

A.4 Assigning Board IDs

Board ID numbers are used to uniquely identify each board in the system for the purposes of addressing bus packets (see section 3.2.1). This section describes how to write a board ID into the EEPROM of a board's AVR microcontroller.

Programming board IDs requires the following materials:

- One backplane board with at least two RS-485 connectors and at least one row of circuit board connection headers. Make sure that no circuit boards are plugged into it.
- The board to which the ID is being assigned.
- One RS-485 transceiver cable.
- One shore power cable.
- One AVR programmer.
- One PC with all necessary software dependencies installed, a copy of the project Git repository, and at least one USB port.

To write the board ID into the EEPROM of an AVR, follow these steps:

1. Select an ID number for the board. The ID should be different from the ID assigned to any other board and must be representable using an 8-bit unsigned integer value.

2. Open the `write_boardid.c` file in the `software/majortom/src/avr/` directory. Set the first value of the `boardIDstr` array to the ID number to be assigned to the board. The remaining values in the array should form a null-terminated string that identifies the type of the board being programmed:

- GPC Board: `'gpc'`
- Radio Board: `'radio'`
- Servo Board: `'servo'`
- Sensors Board: `'sensors'`

When these changes have been made, save the file.

3. Build the board ID writing program by running

```
$ make build-avr/write_boardid.hex
```

in the `software/majortom/` directory.

4. Plug the board to be programmed into the backplane. Power the backplane using the shore power cable.

5. Connect the AVR programmer to a USB port on the PC and to the appropriate site on the target sensors board. Write the board ID writing program into memory on the board's AVR by running

```
$ ./avr-program.sh build-avr/write_boardid.hex
```

at the command prompt inside the `software/majortom/` directory.

6. At this point, the board should be programmed with its new board ID. To see that check that the write was successful, use an RS-485 transceiver cable to listen to traffic on bus 2. The program will continuously stream out the ASCII hexadecimal representation of the new ID on that bus. Alternatively, use the `avrdude` program's terminal mode to examine the contents of the EEPROM directly by connecting an AVR programmer to both the target board and the PC and running

```
$ ./avr-avrdude-terminal.sh
```

at the command prompt inside the `software/majortom/` directory. This will open up an interactive `avrdude` terminal session for the sensors board AVR. Run the command `dump eeprom` at the `avrdude` prompt to view the EEPROM pages that were written.

A.5 Hardware-in-the-Loop Testing

Hardware-in-the-loop (HITL) testing is useful for trying out changes to the autopilot using a flight simulator before testing them in an actual flight. See section 4.3 for more details. This section gives the procedure for setting up an HITL test.

Setting the system up for HITL testing requires the following materials:

- One backplane board with at least two RS-485 connectors and at least one row of circuit board connection headers. Make sure that no circuit boards are plugged into it.
- One GPC board, programmed with the firmware to be tested.
- One shore power cable.
- One RS-485 transceiver cable.

- One PC with all necessary software dependencies installed, a copy of the project Git repository, and at least one USB port. It must be capable of running the Houston ground control software.
- One PC with the X-Plane flight simulator installed. This can be the same as the PC used to run the ground software, or it can be a separate machine entirely. If a separate machine is used, both PCs must have ethernet ports, and one standard ethernet connection cable is also required.

To test the system in HITL mode, use the following procedure:

1. Plug the GPC board into the backplane. Power the backplane using the shore power cable, and connect one end of the RS-485 transceiver cable to the bus that the GPC will use to issue its packet requests. Connect the other end of the USB cable to an available USB port on the PC that will run the ground software. Be sure to note its assigned device node.
2. If X-Plane is to be run on a computer different from the ground software, connect the ethernet ports of the computers together with an ethernet cable. Use the computers' network configuration utilities to set up an ad-hoc wired network between them. Take note of the IPv4 address assigned to each.

NB: If no network cable is available, a wireless ad-hoc network can also be used.

3. Start up Houston on the PC that will run the ground software. From the "UAV" menu, select "I/O Configuration." When the "I/O Configuration" dialog appears, select the "Network" tab. In the "Local IP" field, enter the IPv4 address of the computer running the ground software. More precisely, if the computer running the ground software is also the computer that will run X-Plane, set this field to 127.0.0.1; otherwise, set it to the address

assigned to the network interface on the computer running the ground software that is connected to the computer that will run X-Plane.

4. Set the the local-IP port number to 38000.
5. In the “X-Plane IP” field, enter the IP address of the computer running X-Plane. Again, if this is the same as the computer being used to run the ground software, set this field to 127.0.0.1. Otherwise, enter the IP assigned to the network interface on the computer running X-Plane that is connected to the computer running the ground software.
6. Set the X-Plane IP port number 49000.
7. If the computer hosing X-Plane runs on a different computer architecture from the computer running the ground software, check the “Endian” box if the endianness of the architectures are different. In particular, if the computer running the ground software is running on an x86 platform and the machine running X-Plane is a Mac, this box must be checked to prevent X-Plane from crashing.
8. Fill in the “RS485 bus” field with the device node of the RS-485 transceiver that will be used to receive packets from the GPC. Set the serial rate to 921600.
9. Click the “Apply” button and close out of the “I/O Configuration” dialog.
10. Start up X-Plane. Set X-Plane to listen for UDP packets on the correct IP. Select the airframe model and world location to be be used for the test.
11. Set the ground software to operate in HITL testing mode by selecting “Hardware-in-the-Loop” from the “UAV” menu.
12. When everything else is ready, select “Activate” from the UAV menu to begin the HITL test.

A.6 Software Utilities

This section describes some of the PC utilities the team created in addition to the Houston ground control software to help with processing telemetry data and other tasks.

teldecode The `teldecode` utility is used for processing logfiles generated by Houston. In particular, it is used for extracting and displaying downlinked telemetry data, but it can also extract any of the other data stored in the logfile, including logged RS-458 bus packets.

`teldecode` reads data from standard input and writes to standard output, so it can be easily used as part of a data processing pipeline. For instance, running

```
$ teldecode < telemetry.log | grep "gyro_axis1" | cut -f 2 -d "="
```

will produce a list of all downlinked pitch gyroscope data stored in `telemetry.log`.

tel2csv.pl `tel2csv.pl` is a Perl script which is used in conjunction with `teldecode` to convert logged telemetry data into the comma-delimited CSV format so that it can be imported into a spreadsheet program for further analysis. Like `teldecode`, `tel2csv` reads all of its data on standard input and writes the results of its processing to standard output. For example, the command pipeline

```
$ teldecode < telemetry.log | tel2csv.pl > teldata.csv
```

will dump the telemetry data stored in `telemetry.log` to the file `teldata.csv`.

busmonitor and busmonitor2 `busmonitor` and `busmonitor2` are both programs that can be used for monitoring traffic traveling on one of the four RS-485 system buses. `busmonitor` writes all of the traffic it observes to standard output and is capable of outputting observed bytes either in raw-binary form or in ASCII-encoded hexadecimal. `busmonitor2` offers only

ASCII-encoded hexadecimal output but displays the traffic in a more organized format using a simple ncurses-based interface. Unlike `busmonitor`, `busmonitor2` also parses the traffic into packets and even parses the packet headers, allowing the traffic to be displayed as a sequence of packets instead of just as a stream of bytes.

These programs were useful for early debugging efforts but were largely superseded with the advent of the logging capabilities of the Houston ground control software and the `teldecode` log parser. Nevertheless, they still a few specialized uses. For instance, `busmonitor` is used in binary output mode for acquiring sensor calibration data (see section A.7).

cd2matlab `cd2matlab` is a utility for taking raw sensors calibration data dumps and converting them to the format expected by the MATLAB calibration scripts. For more information on this utility, see section A.7.

A.7 Sensor Calibration Procedure

This section describes the procedures for taking sensor calibration data, using it to generate calibration values, and loading them into EEPROM on the sensors board for application.

There are four types of sensors that must be calibrated: the accelerometers, magnetometers, gyroscopes, and the differential pressure sensor used for taking airspeed data. The BMP085 static pressure and temperature sensor from Bosch (see section 3.1.4) comes from the factory loaded with calibration values, which the sensors board reads as part of the I2C startup sequence. It may be desirable to perform additional calibration, but procedures for doing this have not yet been developed.

The calibration procedures make use of the ground software in addition to several other software utilities. For a description of these utilities, see section A.6. A computer with MATLAB installed is required to run the calibration scripts.

A.7.1 Step 1: Data Collection

The first step in the calibration process is to take calibration data. The procedure varies for each type of sensor.

A.7.1.1 Accelerometers

The procedure for acquiring accelerometer calibration data requires the following materials:

- One backplane board with at least three RS-485 connectors and at least one row of circuit board connection headers. Make sure that no circuit boards are plugged into it.
- Sensors board with accelerometers to be calibrated.
- One shore power cable.
- Two RS-485 transceiver cables.
- One AVR programmer.
- One PC with all necessary software dependencies installed, a copy of the project Git repository, and at least two USB ports.

To take accelerometer calibration data, use the following procedure:

1. Open the `sensors03.h` source file in the `software/majortom/src/avr/` subdirectory of the project repository. Near the top of the file (within the first 30 lines) should be a line containing a `#define SENSORS_USE_RAW_VALS` preprocessor directive. If this line is commented out, comment it in and save the file.

Defining this symbol sets up the sensors firmware to use raw sensor values instead of trying to apply any calibration values that may already be stored on the device. It also

ensures that the values are stored in a manner that is compatible with the calibration MATLAB scripts.

2. Open the `sensors03_take_caldata.c` source file in the `software/majortom/src/avr/` subdirectory of the project repository. Near the top of the file is a line with a preprocessor directive that defines the symbol `DATA_CAPTURE_BUS`, e.g. `#define DATA_CAPTURE_BUS 2`. The value of this preprocessor symbol is a number between and including 0 and 3 that corresponds to the bus to which calibration data will be dumped for capture. For example, `#define DATA_CAPTURE_BUS 2` sets bus 2 as the data capture bus. Change this value to the desired bus number and save the file.
3. Still in `sensors03_take_caldata.c`, near the top of the file is a line with a preprocessor directive defining the `USE_MANUAL_DATA_CAPTURE` symbol. Make sure that this line is not commented out and save the file.

Defining the `USE_MANUAL_DATA_CAPTURE` symbol configures the sensors firmware to dump calibration values out to the data capture bus only when the user tells it to by sending a specific character over a different bus. If this symbol is not defined, the sensors board will stream data continuously onto the data capture bus. For accelerometer calibration, manual data capture is used.

4. Compile the `sensors03_take_caldata.hex` firmware program by running

```
$ make build-avr/sensors03_take_caldata.hex
```

in the `software/majortom/` directory.

5. Plug the sensors board with the accelerometers to be calibrated into the backplane.
6. Power the backplane by plugging the wall-adaptor end of the shore power cable into an available wall socket and the other end into one of the RS-485 jacks on the backplane.

7. Connect an AVR programming header to a USB port on the PC and to the appropriate site on the target sensors board. Write the calibration data dump program into memory on the sensors board AVR by running

```
$ ./avr-program.sh build-avr/sensors03_take_caldata.hex
```

at the command prompt inside the `software/majortom/` directory. If the programming of is successful, unplug the AVR programmer from the PC and the sensors board and set it aside. Otherwise, fix any errors that arise and make sure that the board is programmed before continuing.

8. Connect two RS-485 transceivers to the PC. Plug one into bus 0 and the other into the data capture bus defined in step 2. Be sure to note the device node assigned to each transceiver. For convenience, it will be assumed for the remainder of this procedure that the transceiver connected to bus 0 has device node `/dev/ttyUSB0` and that the one connected to the data capture bus is on `/dev/ttyUSB1`.
9. Open up a `minicom` serial console on bus 0:

```
$ minicom -D /dev/ttyUSB0
```

Set the serial speed to 921600 bps. This console will be used to signal the sensors board when it is time for it to capture data.

10. Capture of the data will be done using using the `busmonitor` program. If necessary, build it by issuing the command

```
$ make build-pc/busmonitor
```

in the `software/majortom/` directory.

11. Enter the `software/majortom/build-pc/` directory and set the `busmonitor` program to begin listening on the data capture bus and saving any packets to an output file. For example,

```
$ ./busmonitor /dev/ttyUSB1 921600 > caldata.dat
```

will monitor the bus connected to the RS-485 transceiver with device node `/dev/ttyUSB1` and will save all data to a file named `caldata.dat`.

12. Position the sensors board in the desired orientation for measurement by rotating the board assembly. Calibration requires data from six different orientations, three with each principal axis aligned parallel to the direction of gravity, and three with each principal axis aligned antiparallel (i.e., pointing in the direction exactly opposite) to the direction of gravity. (See the accelerometer datasheet for axis positioning.) The order in which each set of data is taken does not matter.
13. Holding the board steady in the desired orientation, use the `minicom` terminal to send the character 'A' (capital 'A', ASCII 0x41) over bus 0 to the sensors board. The board will respond by sending data back across the data capture bus, which will be picked up by the `busmonitor` program and stored in the output file. Repeat this step 10 times to take 10 measurements.

NB: The number of measurements taken may be increased beyond 10 if desired; however, one must make sure to take the same number of measurements for each orientation in order to avoid biasing the zero-offset measurements.

14. Repeat steps 12-13 for each remaining orientation.
15. Stop the `busmonitor` data capturing process by sending it a `CTRL-C` character. Take the data file and save it somewhere where it can be accessed for use in the pre-processing step that follows.

A.7.1.2 Magnetometers

The procedure for acquiring magnetometer calibration data requires the following materials:

- Airframe fuselage with backplane and motor installed.
- Sensors board with magnetometers to be calibrated.
- One servo board.
- One nickel-cadmium battery with a connector attached for use with the low-voltage battery input on the servo board.
- One shore power cable.
- One RS-485 transceiver cable.
- One AVR programmer.
- One PC with all necessary software dependencies installed, a copy of the project Git repository, and at least one USB port.

To take magnetometer calibration data, follow these steps:

1. Complete steps 1 and 2 of the accelerometer calibration procedure, above.
2. Still in `sensors03_take_caldata.c`, near the top of the file is a line with a preprocessor directive defining the `USE_MANUAL_DATA_CAPTURE` symbol. Make sure that this line is commented out and save the file. For magnetometer calibration, manual data capture is not used; data must be continuously streamed to the bus.
3. Complete step 4 of the accelerometer calibration procedure, above.
4. Plug the servo board and the sensors board with the accelerometers to be calibrated into the backplane inside the airframe.

5. Complete steps 6 and 7 of the accelerometer calibration procedure, above. (When connecting the AVR programmer, it may be easier to remove the sensors board from the backplane, attach the programmer, and then plug the board back into the backplane.)
6. Disconnect the shore power cable from the backplane.
7. Move the data collection setup to a location outdoors, away from buildings and large metal objects. (These distort the Earth's magnetic field in their proximity, damaging the quality of the gathered data). Be sure to take the nickel-cadmium battery, which will be used to power the system without shore power while data is being collected. Make sure that the battery is charged.
8. Connect one RS-485 transceiver cable to the PC. Plug it into the data capture bus defined in the `sensors03_take_caldata.c` source file. Be sure to note the device node assigned to the transceiver. For convenience, we will assume for the remainder of this procedure that the transceiver is on `/dev/ttyUSB1`.
9. The `busmonitor` program is used to capture the required data. Complete steps 10 and 11 of the accelerometer calibration procedure.
10. Connect the nickel-cadmium battery to the low-voltage battery connection site on the servo board. (It may be easier to remove the servo board from the backplane, connect the battery, and then plug the board back into the backplane.) Since the system should now be powered, data should now be streaming to the PC over the bus. You can verify this by watching the size of the data dump file and seeing if it grows with time.
11. Carefully pick up the plane and rotate it through a wide range of random orientations and headings. Be sure to rotate it a full 360 degrees about each principal axis (axial, trans-axial, and normal) at least once: the more points collected from the various octants of the ellipsoid, the better the resulting fit will be.

12. After collecting data for about 60-90 seconds, stop the `busmonitor` data capturing process by sending it a `CTRL-C` character. Take the data file and save it somewhere where it can be accessed for use in the pre-processing step that follows.
13. Disconnect the nickel-cadmium battery. Be sure to recharge it before its next use.

A.7.1.3 Gyroscopes

The procedure for acquiring gyroscope calibration data requires the following materials:

- One backplane board with at least two RS-485 connectors and at least four rows of circuit board connection headers. Make sure that no circuit boards are plugged into it.
- Sensors board with gyroscopes to be calibrated.
- One servo board.
- One radio board, programmed with the radio firmware that will be used in actual flight. In particular, it must be capable of transmitting telemetry packets.
- One GPC board programmed with the GPC firmware that will be used in actual flight. In particular, it must be capable of issuing requests for high-rate sensors data and using the replies to assemble telemetry packets containing the gyroscope data, which it then ships to the radio board for transmission.
- One nickel-cadmium battery with a connector attached for use with the low-voltage battery input on the servo board.
- One shore power cable.
- One AVR programmer.
- XTend radio ground module.

- One PC with all necessary software dependencies installed, a copy of the project Git repository, and at least one USB port. The computer must be capable of running the “Houston” ground control software.
- One $33\frac{1}{3}$ RPM turntable with printed calibration pattern. Turntables with other rotational rates can also be used.
- One LED with through-hole leads. Brighter is better: this LED will be used to create a stroboscope tachometer to make a more precise measurement of the turntable’s rotational rate.
- One function generator with a BNC output connector.
- One oscilloscope with BNC input connectors. It is very helpful if the oscilloscope has a built-in frequency measurement feature.
- One pair of BNC clip leads.
- One BNC cable.
- One BNC T-connector.

To take gyroscope calibration data, use the following procedure:

1. Complete step 1 of the accelerometer calibration procedure.
2. Re-compile the main set of sensors firmware by issuing

```
$ make build-avr/main_sensors03.hex
```

in the `software/majortom/` directory. Note that the firmware must be configured to at least have the sensors board respond properly to requests for high-rate data.

3. Plug the servo board, target sensors board, radio board, and GPC board into the backplane.
4. Power the backplane by plugging the wall-adapter end of the shore power cable into an available wall socket and the other end into one of the RS-485 jacks on the backplane.
5. Connect an AVR programming header to a USB port on the PC and to the appropriate site on the target sensors board. Write the calibration data dump program into memory on the sensors board AVR by running

```
$ ./avr-program.sh build-avr/main_sensors03.hex
```

at the command prompt inside the `software/majortom/` directory. If the programming of is successful, unplug the AVR programmer from the PC and the sensors board and set it aside. Otherwise, fix any errors that arise and make sure that the board is programmed before continuing.

6. Disconnect the shore power cable.
7. Connect the XTend ground module to a USB port on the PC. Be sure to note the device node that it is assigned. For convenience, it will be assumed for the remainder of this procedure that the radio has been assigned `/dev/ttyUSB0`.
8. Load up the “Houston” ground software by running

```
$ wx/GroundControl
```

at the command prompt inside the `software/houston` directory. If necessary, build the ground software first by issuing

```
$ make wx/GroundControl
```

inside the same directory.

9. Inside the ground software, open the “UAV” menu and select “I/O Configuration.” In the dialog box that appears, click on the “Network” tab. Make sure that the device node and serial speed for the XTend radio are correct. If you change any values, click the “Apply” button. Close the “I/O Configuration” dialog.
10. Again inside the ground software, open the “UAV” menu and select the “Live Flight” option. With this, the ground software is set up for data collection.
11. Plug the BNC T-adapter into the output port on the function generator. Using the BNC cable, connect one side of the T-adapter to an oscilloscope, and using the BNC clip leads, connect the other side of the T-adapter to the LED. Set the function generator to output a square wave of a “reasonable” amplitude and frequency. (The frequency will be adjusted in the next step, but the amplitude must not exceed the limits of the LED.)
12. Aim the LED at the calibration pattern on the turntable and have the turntable begin rotating. Once the turntable has reached its steady-state speed, adjust the LED blink frequency using the function generator until it matches that of the rotating pattern. (The pattern will appear to stop rotating within the LED’s field of illumination.) Measure this frequency using the oscilloscope and use it along with the pattern’s spatial frequency to calculate the rotational rate of the turntable. Write this number down for future reference.
NB: Beware of aliasing effects. For example, if the LED is blinking at half the rate at which the pattern is rotating, the pattern will still appear to be stopped, even though the rates do not match. One way to check for aliasing is to double the frequency of the LED and see if the pattern still stops. If it does, then the previous frequency was too low. Additionally, one can compare the measured rotational rate to the rated speed of the turntable. If these numbers do not match fairly closely, it is possible that the measured

rate was made using an alias frequency instead of the true value.

13. Disconnect the stroboscope tachometer setup and set it aside.
14. Mount the system on the turntable in the desired orientation. There are three orientations for which measurement data must be taken, one for rotation about each gyroscope axis. The system should be mounted so that it rotates in the clockwise direction about the axis being measured. (Depending on the axis, this corresponds to one of pitch-down, roll-left, or yaw-right motion.)
15. Connect the nickel-cadmium battery to the low-voltage battery connection site on the servo board. (It may be easier to remove the servo board from the backplane, connect the battery, and then plug the board back into the backplane.) Since the system should now be powered, telemetry data should be being sent to the PC. You can verify this by checking for the flashing lights on the ground radio module, but *do not* set the ground software to being saving the telemetry just yet.
16. Set the turntable to begin rotating, and wait for it to reach a steady-state speed.
17. Inside the ground software, select “Activate” from the “UAV” menu. If everything is set up correctly, the software should be receiving telemetry that contains the gyroscope values from the rotating assembly. Note that it is extremely important that this step be performed *after* the assembly is set in motion and not before.
18. After collecting data for 30-60 seconds, de-select the “Activate” option in the “UAV” menu of the ground software, stop the rotating assembly, and disconnect the nickel-cadmium battery. A telemetry file should have been created in the `/tmp` directory with the data downlinked while the assembly was in motion. Save this file somewhere where it can be accessed for the data pre-processing step that follows. Make sure that the filename indicates which axis was being measured.

19. Repeat steps 14-18 for each remaining orientation.

20. Repeat steps 15 and 17-18 with the boards in a stationary, non-rotating configuration.

This measurement will be used to correct for zero-offsets in the gyroscope values. Save the data file somewhere where it can be accessed for the data pre-processing step that follows. Make sure that the filename indicates that the measurement was made with the boards stationary.

You should end up with four telemetry logs: three that each have rotational data for one of the gyroscope axes apiece and one with stationary data taken for all three axes simultaneously.

A.7.1.4 Differential Pressure Sensor

The easiest method for calibrating the differential pressure sensor is to use an already-calibrated sensor as a reference. The team was fortunate enough to have access to such a system at the wind tunnel located in the basement of Rice's Ryon Laboratory. The procedure outlined here assumes the use of this (or a similar) setup.

The procedure for acquiring differential pressure calibration data requires the following materials:

- One backplane board with at least two RS-485 connectors and at least one row of circuit board connection headers. Make sure that no circuit boards are plugged into it.
- Sensors board with sensor to be calibrated.
- One shore power cable.
- One RS-485 transceiver cable.
- One AVR programmer.

- One pitot tube with plastic tubing for connection to the input ports on the differential pressure sensor.
- One PC with all necessary software dependencies installed, a copy of the project Git repository, and at least one USB port.

To take differential pressure calibration data, use the following procedure:

1. The firmware setup for gathering differential pressure calibration data is the same as that for magnetometer data collection. Complete steps 1-6 of the magnetometer calibration procedure, above.
2. Use plastic tubing to attach a pitot tube to the input ports on the differential pressure sensor. Be sure to check the polarity is correct. (The easiest way to check polarity is to take a set of calibration data as described below and then look at the values. The sensor should give positive readings for increased flow rates.)
3. Mount the pitot tube inside the wind tunnel. *Only* the pitot tube should be placed in the wind tunnel; the backplane with the sensors board must remain outside of the tunnel for easy access.
4. Connect one RS-485 transceiver cable to the PC. Plug it into the data capture bus defined in the `sensors03_take_caldata.c` source file. Be sure to note the device node assigned to the transceiver. For convenience, we will assume for the remainder of this procedure that the transceiver is on `/dev/ttyUSB1`.
5. Set the wind tunnel flow rate to the desired speed, as measured by the wind tunnel's own pitot-static system. This procedure assumes the use of calibration flow speeds that generate differential pressures of 0, 0.05, 0.12, 0.20, 0.30, and 0.44 inches of water. At the Ryon Lab wind tunnel, these correspond to flows of 0, 10, 15, 20, 25, and 30 mph,

respectively. Other pressures/flow rates can be used, but this will require changes to the calibration scripts later on.

6. Make sure that the backplane is unpowered.
7. When the wind tunnel flow has stabilized, set up the `busmonitor` program to capture data as described in steps 10 and 11 of the accelerometer calibration procedure.
8. Connect the shore power cable to the backplane. The sensors board should begin streaming its data over the bus, and the `busmonitor` program should capture this data and save it to a file.
9. After collecting data for about 15 seconds, disconnect the shore power cable from the backplane. Stop the `busmonitor` data capturing process by sending it a `CTRL-C` character. Take the data file and save it somewhere where it can be accessed for use in the pre-processing step that follows.
10. Repeat steps 5-9 for each desired flow rate. You should end up with six data files, one for each flow rate tested.

A.7.2 Step 2: Pre-Processing

In this step, the raw data dumps generated by the previous step are converted to the formats required by the calibration scripts.

A.7.2.1 Accelerometer, Magnetometer, and Differential Pressure Data

To pre-process calibration data from these sensors, run the raw data file produced in the data collection step through the `cd2matlab` program. This program strips away frame delimiters and escape bytes added by the `sensors03_take_caldata.c` program to help determine boundaries between data packets. First, if necessary, build the `cd2matlab` program by running

```
$ make build-pc/cd2matlab
```

in the `software/majortom/` directory.

The `cd2matlab` program takes the name of the data file to be processed as an input argument and writes the processed data to standard output. For instance, if raw accelerometer data was saved to `raw_data.dat` in the `software/majortom/build-pc/` directory, it can be processed by running

```
$ cd2matlab raw_data.dat > caldata_accel.dat
```

in the `software/majortom/build-pc/` directory. The processed data will be written to the file `caldata_accel.dat`.

Process each data file generated in the data collection step in this manner. For the accelerometer and magnetometer data, this means the one file that the procedures for each of these sensors generate. For differential pressure data, the data file from each individual flow rate must be processed separately. Be sure to give each processed data file a different name that describes its contents and save them for use in the next step.

A.7.2.2 Gyroscope Data

The gyroscope data must be extracted from telemetry logfiles generated during the data collection process. This is accomplished by using the `teldecode` program to read the telemetry log and the Unix utilities `grep` and `cut` to extract the relevant values.

For the purpose of this example, it is assumed that the gyroscope telemetry logs are contained in the files `gyro_axis1_pitch.log`, `gyro_axis2_roll.log`, `gyro_axis3_yaw.log`, and `gyro_stationary.log` and that they have been moved to the `software/majortom/build-pc` directory for processing.

First, if necessary, build the `teldecode` program by issuing

```
$ make build-pc/teldecode
```

in the `software/majortom/` directory. Change to the `software/majortom/build-pc` directory and run the following commands:

```
$ teldecode < gyro_axis1_pitch.log | grep "gyro_axis1" | cut -f 2 -d "=" \  
    caldata_gyro_rot1.dat
```

```
$ teldecode < gyro_axis2_roll.log | grep "gyro_axis2" | cut -f 2 -d "=" \  
    caldata_gyro_rot2.dat
```

```
$ teldecode < gyro_axis3_roll.log | grep "gyro_axis3" | cut -f 2 -d "=" \  
    caldata_gyro_rot3.dat
```

```
$ teldecode < gyro_stationary.log | grep "gyro_axis1" | cut -f 2 -d "=" \  
    caldata_gyro_stat1.dat
```

```
$ teldecode < gyro_stationary.log | grep "gyro_axis2" | cut -f 2 -d "=" \  
    caldata_gyro_stat2.dat
```

```
$ teldecode < gyro_stationary.log | grep "gyro_axis3" | cut -f 2 -d "=" \  
    caldata_gyro_stat3.dat
```

This will save the rotational and stationary data for axis 1 to the files `caldata_gyro_rot1.dat` and `caldata_gyro_stat1.dat`, respectively, and similar for the other axes. Take these output files and save them for use in the next step.

A.7.3 Step 3: Model Fitting and Analysis

In this step, models are fit to the calibration data, but the model parameters are not prepared for loading into the EEPROM on the sensors board. The user examines the quality of the computed models and decides if they are suitable for use or if another set of calibration data should be taken instead.

Fitting models to the calibration data is accomplished through the use of the following MATLAB scripts:

- `cal_accel.m` – Generate accelerometer calibration values.
- `cal_mag.m` – Generate magnetometer calibration values.
- `cal_gyro.m` – Generate gyroscope calibration values.
- `cal_airspeed.m` – Generate differential pressure sensor calibration values.

For more information on these routines and how they work, see section 4.2 and the comments within the individual files themselves. The user should not need to access any of these routines directly but should instead use the interface provided to them through the `caltest.m` and `gen_cal_prog.m` scripts. There are only two exceptions to this:

- The `RP_ROTATION_RATE` variable in the `cal_gyro.m` file needs to be updated with the rotation rate of the turntable measured in step 12 of the gyroscope calibration procedure. Convert the measurement made to have units of mrad/s and store the result in `RP_ROTATION_RATE`.
- If different pressure levels from those listed in step 5 of the differential pressure sensor calibration procedure were used for taking differential pressure data, these values (in inches of water) will need to be substituted into the 'p' array at the start of the function in the `cal_airspee.m` file. At the same time, their corresponding airspeed (in miles per hour) will need to be substituted into the 'a' array in the same file.

The `caltest.m` script is used for analyzing calibration data and the computed calibration models before the user is ready to commit to storing the values in the EEPROM on the actual sensors board for use. It accepts a single string argument that indicates which type of calibration is to be performed:

- 'accel' – Perform accelerometer calibration.
- 'mag' – Perform magnetometer calibration.
- 'gyro' – Perform gyroscope calibration.
- 'airspeed' – Perform differential pressure sensor calibration.

The paths to the data files used for calibration are coded into the script and must be changed before the script can be used to look at new set of data.

To use `caltest.m` to analyze calibration data, use the following procedure:

1. Decide which sensor data to analyze and locate all of the corresponding data files.
2. Edit the `caltest.m` script file in the `software/majortom/src/utils/` directory. At the top of the `caltest()` function are some variables that hold the paths to the calibration data files:
 - `acc_dat_file` – Path to accelerometer calibration data file, after pre-processing with `cd2matlab`.
 - `mag_dat_file` – Path to magnetometer calibration data file, after pre-processing with `cd2matlab`.
 - `gyro_stat_dat_files` – Cell array of paths to files with gyroscope data extracted from the telemetry logs generated with the gyroscopes at rest.
 - `gyro_rot_dat_files` – Cell array of paths to files with gyroscope data extracted from the telemetry logs generated with the gyroscopes in motion.
 - `airspeed_s_dat_files` – Cell array of paths to differential pressure sensor data files for each flow rate, after pre-processing with `cd2matlab`.

Change the values of these variables to contain the locations of the data to be analyzed. When finished, make sure to save the file.

NB: The order in which the paths are stored in the cell array variables above is very important. Read the comments in the headers and bodies of the `cal_gyro.m` and `cal_airspeed.m` scripts for information on how these arrays must be structured.

3. Run MATLAB. Change the working directory to the `software/majortom/utils` directory and run the `caltest.m` script at the prompt with the string argument corresponding to the sensor type to be analyzed. For example, `caltest('accel')` will run the accelerometer calibration routine on the data file specified in the `acc_dat_file` variable defined in the `caltest.m` script itself.
4. The script will generate some plots of the data and the fit models and will print some numerical data (e.g., mean square error, etc.) to the command window. Using this data, decide if the model looks acceptable or if another round of data collection is necessary. If the generated models are acceptable, proceed to the next step to store the calibration values in the EEPROM on the sensors board.

A.7.4 Step 4: Storing Values in EEPROM

Writing the calibration values to EEPROM is accomplished by using the `gen_cal_prog.m` script to create a program that loads the values into EEPROM when executed on the sensors board AVR. To do this, use the following procedure:

1. Edit the `gen_cal_prog.m` file in the `software/majortom/src/utils/` directory. Just as with the `caltest.m` program, the paths to the calibration data files to use are stored in variables within the `gen_cal_prog.m` script itself, and these must be updated to point to the data files to use. For a list of the variables that need to be changed and their

functions, see step 2 of the procedure for using `caltest.m` in section A.7.3, above. When finished, make sure to save the file.

2. Run MATLAB. Change the working directory to the `software/majortom/utils` directory and run the `gen_cal_prog.m` script at the prompt. This will run all of the calibration procedures for all the sensors, generate all of the calibration values, and create a file called `sensors03_write_caldata.c` in the `software/majortom/src/avr/` directory that will write them all into the EEPROM on the sensors board AVR.

NB: The `gen_cal_prog.m` program works by taking a pre-constructed template source file and then substituting the calibration values into certain lines in that template. Because MATLAB's native text processing facilities are poor, the `gen_cal_prog.m` calls the `sed` program to accomplish this task. This means that `sed` must be present on the system for this procedure to work.

3. Compile the `sensors03_write_caldata.c` program by running

```
$ make build-avr/sensors03_write_caldata.hex
```

at the command prompt inside the `software/majortom/` directory.

4. Write the `sensors03_write_caldata.hex` program into flash on the target sensors board AVR using the standard AVR programming procedure given in section A.3.1. To see that check that the write was successful, use an RS-485 transceiver cable to listen to traffic on bus 2. The program will continuously stream out the calibration values just written on that bus. Alternatively, use the `avrdude` program's terminal mode to examine the contents of the EEPROM directly by connecting an AVR programmer to both the target sensors board and the PC and running

```
$ ./avr-avrdude-terminal.sh
```

at the command prompt inside the `software/majortom/` directory. This will open up an interactive `avrdude` terminal session for the sensors board AVR. Run the command `dump eeprom` two or three times at the `avrdude` prompt to view the EEPROM pages that were written.

5. Open the `sensors03.h` file and comment out the line defining the `SENSORS_USE_RAW_VALS` symbol mentioned in step 1 of the accelerometer calibration data collection procedure.
6. Re-compile the main set of sensors firmware by issuing

```
$ make build-avr/main_sensors03.hex
```

in the `software/majortom/` directory.

7. Write the `main_sensors03.hex` program into flash on the target sensors board AVR using the standard AVR programming procedure given in section A.3.1.

The sensors board should now be loaded with the set of main sensors firmware, set to use the calibration values just written to EEPROM.

A.8 Compiling the ARM Development Toolchain

While compilation of the AVR development toolchain is fairly straightforward, the ARM development toolchain requires a slightly more specialized procedure in order to enable software emulated floating-point operations. If for some reason the user is unable to use the team's provided binary package (see section A.2), the ARM toolchain can be built from source using the following procedure. This assumes the user is working in a Linux environment with the usual development utilities (`gcc`, `make`, etc.) installed.

1. Create a directory in which to perform the build. For the sake of this procedure, it will be assumed that the build directory is `/usr/src/build/arm-elf/`. If a different directory is used, the instructions below will need to be modified accordingly.
2. Copy the following files from the `software/toolchains/arm-elf/` directory in the Git repository into the build directory:

- `99-gcc-arm-elf-multilib.patch`
- `INSTALL.txt`
- `do-binutils`
- `do-gcc`
- `do-newlib`
- `gcc_config_arm_t-arm-elf`

3. Acquire the following standard source packages from the Internet and save them in the build directory:

- `binutils-2.20.1.tar.bz2`
- `gcc-core-4.4.4.tar.bz2`
- `newlib-1.18.0.tar.gz`

4. Unpack each of these files in the build directory:

```
$ cd /usr/src/build/arm-elf/  
$ bunzip2 -cd binutils-2.20.1.tar.bz2 | tar -xv  
$ bunzip2 -cd gcc-core-4.4.4.tar.bz2 | tar -xv  
$ gunzip -cd newlib-1.18.0.tar.gz | tar -xv
```

This will create the following directories:

- `/usr/src/build/arm-elf/binutils-2.20.1`
- `/usr/src/build/arm-elf/gcc-4.4.4`
- `/usr/src/build/arm-elf/newlib-1.18.0`

5. To keep everything clean and separated, these builds for these packages will be performed in separate directories. Create them by running

```
$ cd /usr/src/build/arm-elf/  
$ mkdir build-binutils build-gcc build-newlib
```

at the command prompt.

6. Configure, build, and install the binutils package by running the following commands:

```
$ cd /usr/src/build/arm-elf/build-binutils/  
$ sh ../do-binutils  
$ make  
$ sudo make install
```

It will take a while for the build to complete. The last command will install programs into `/usr/local/bin/` and will also create the `/usr/local/arm-elf/` directory and several subdirectories.

7. The next step in the process is to build gcc, but first some of the header files from newlib must be copied into the new `/usr/local/arm-elf` directory structure. Run

```
$ mkdir -p /usr/local/arm-elf/include/  
$ cp -av /usr/src/build/arm-elf/newlib-1.18.0/newlib/libc/include/* \  
    /usr/local/arm-elf/include/
```

to do this.

8. Also prior to building gcc, the multilib configuration file must be patched. Run

```
$ cd /usr/src/build/arm-elf/  
$ patch -p1 < ./99-gcc-arm-elf-multilib.patch
```

to do this.

9. Build gcc by running the following commands:

```
$ cd /usr/src/build/arm-elf/build-gcc/  
$ sh ../do-gcc  
$ make  
$ sudo make install
```

It will take a long time for the build to complete. The last command will put programs into `/usr/local/bin/` and lots of files into `/usr/local/arm-elf/`, `/usr/local/lib/gcc/arm-elf/`, and `/usr/local/libexec/gcc/arm-elf/`.

10. Configure and build newlib:

```
$ cd /usr/src/build/arm-elf/build-newlib/  
$ sh ../do-newlib  
$ make  
$ sudo make install
```

All of newlib's files should go into `/usr/local/arm-elf/include/` and `/usr/local/arm-elf/lib/`.

11. With the completion of the last step, the ARM toolchain has been built. If desired, the build directory can now be removed:

```
$ rm -rf /usr/src/build/arm-elf/
```

A.9 Compiling Open OCD

This section describes the procedure for compiling the Open On-Chip Debugger for use with programming the ARM. It is assumed that the user has already installed `libFTDI` (version 0.18 or later) and `libconfuse` (version 2.5 or later). These packages are straightforward to compile and install and do not require any special compile-time options for them to work for this project.

1. Get the source for Open OCD from the Internet (e.g., from the Open OCD project page on SourceForge). As of this writing the latest version of Open OCD is 0.4.0, and the name of the file containing the source is `openocd-0.4.0.zip`.
2. Navigate to the directory in which the source was saved, and run

```
$ unzip openocd-0.4.0.zip
$ cd openocd-0.4.0
```

to unpack the source and switch to the build directory.

3. Issue

```
$ ./configure --enable-parport --enable-ft2232_libftdi
$ make
$ sudo make install
```

to build and install Open OCD. The `--enable-parport` option sets up Open OCD to work with the parallel port ARM-JTAG cable, and `--enable-ft2232_libftdi` enables support for the ARM-USB-OCD cable.

4. If desired, the build directory may be removed after the previous step is complete:

```
$ cd ..
$ rm -r openocd-0.4.0
```

A.10 Safety Precautions

A.10.1 Lithium-Polymer Batteries

The Lithium-Polymer batteries used in the aircraft have a surprising energy density. These must be charged and stored carefully and safely to avoid short circuits. The batteries are rated to safely discharge 175 amps, which is well in excess of what the three-phase motor can draw. The charger listed in Section C.3.3 is capable of safely charging the main battery.

The backup battery in the aircraft and the R/C transmitter use Nickel-Cadmium batteries. The charger in Section C.3.3 will also charge the backup battery safely when configured properly.

A.10.2 R/C Flying

There are many hazards involved in R/C flying. Following established R/C flight regulations, as documented in the AMA safety code [41], can reduce the risk of injury and mishap during flight operations.

When in an active configuration, the propeller poses a potential hazard. If the R/C transmitter is not turned on when the aircraft is powered, it may start in an undefined state. *Before activating the motor controller, ensure that the R/C transmitter is on.* Additionally, metal-bladed propellers may not be used, according to regulations.

R/C flying should only be performed in safe areas, where there is minimal risk to others and to property. Team Electric Owl recommends designated R/C fields, such as Dick Scobee Field in George Bush Park in west Houston.

A.10.3 Construction

Standard precautions should be taken when handling Cyanoacrylate-based adhesives in airframe construction, as these can adhere to flesh. Additionally, soldering components to the boards provides a potential source of burns. Food should be kept away from soldering equipment to prevent lead contamination.

A.11 Legal Requirements

A.11.1 FCC Radio Frequency Regulations

Radio communications with the flying aircraft are subject to FCC regulations. This falls under Title 47 of Federal Code: Telecommunication [26]. Operation within HAM bands should follow ARRL rules [43].

At present, the aircraft uses commercially-available transmitters in the unlicensed 900MHz and 2.4GHz bands below transmission power limits; however, the operator should be aware of these restrictions, and any additional radio links added to the aircraft verified to conform to these regulations.

A.11.2 FAA Flight Regulations

Flight operations of model and unmanned aircraft are subject to regulation by the FAA. Restrictions on model aircraft flight are documented in *Model Aircraft Operating Standards* [27]. Additional regulations on unmanned autonomous flight are available in *Unmanned Aircraft Operations in the National Airspace System* [28].

B Schematics and CAD Drawings

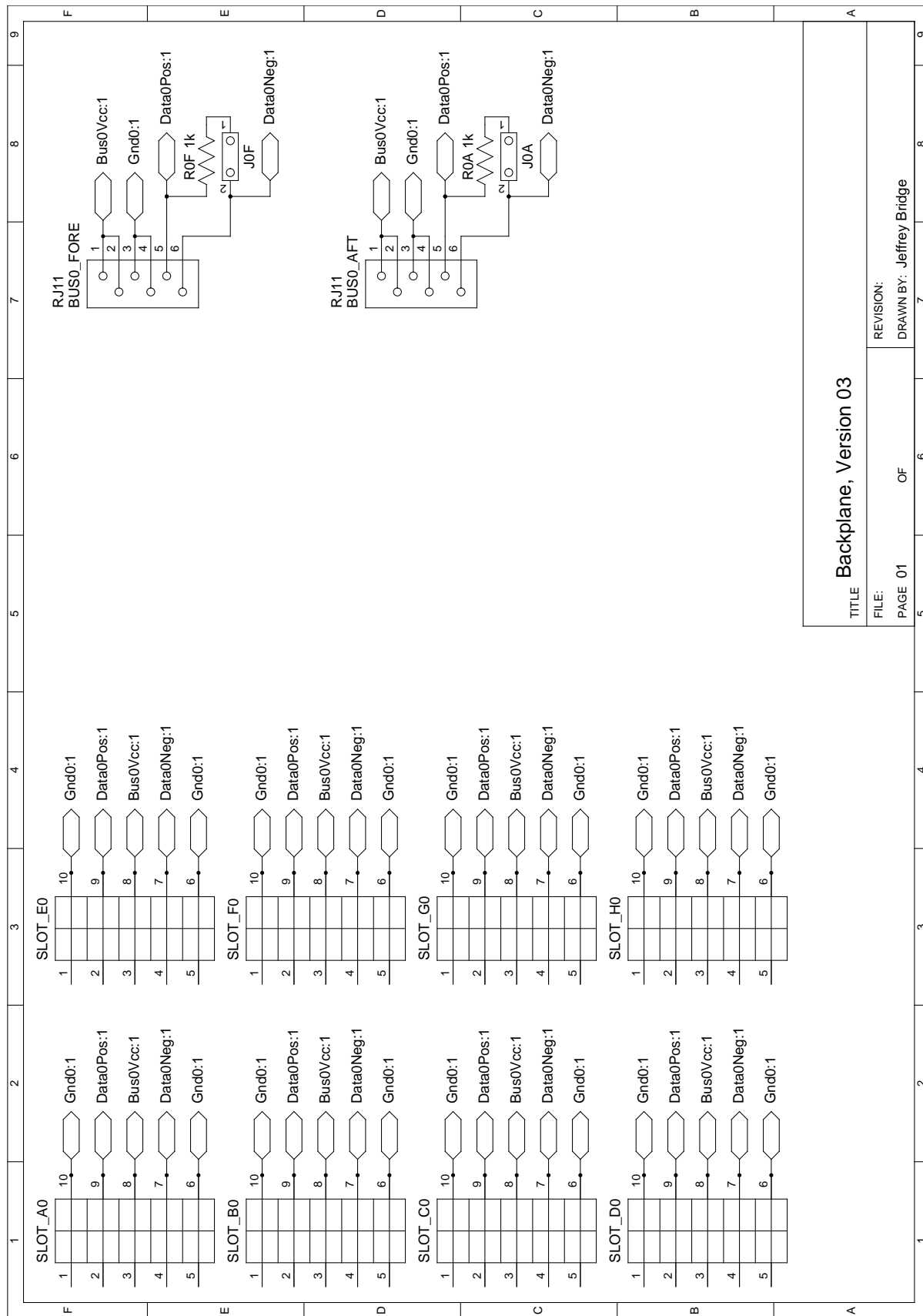


Figure B.1: Circuit schematic for backplane board, hardware revision 03, page 1 of 4.

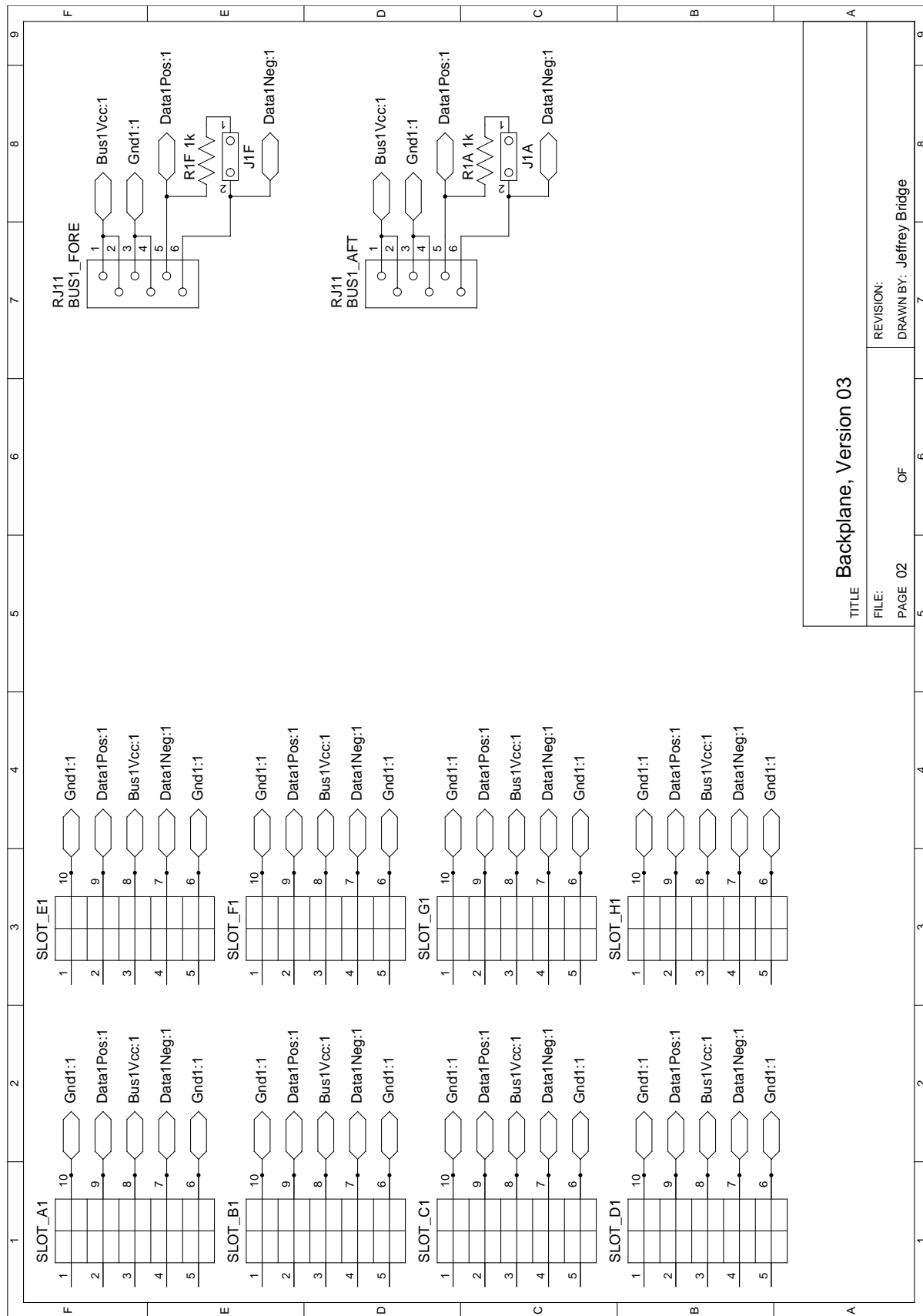


Figure B.2: Circuit schematic for backplane board, hardware revision 03, page 2 of 4.

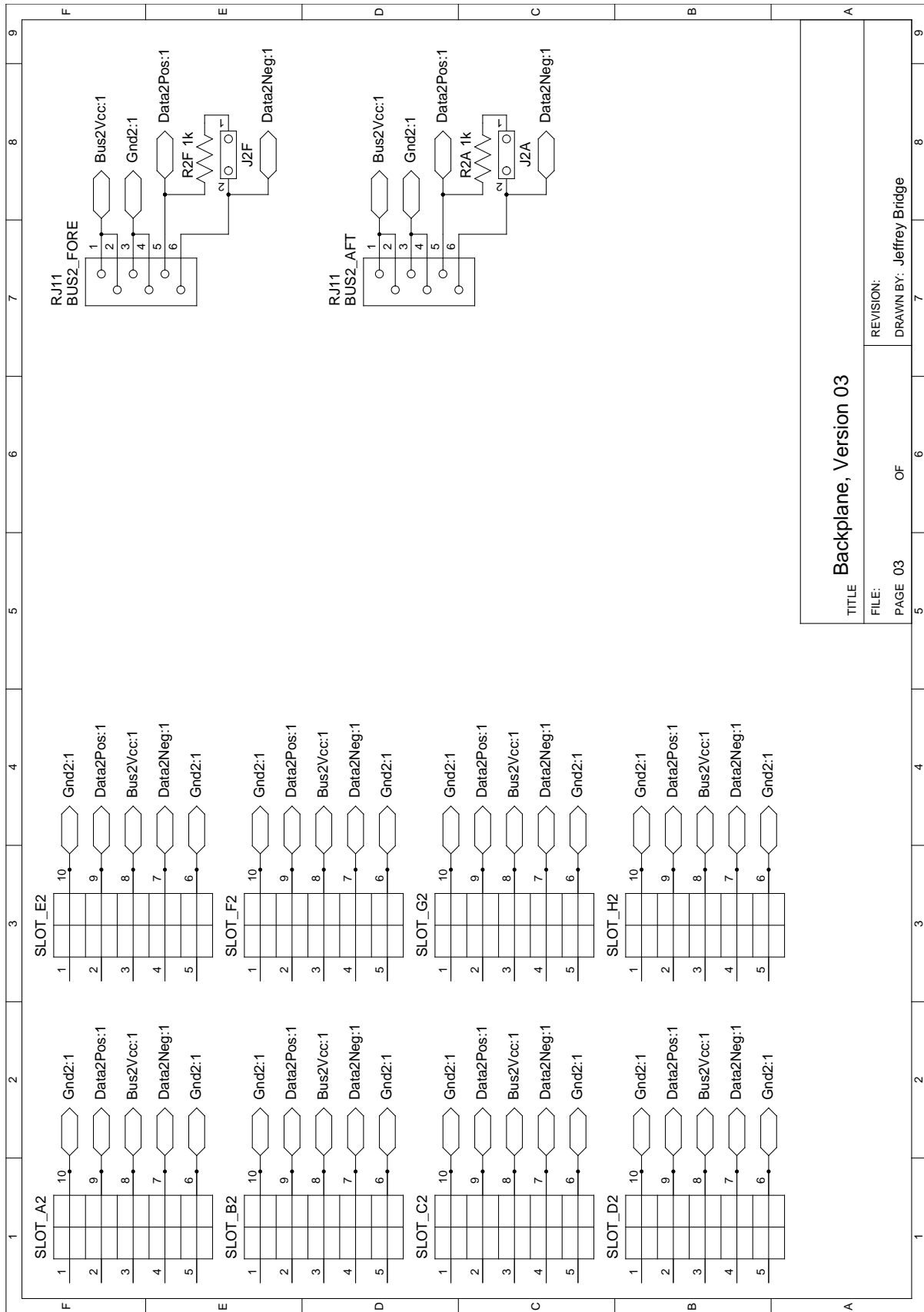


Figure B.3: Circuit schematic for backplane board, hardware revision 03, page 3 of 4.

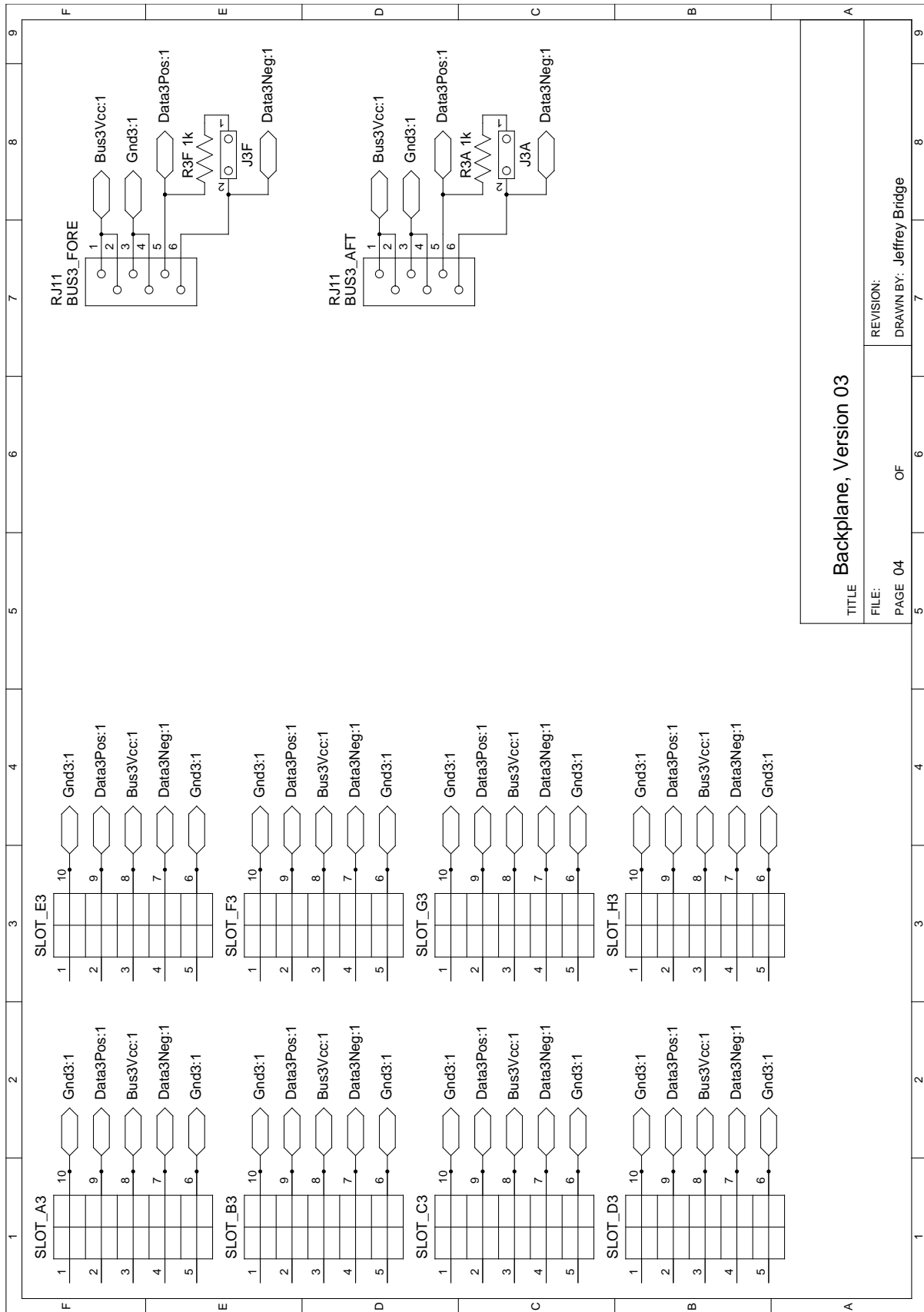


Figure B.4: Circuit schematic for backplane board, hardware revision 03, page 4 of 4.

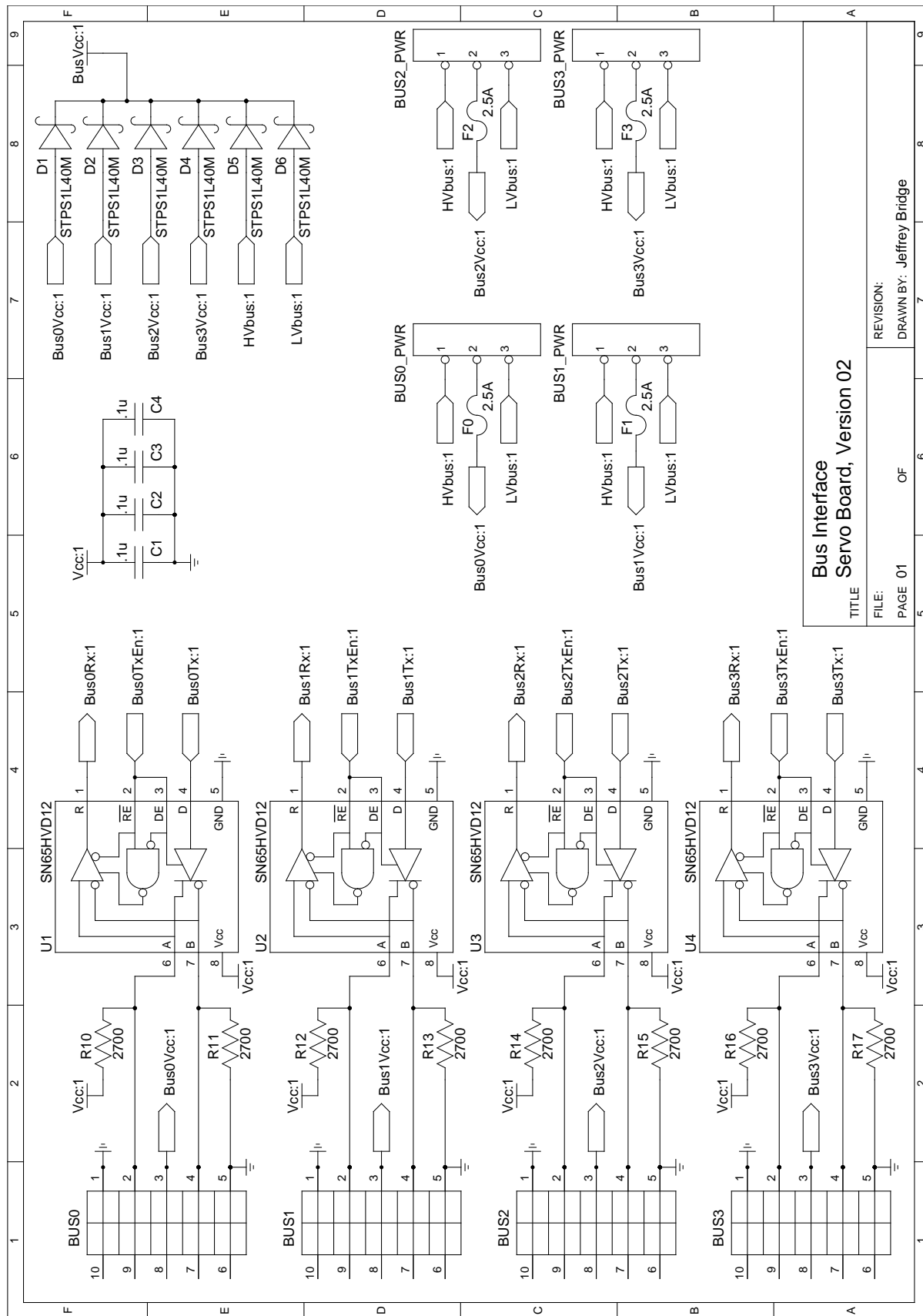


Figure B.5: Circuit schematic for Servo board, hardware revision 03, page 1 of 8.

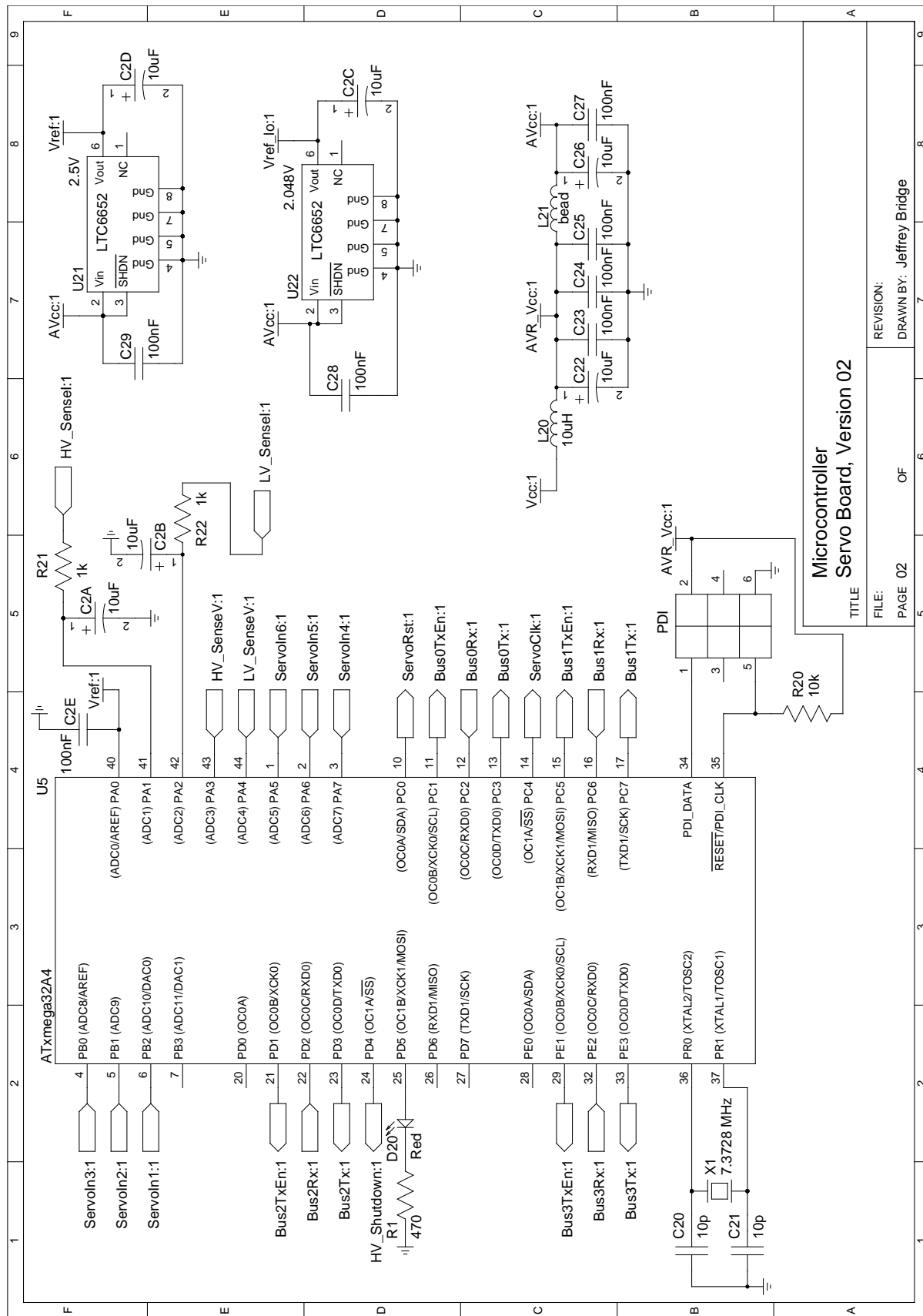


Figure B.6: Circuit schematic for Servo board, hardware revision 03, page 2 of 8.

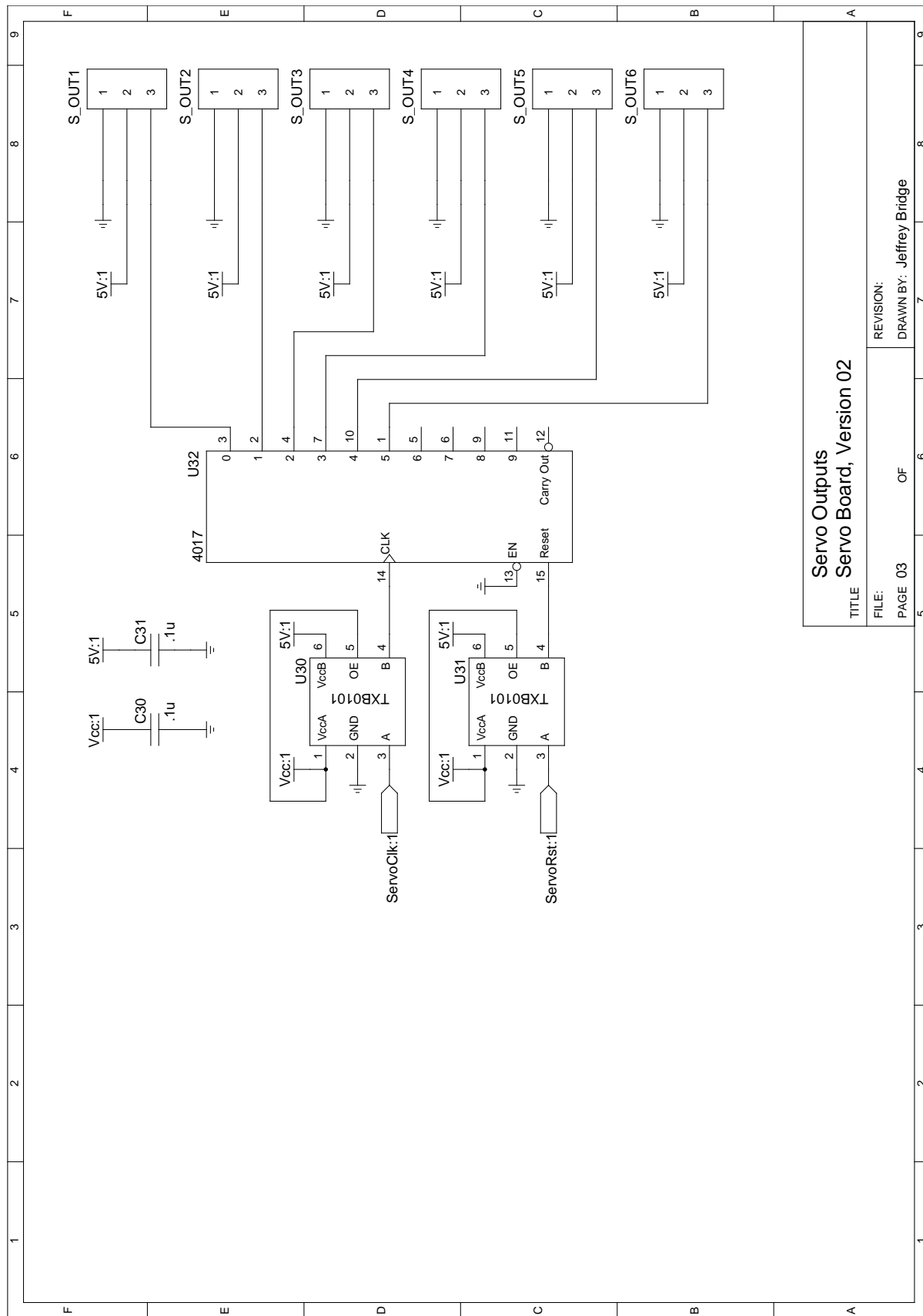


Figure B.7: Circuit schematic for Servo board, hardware revision 03, page 3 of 8.

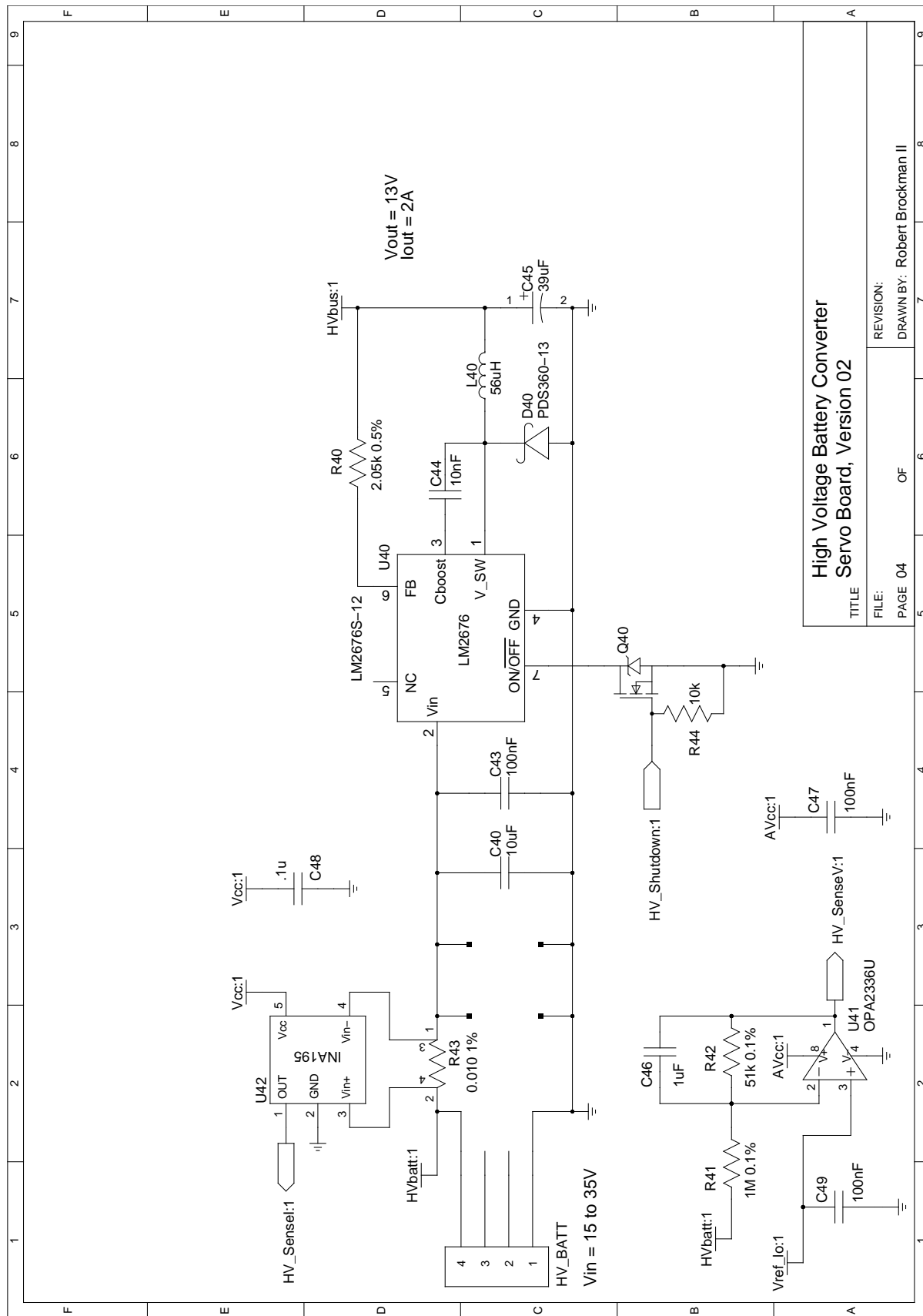


Figure B.8: Circuit schematic for Servo board, hardware revision 03, page 4 of 8.

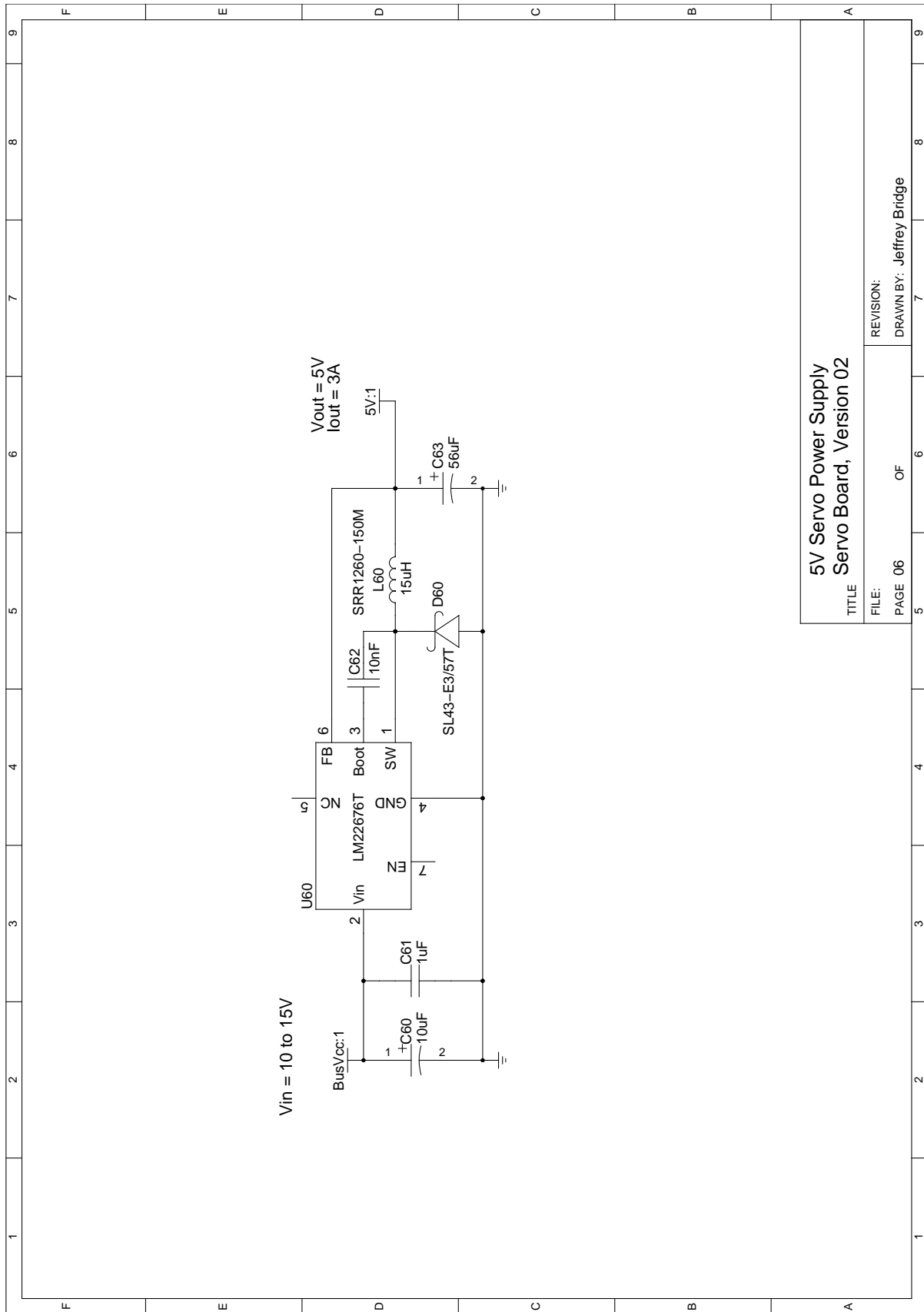


Figure B.10: Circuit schematic for Servo board, hardware revision 03, page 6 of 8.

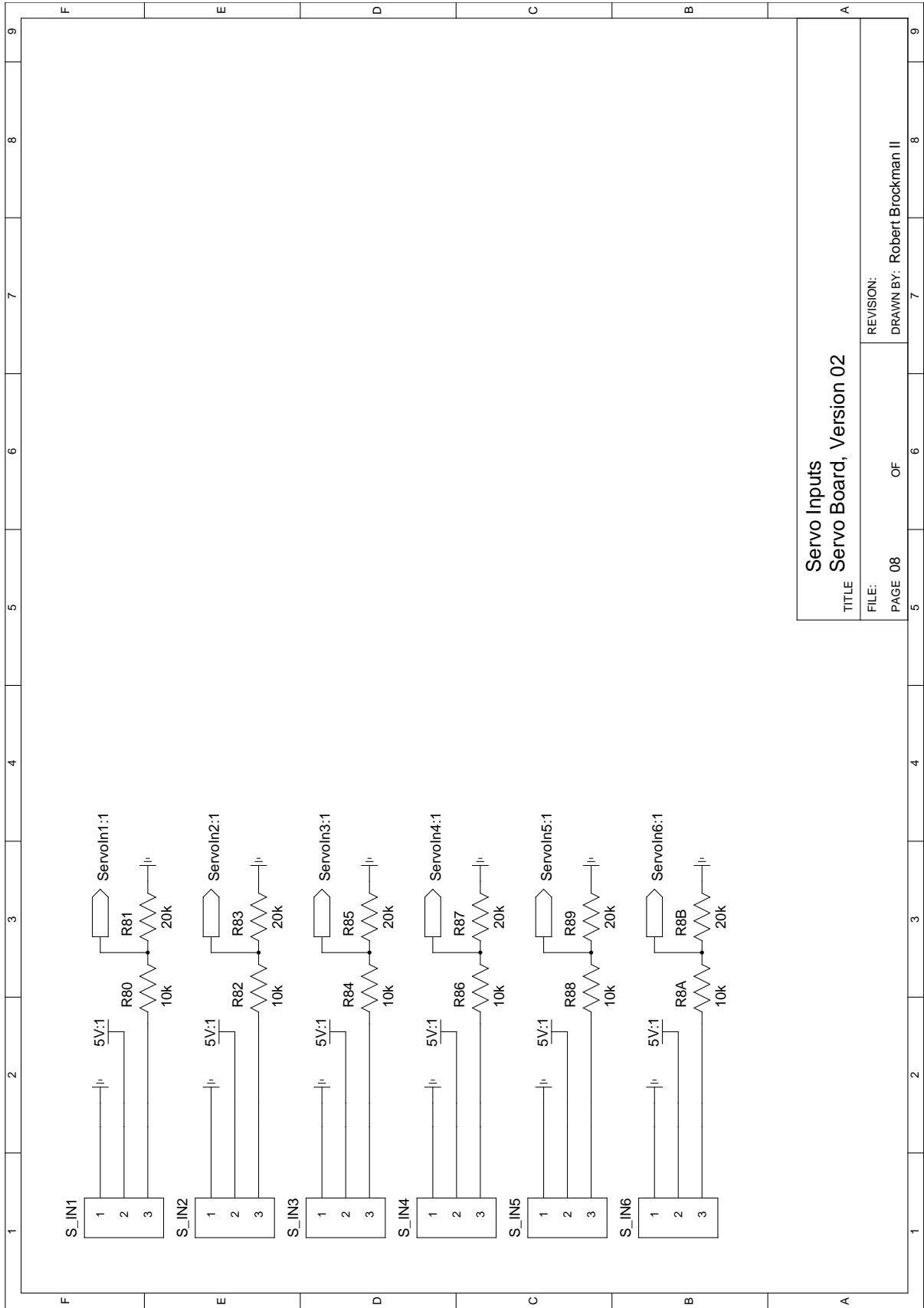


Figure B.12: Circuit schematic for Servo board, hardware revision 03, page 8 of 8.

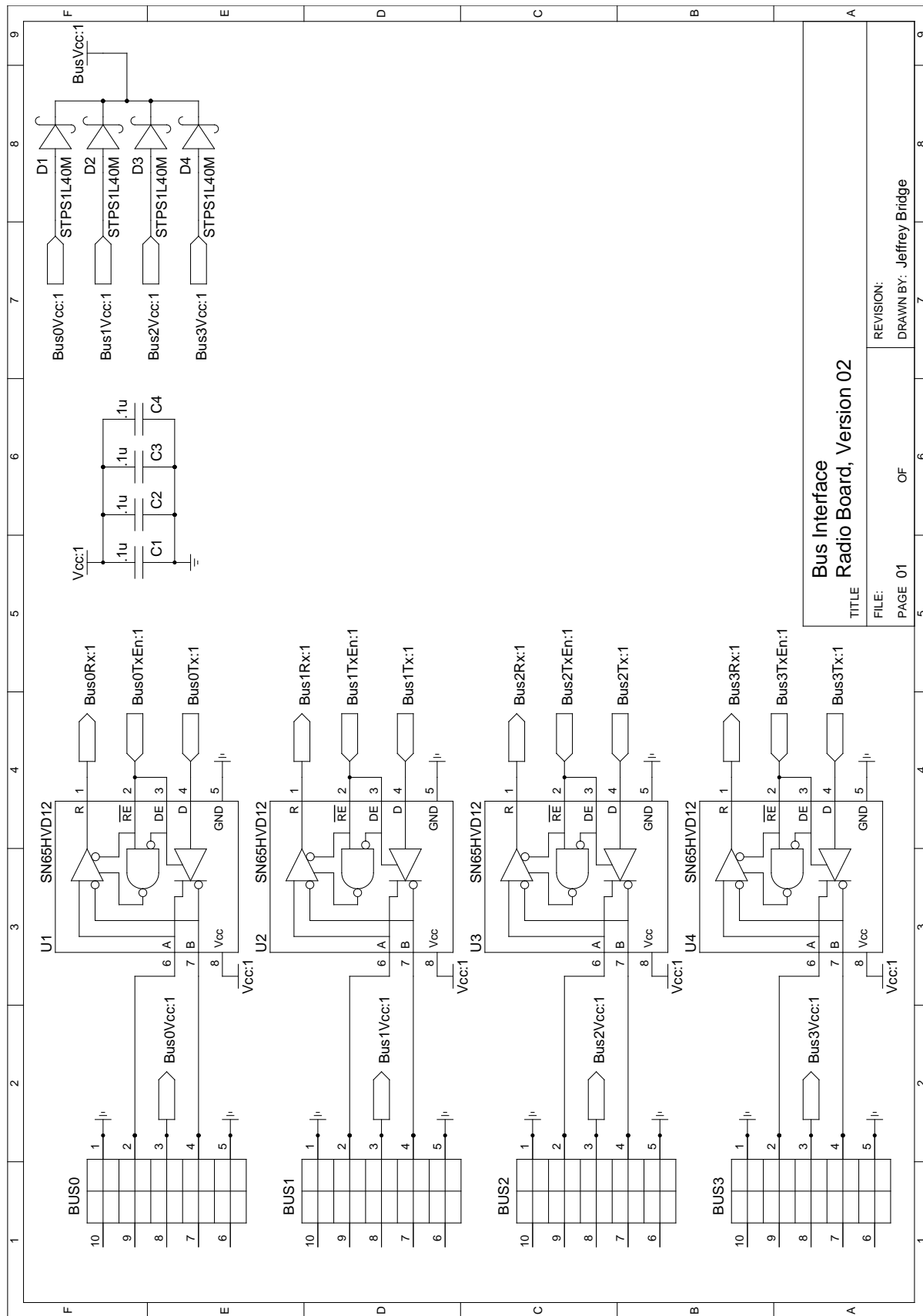


Figure B.13: Circuit schematic for radio board, hardware revision 03, page 1 of 5.

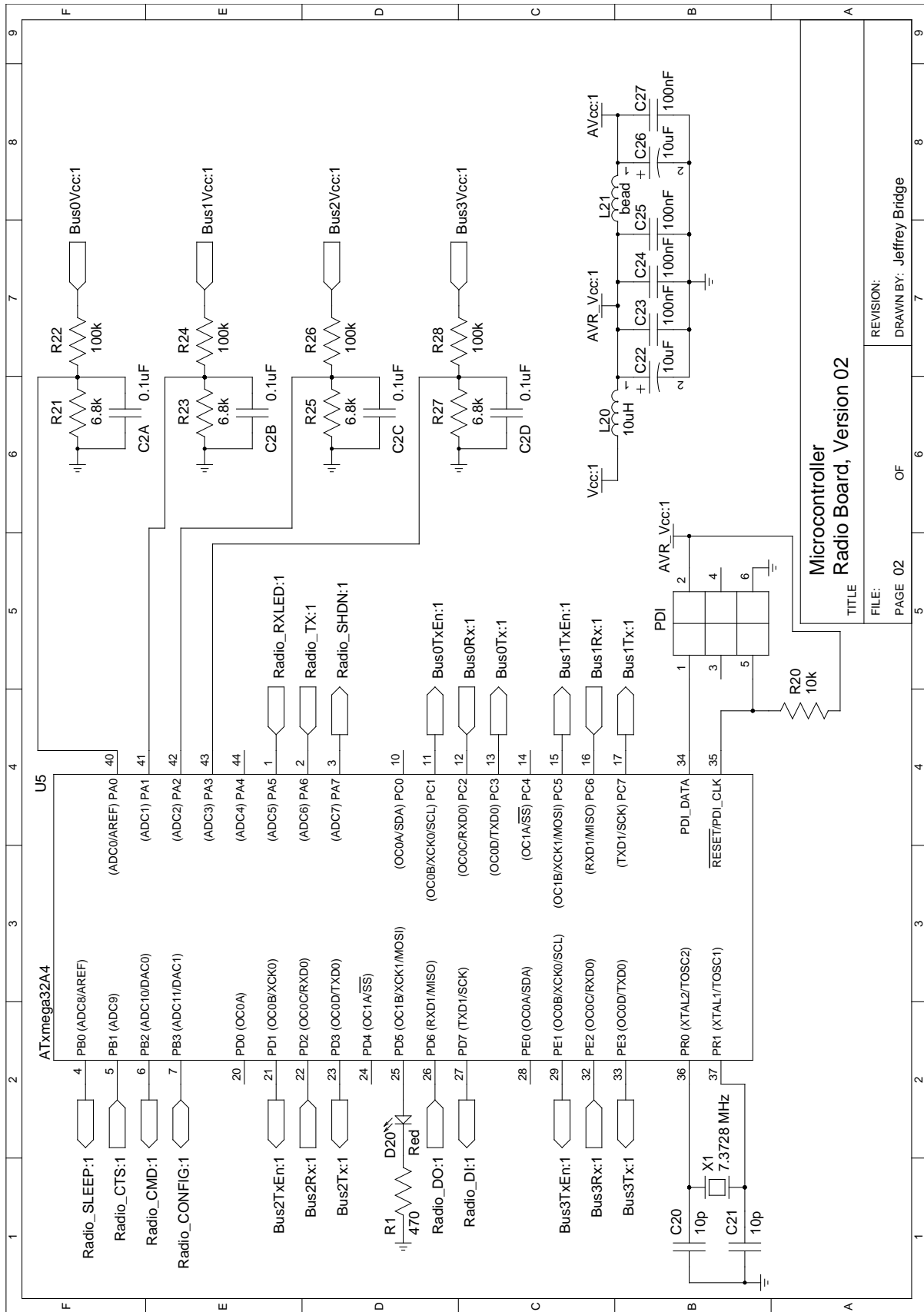
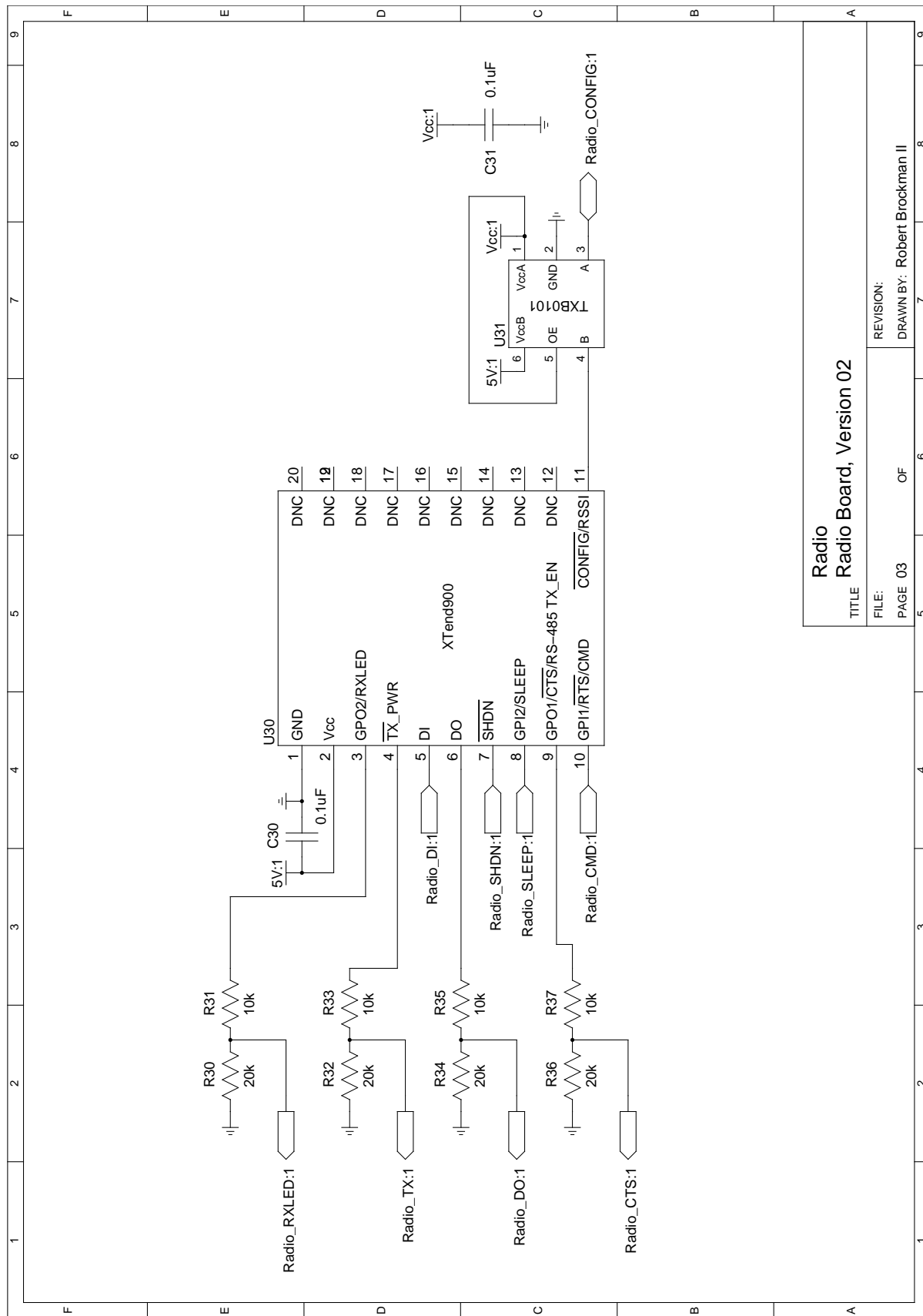


Figure B.14: Circuit schematic for radio board, hardware revision 03, page 2 of 5.



| | |
|----------------------------------|------------------------------|
| Radio Radio Board, Version 02 | |
| TITLE | REVISION: |
| FILE: | DRAWN BY: Robert Brockman II |
| PAGE 03 | OF |

Figure B.15: Circuit schematic for radio board, hardware revision 03, page 3 of 5.

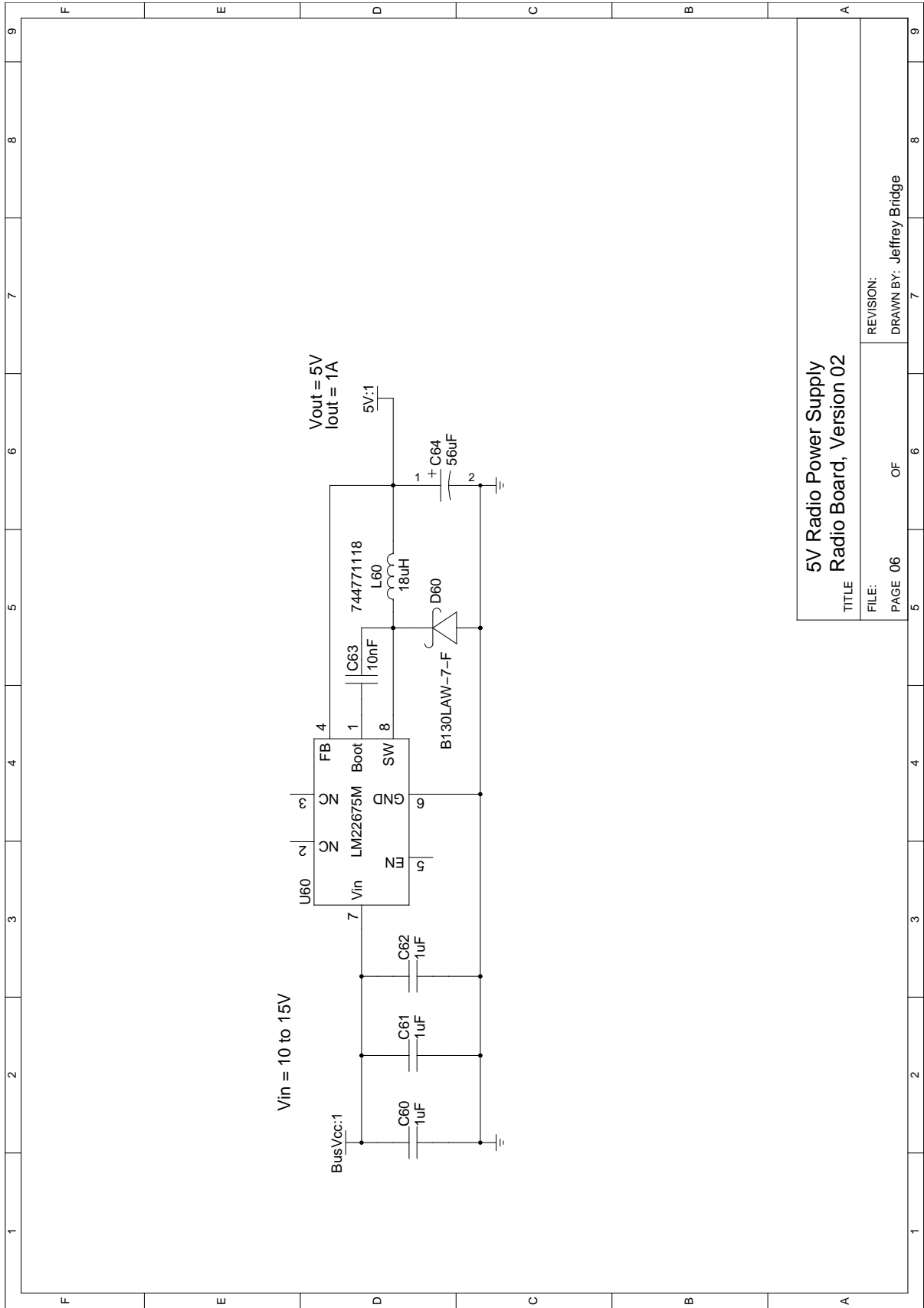


Figure B.16: Circuit schematic for radio board, hardware revision 03, page 4 of 5.

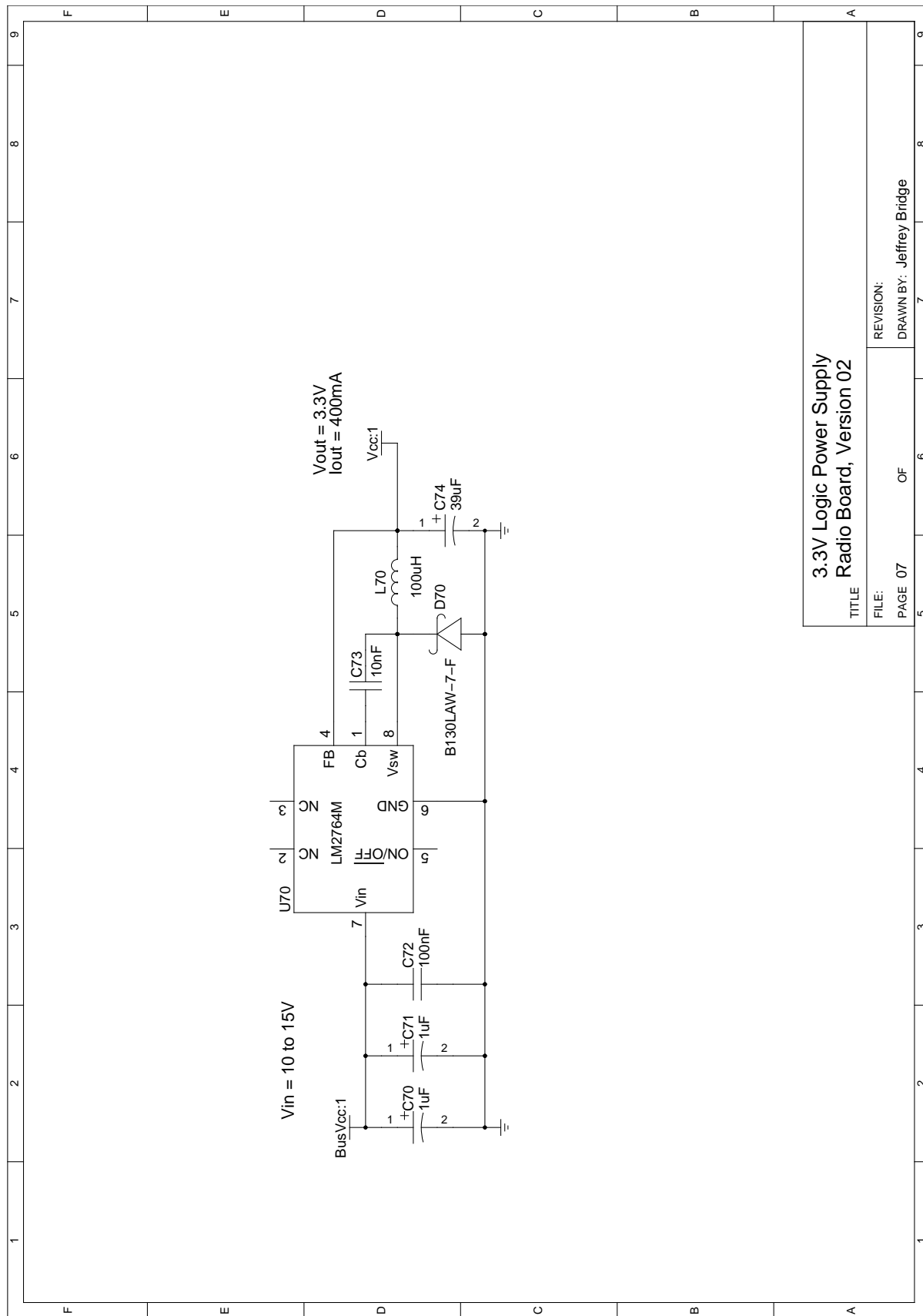


Figure B.17: Circuit schematic for radio board, hardware revision 03, page 5 of 5.

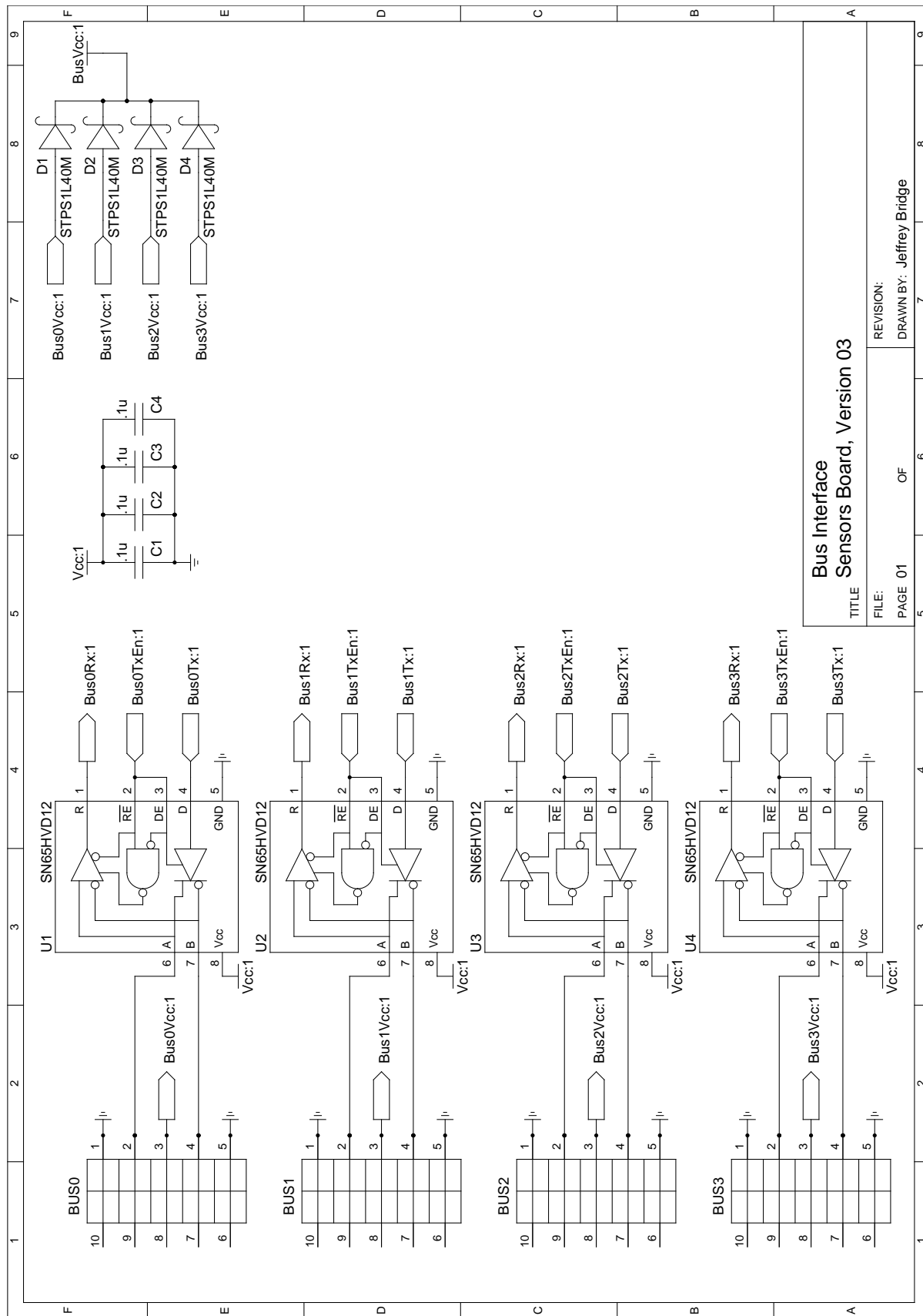


Figure B.18: Circuit schematic for sensors board, hardware revision 03, page 1 of 8.

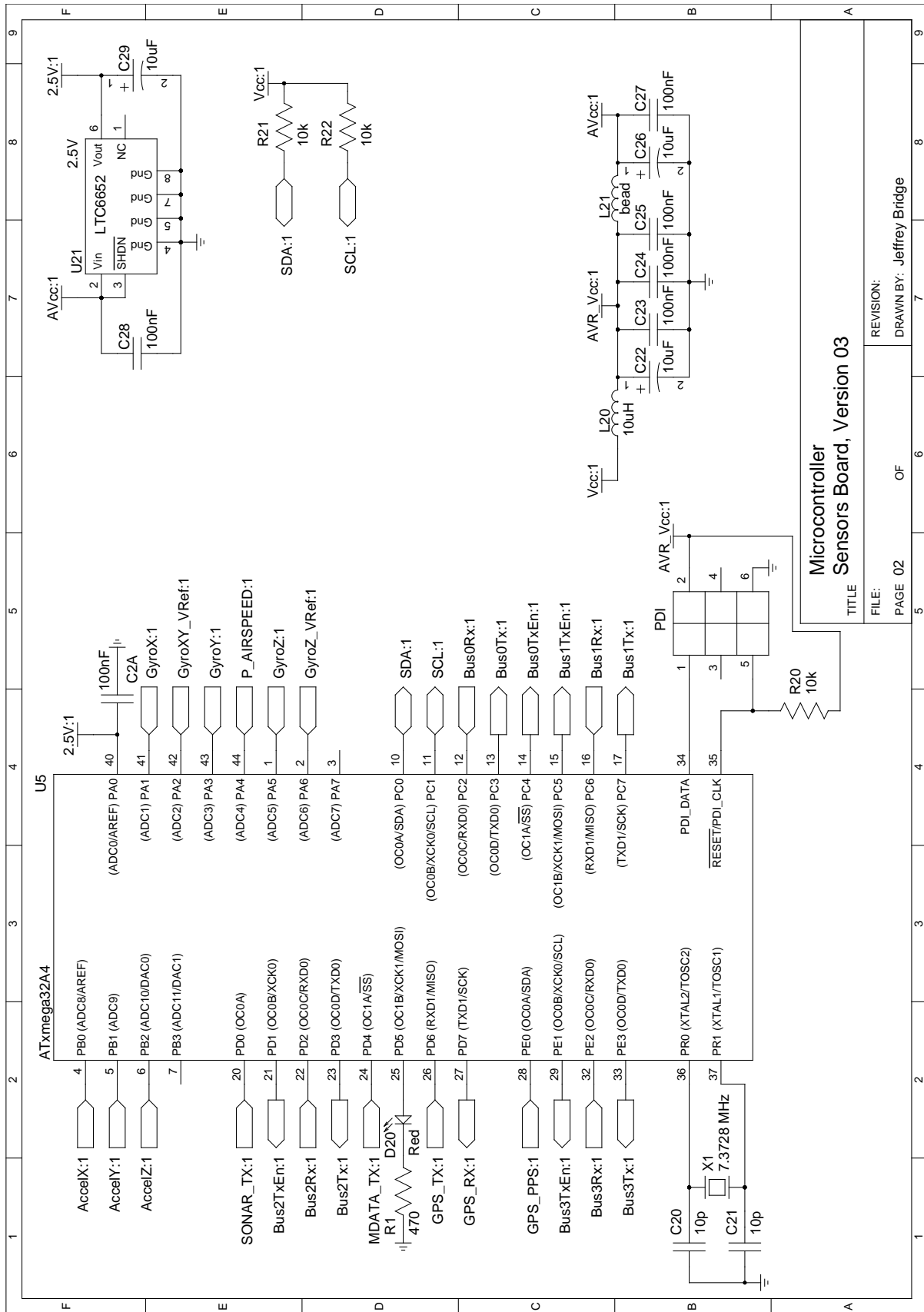


Figure B.19: Circuit schematic for sensors board, hardware revision 03, page 2 of 8.

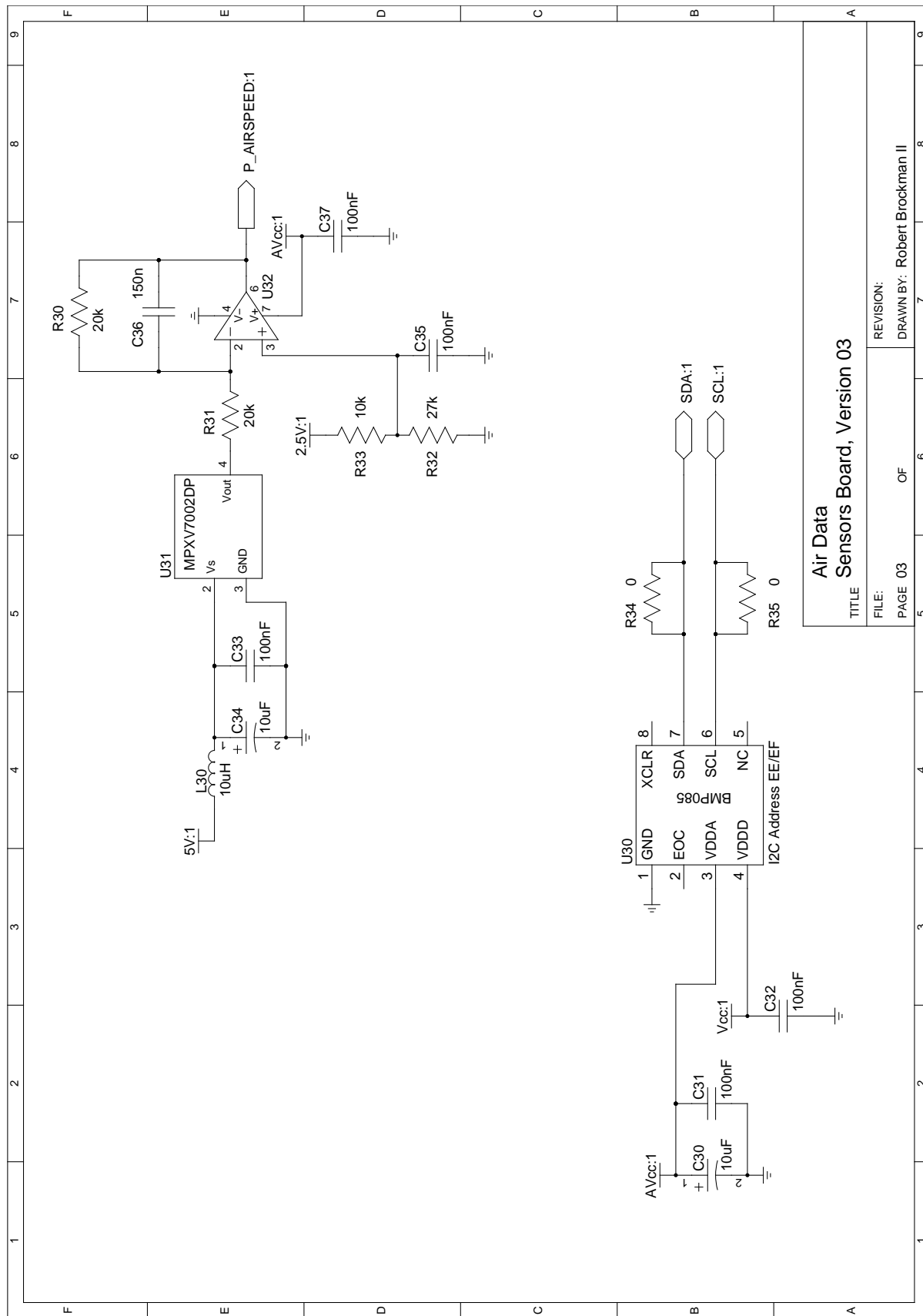


Figure B.20: Circuit schematic for sensors board, hardware revision 03, page 3 of 8.

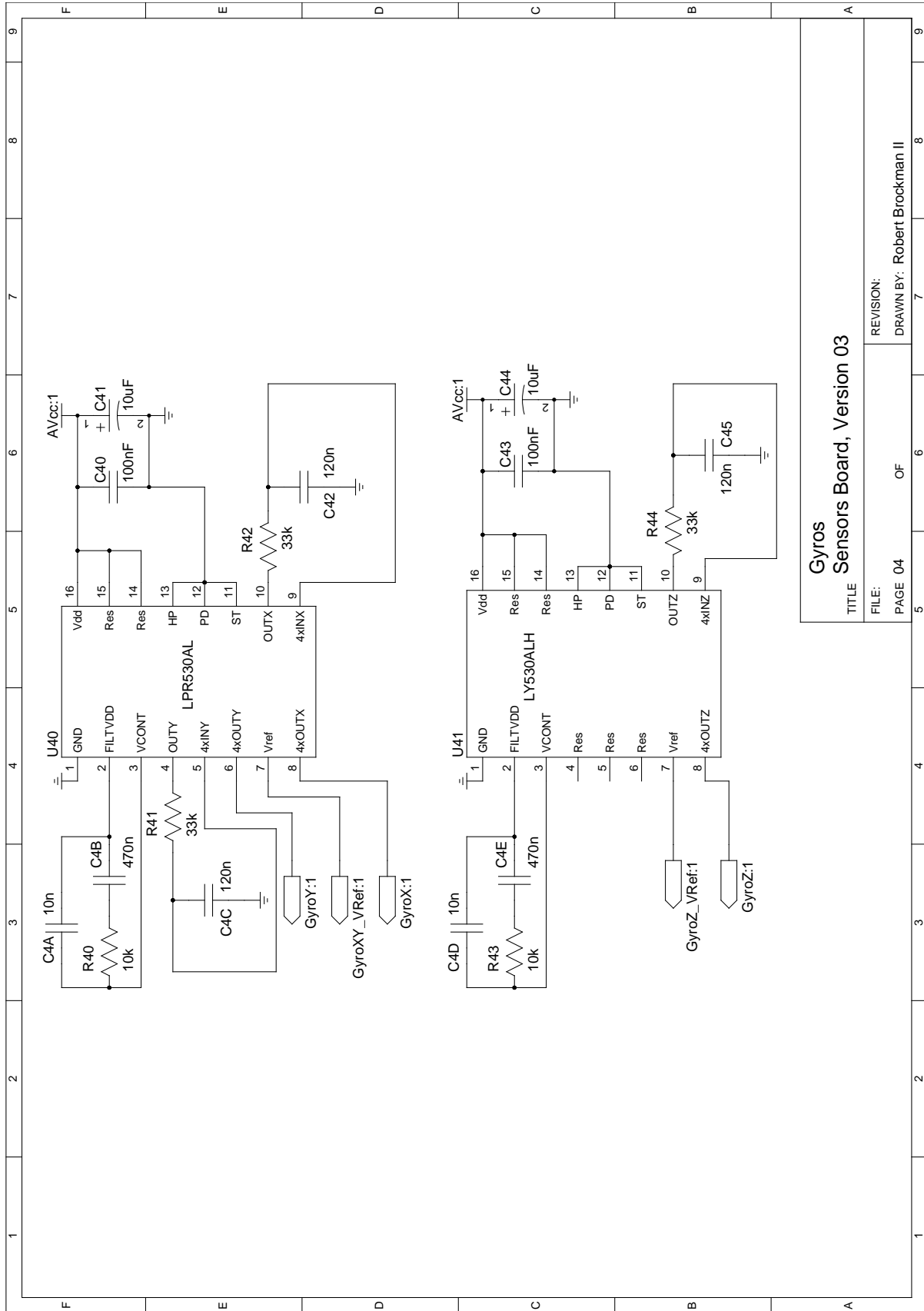


Figure B.21: Circuit schematic for sensors board, hardware revision 03, page 4 of 8.

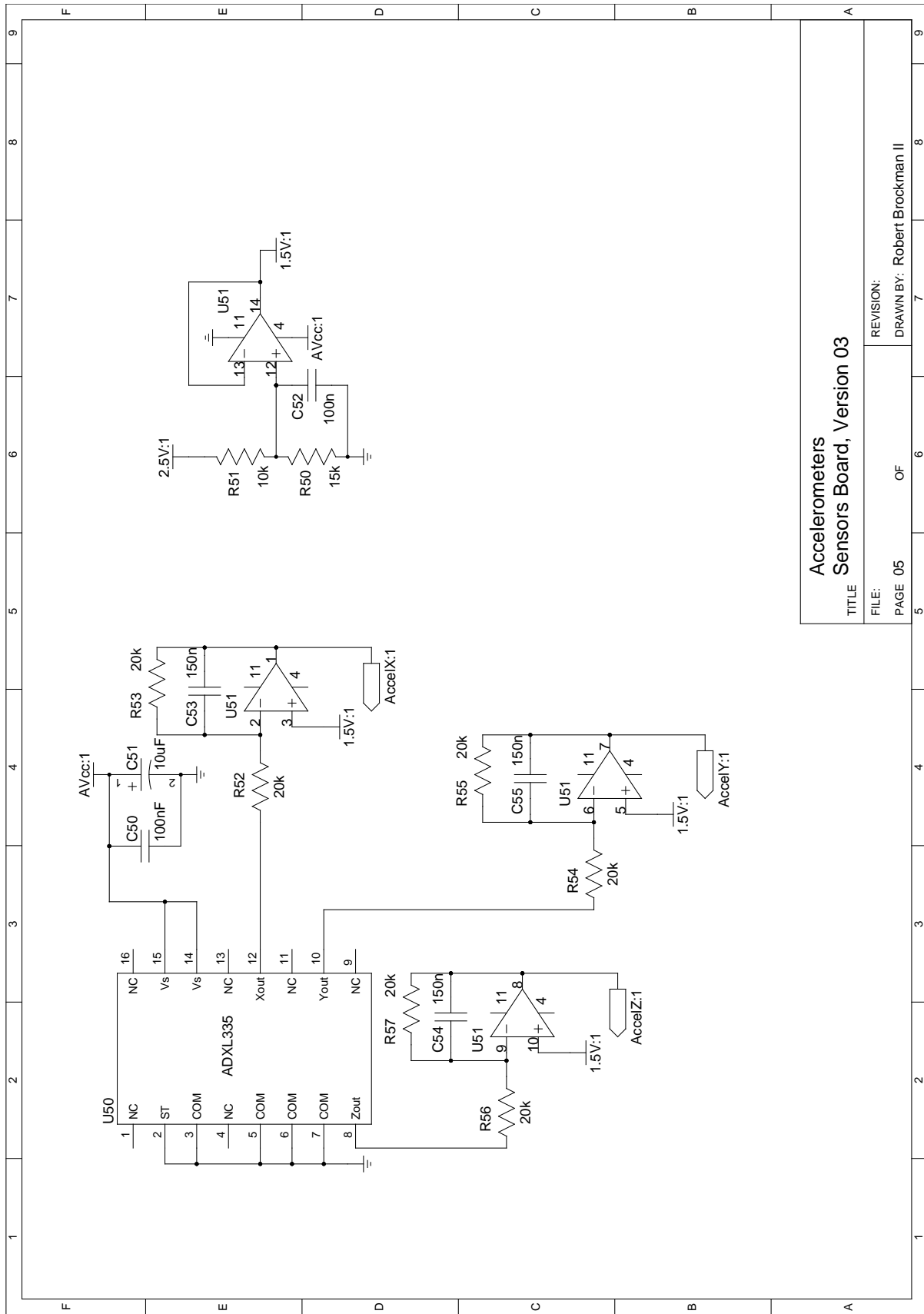


Figure B.22: Circuit schematic for sensors board, hardware revision 03, page 5 of 8.

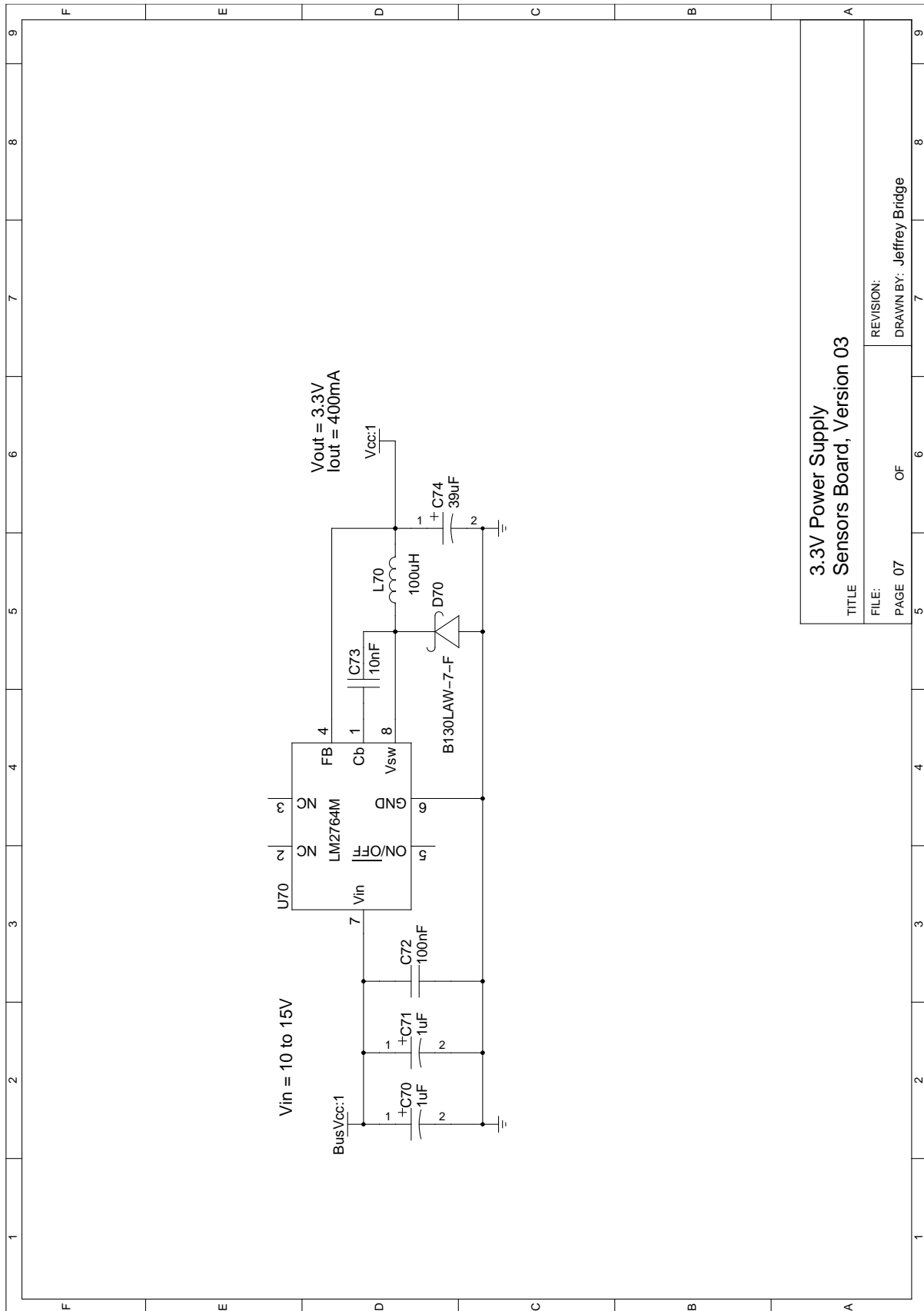
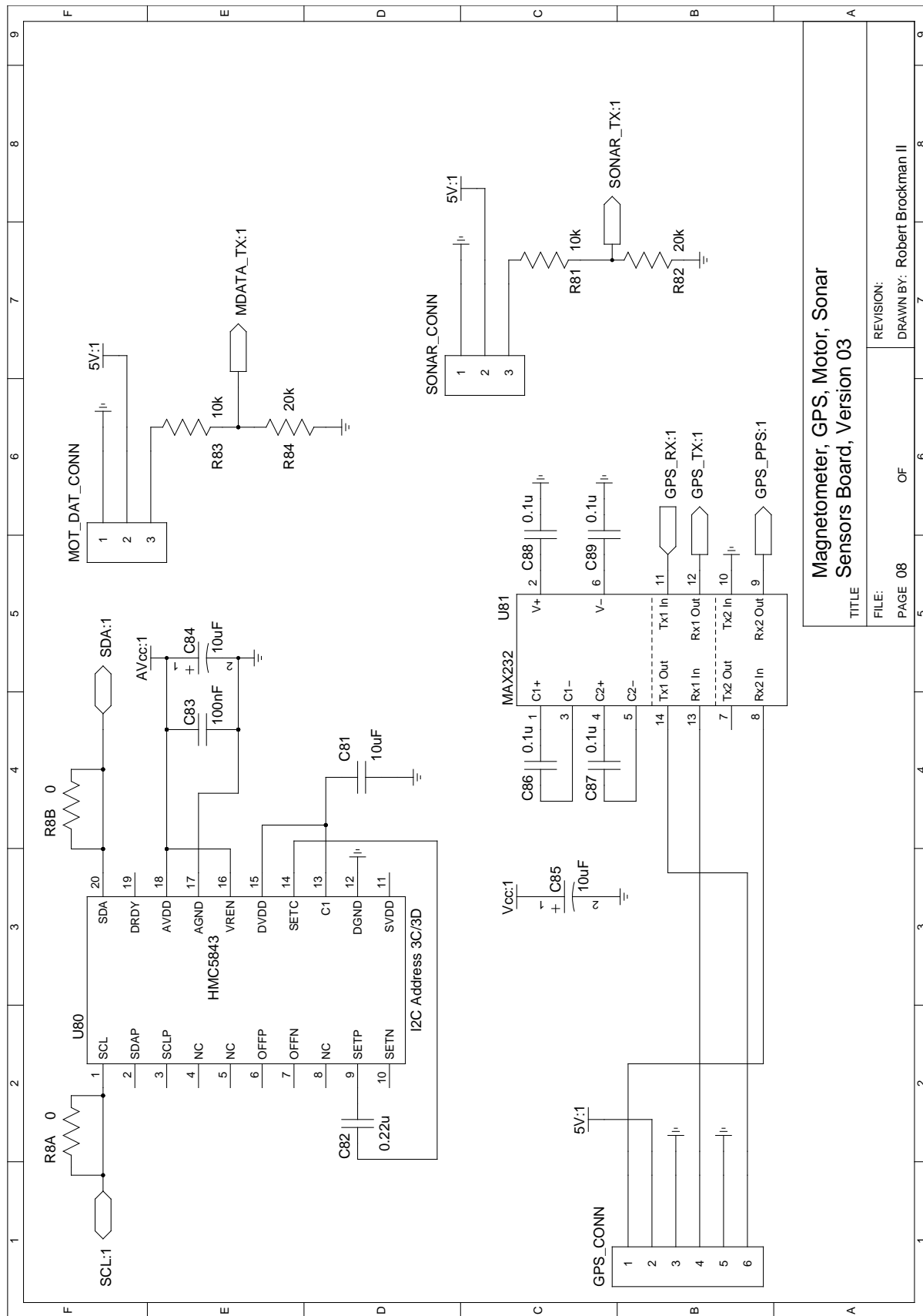


Figure B.24: Circuit schematic for sensors board, hardware revision 03, page 7 of 8.



| | | | |
|---------|--|---|--|
| TITLE | | Magnetometer, GPS, Motor, Sonar Sensors Board, Version 03 | |
| FILE: | | REVISION: | |
| PAGE 08 | | DRAWN BY: Robert Brockman II | |
| OF | | | |

Figure B.25: Circuit schematic for sensors board, hardware revision 03, page 8 of 8.

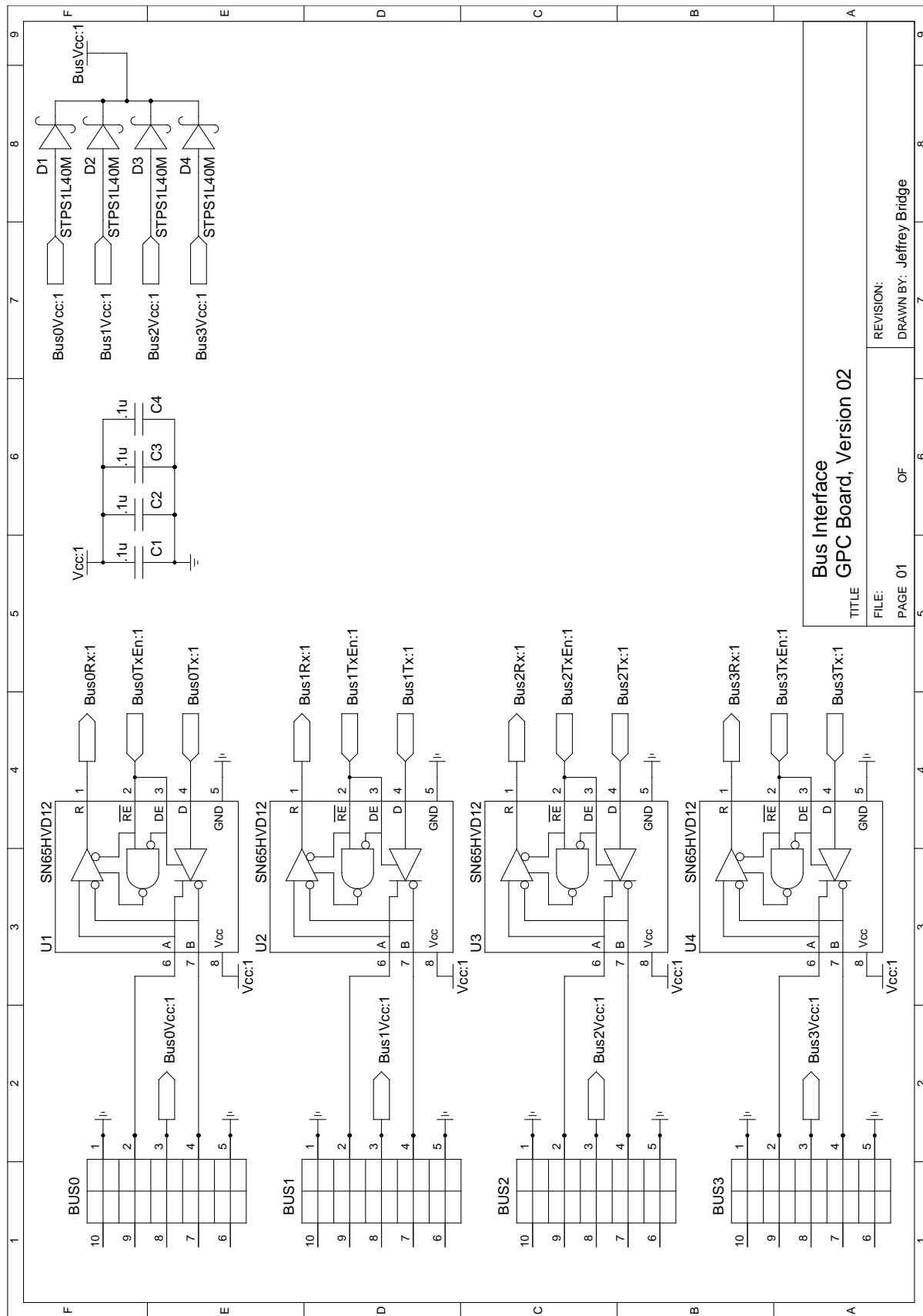


Figure B.26: Circuit schematic for GPC board, hardware revision 02, page 1 of 9.

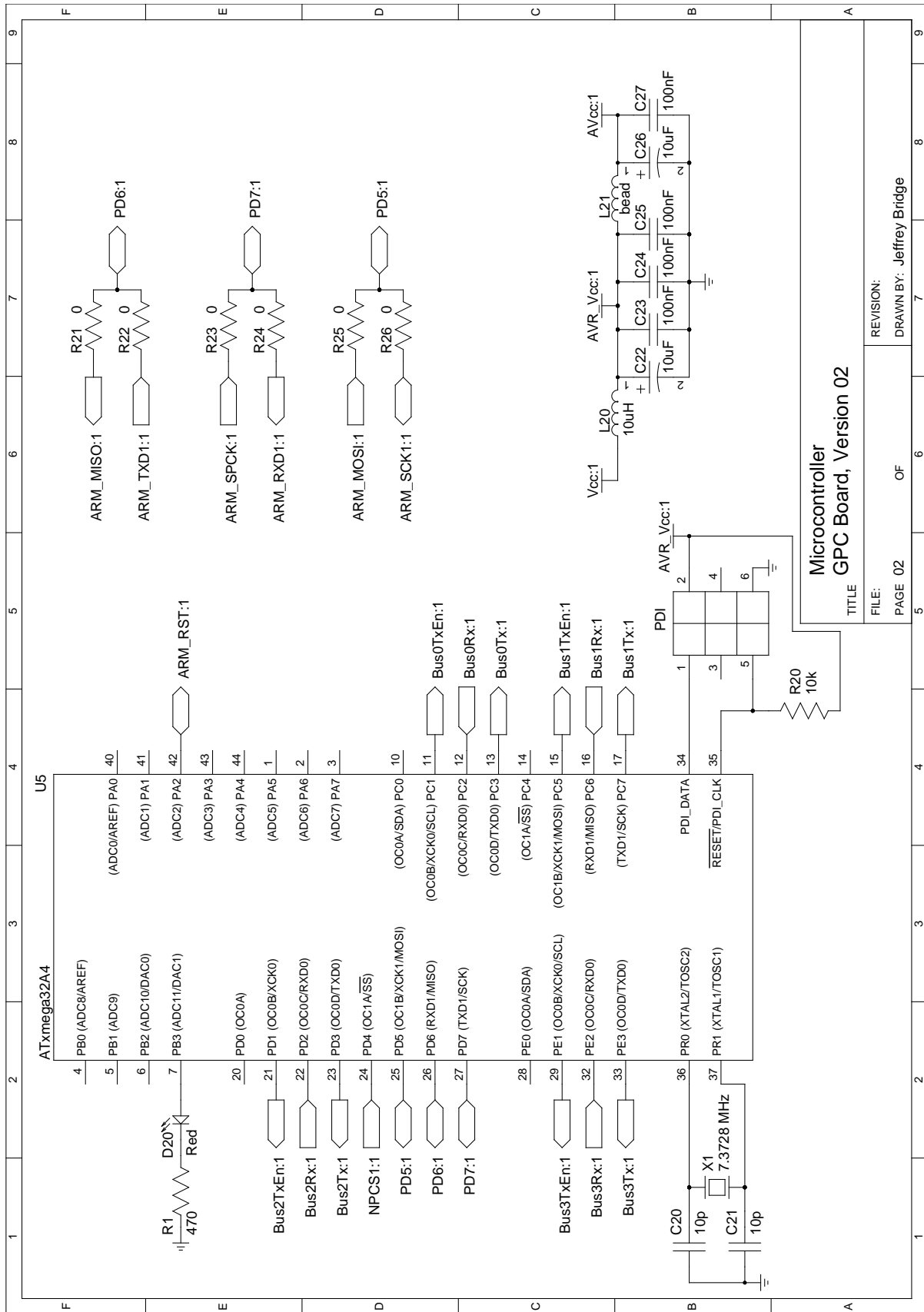


Figure B.27: Circuit schematic for GPC board, hardware revision 02, page 2 of 9.

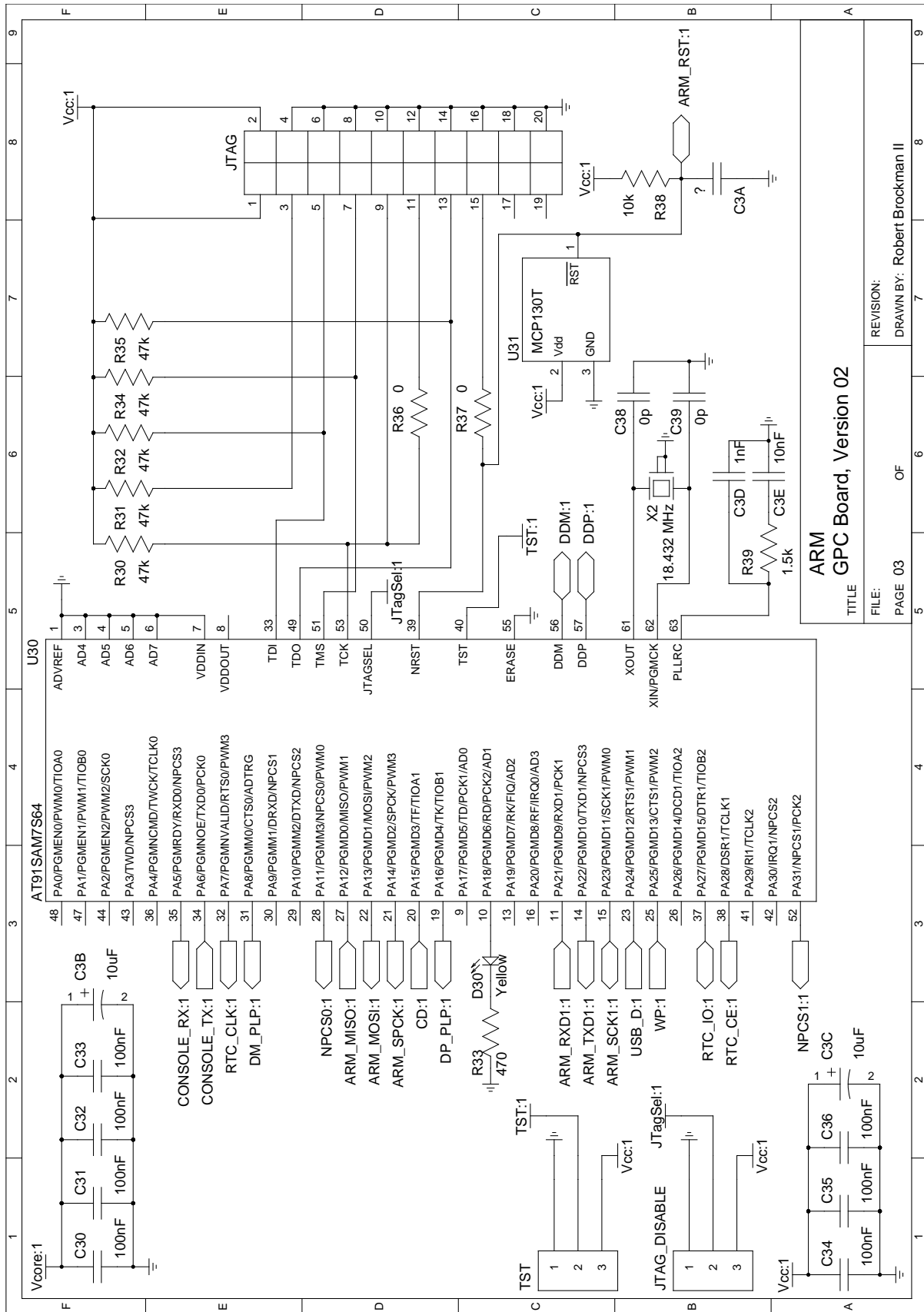


Figure B.28: Circuit schematic for GPC board, hardware revision 02, page 3 of 9.

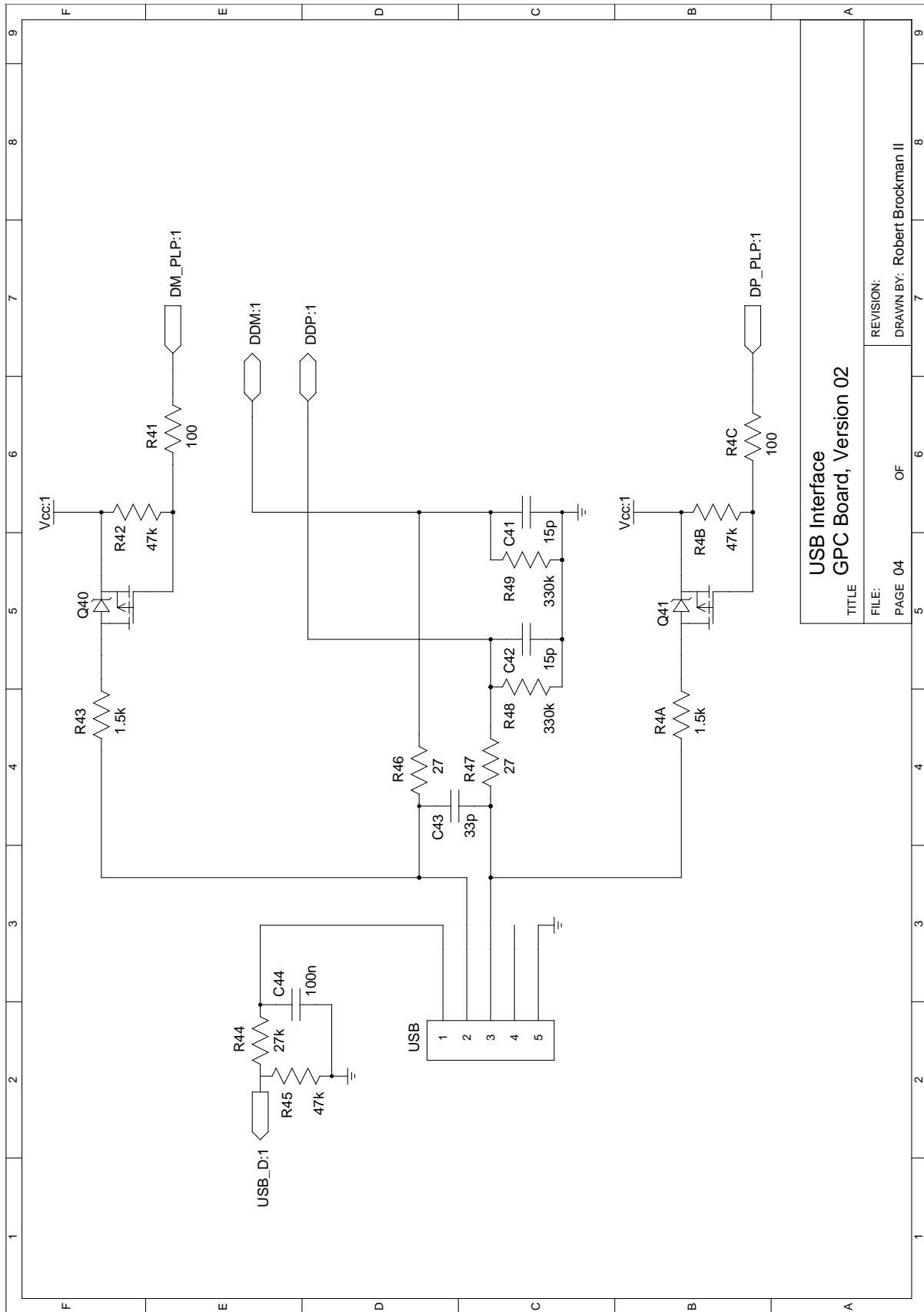


Figure B.29: Circuit schematic for GPC board, hardware revision 02, page 4 of 9.

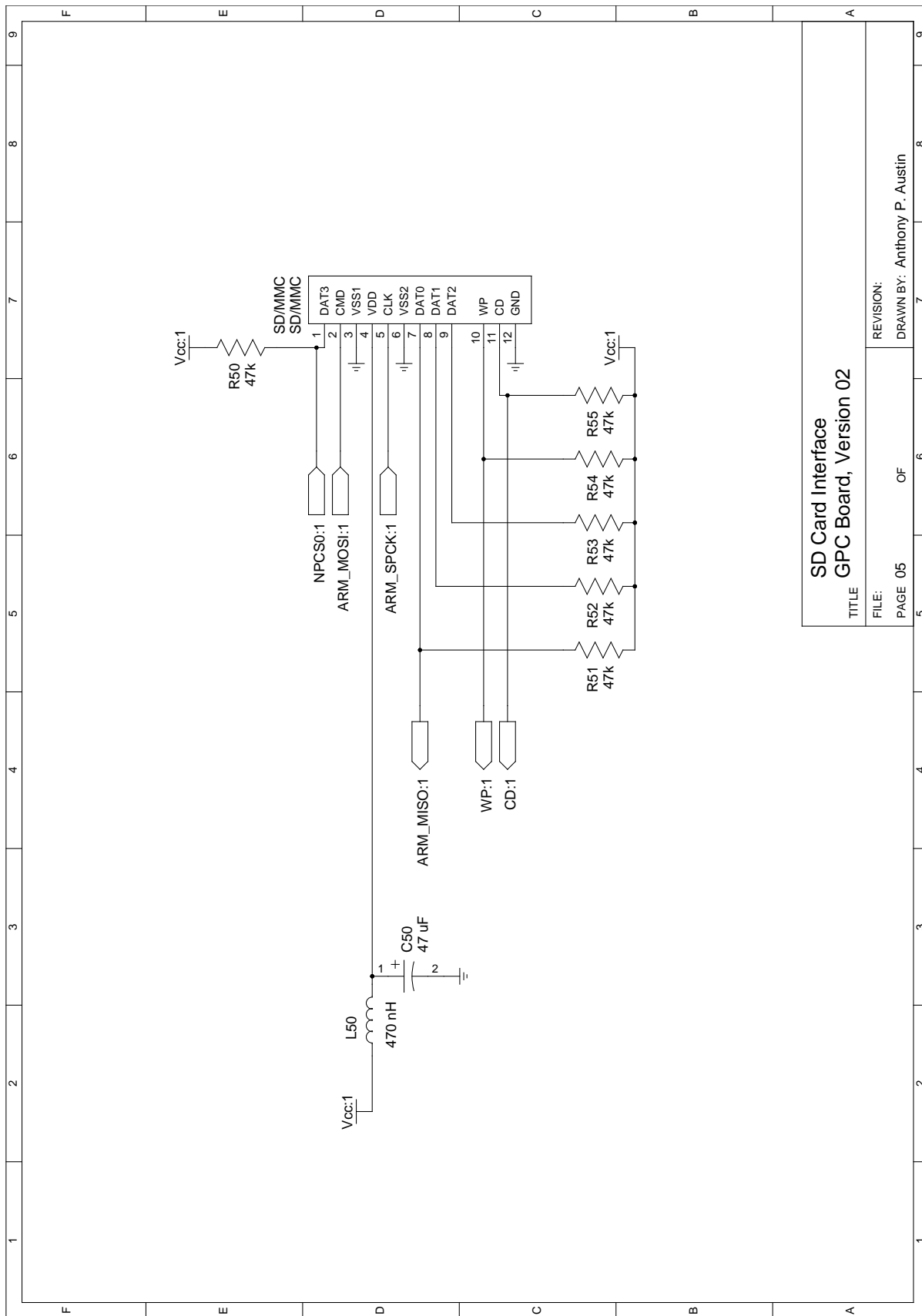


Figure B.30: Circuit schematic for GPC board, hardware revision 02, page 5 of 9.

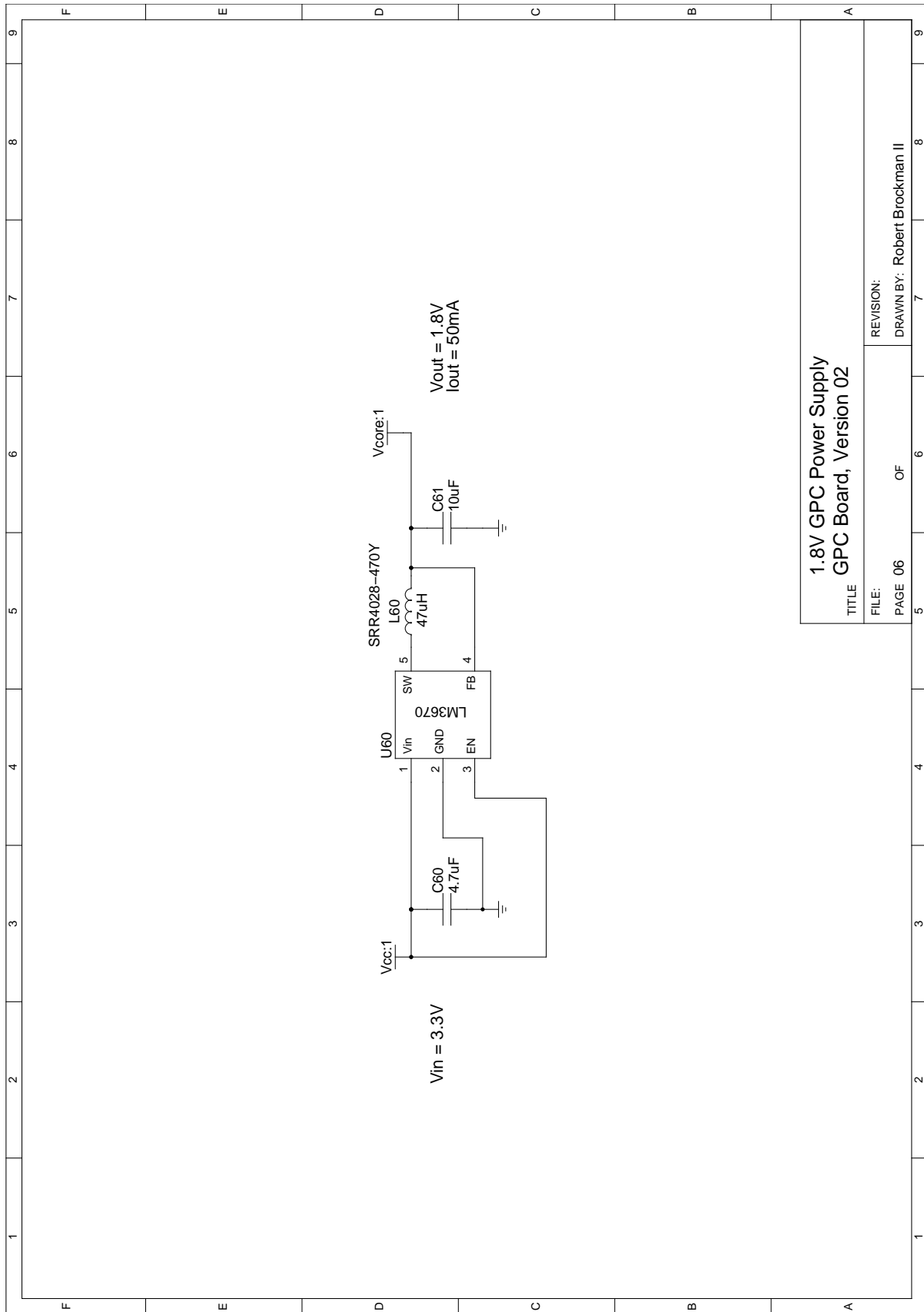


Figure B.31 : Circuit schematic for GPC board, hardware revision 02, page 6 of 9.

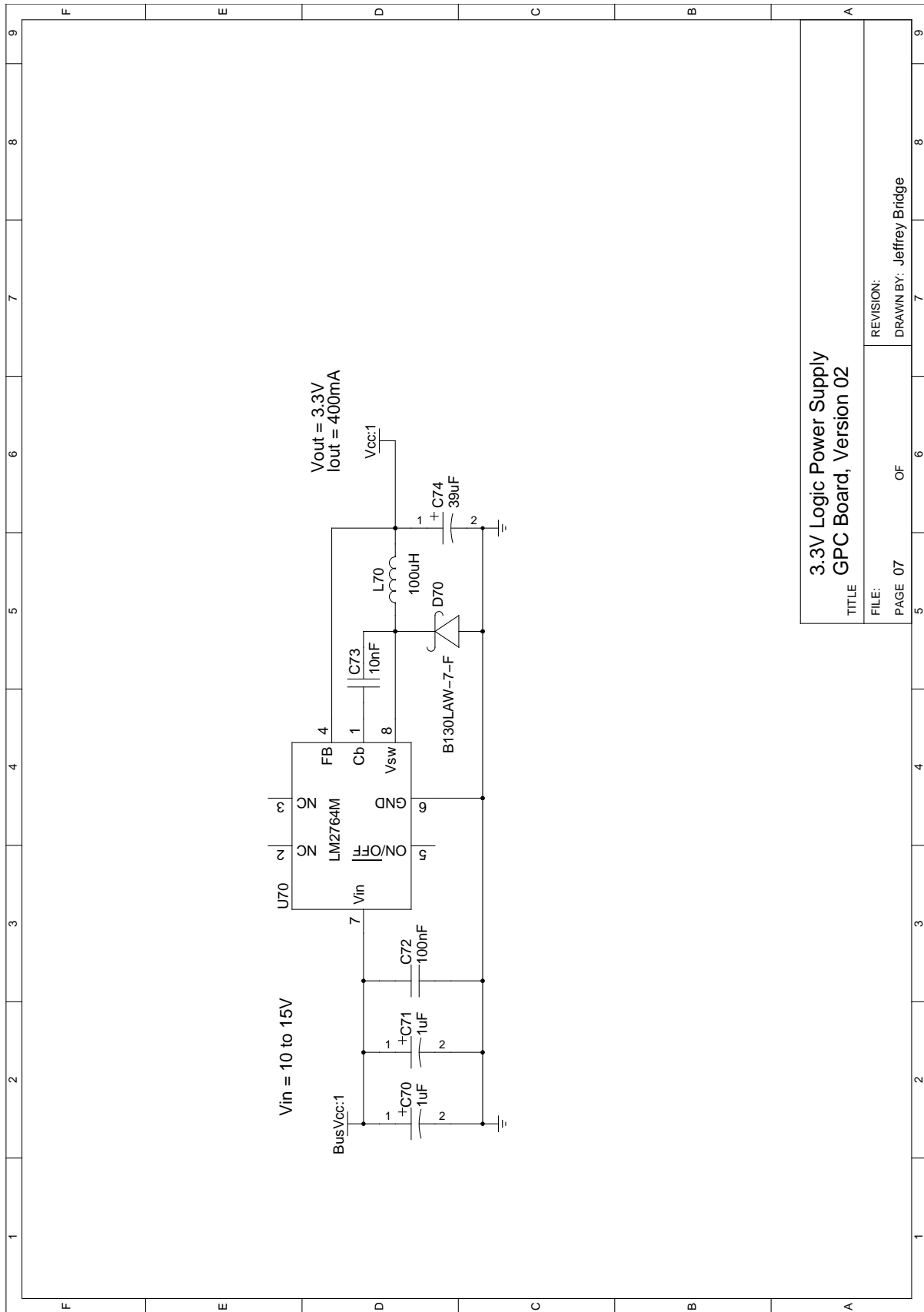


Figure B.32: Circuit schematic for GPC board, hardware revision 02, page 7 of 9.

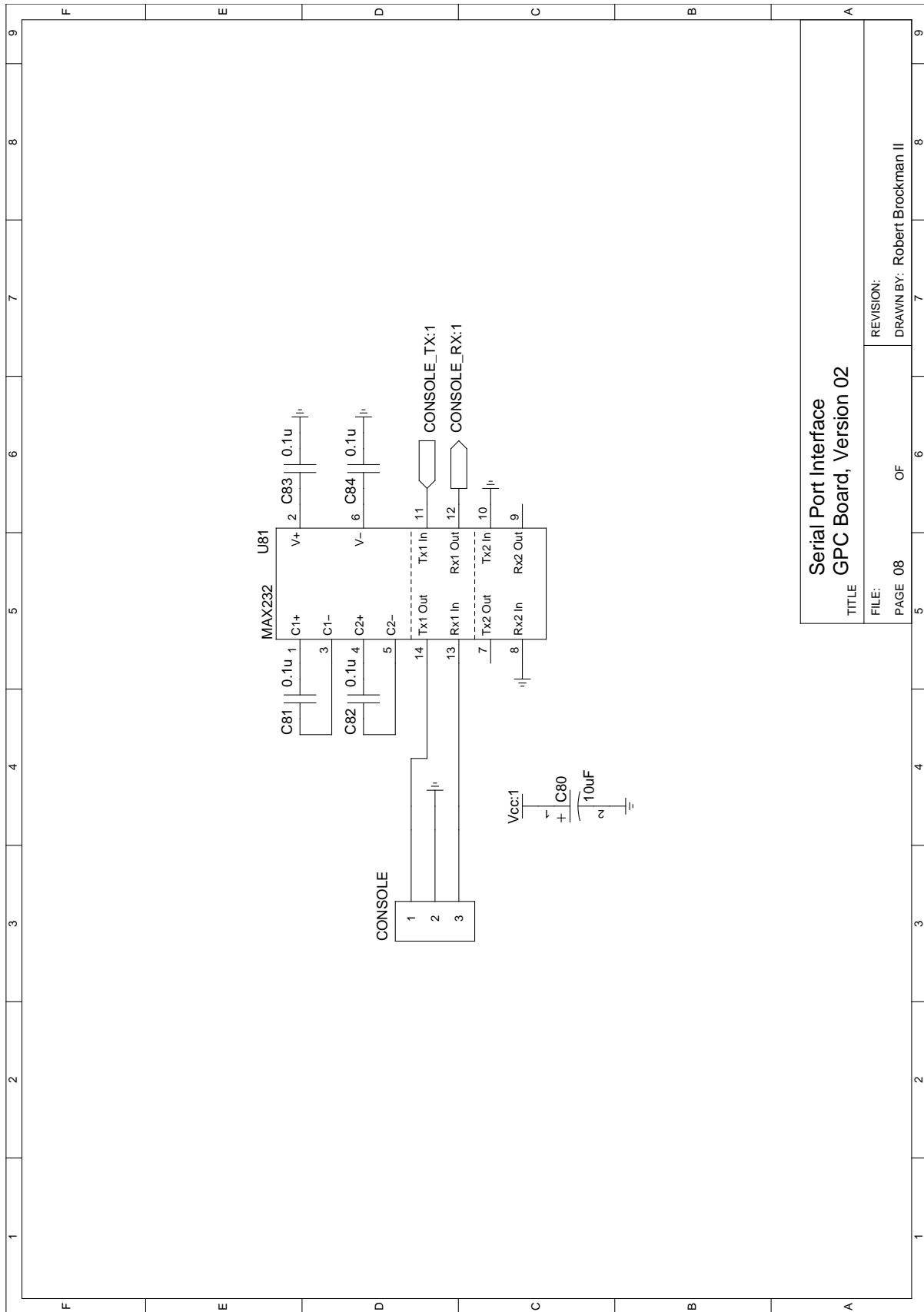


Figure B.33: Circuit schematic for GPC board, hardware revision 02, page 8 of 9.

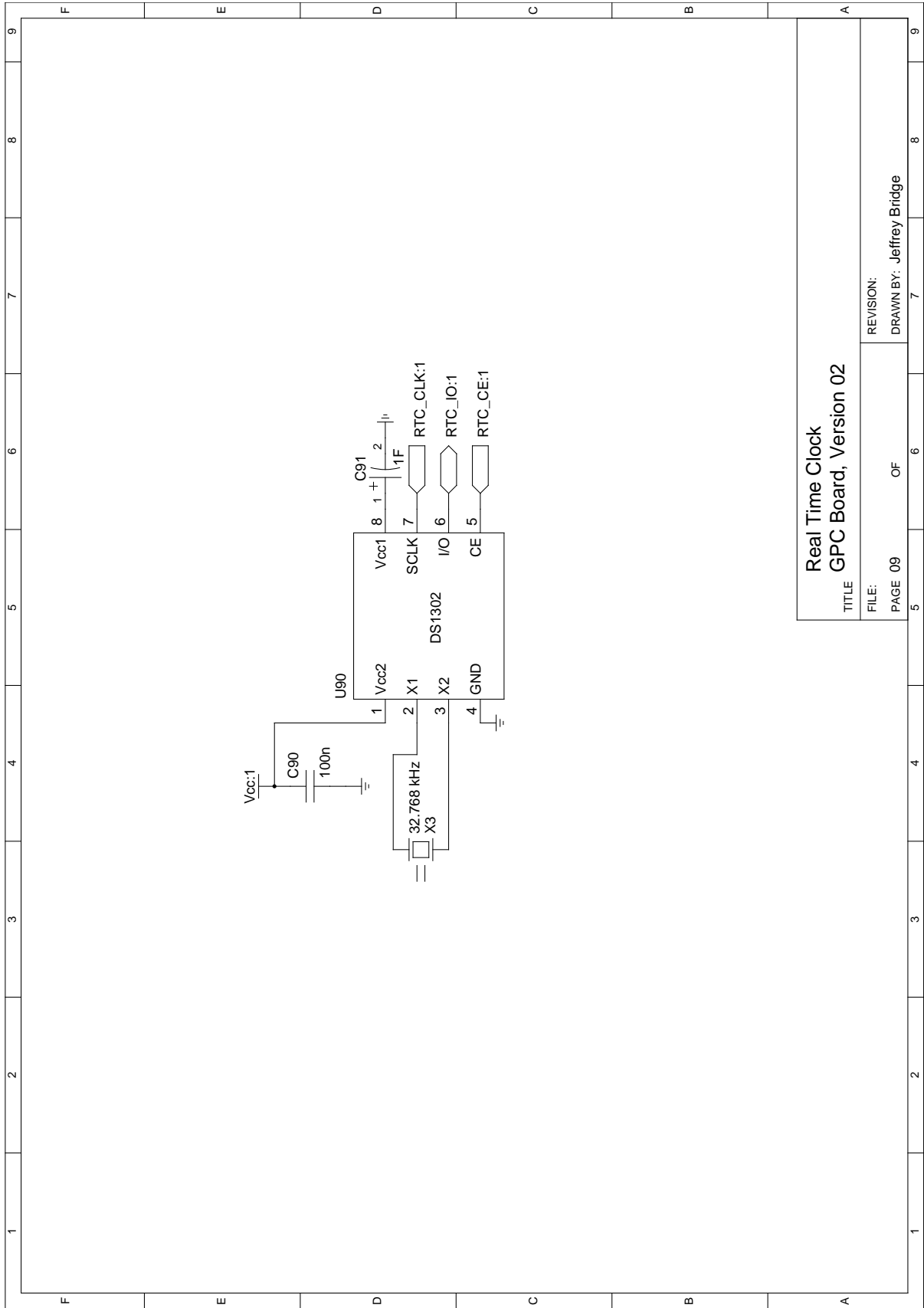


Figure B.34: Circuit schematic for GPC board, hardware revision 02, page 9 of 9.

C Assembly Instructions and Bill of Materials

C.1 Aircraft Hardware

The final prototype aircraft began as an off-the-shelf Senior Telemaster from Hobby Lobby International, Inc. This is a large model aircraft frame with a 2 m wingspan, and is available pre-assembled in a almost-ready-to-fly (ARF) kit.

| Qty | Part | Mfr | Description |
|-----|-----------------------|----------------|--------------------------------------|
| 1 | Senior Telemaster | Hobby Lobby | ARF RC airframe kit |
| 1 | 4120/18 | Axi | Main drive motor |
| 5 | HS-322HD | Hitec | RC Servomotors |
| 1 | #511 Steel Rod | Sullivan | Control Set, straight linkage |
| 2 | #580 Precision Rod | Sullivan | Control Set, carbon-fiber reinforced |
| 2 | 3.25 in rubber wheels | Dubro | Main landing gear |
| 1 | LP 13080E | APC Propellers | Composite propeller 13x8E |
| 1 | AR6200 | Spektrum | RC receiver |
| 1 | VEN-15021 | Venom Power | 5000mah 22.2V Li-Po battery |
| 1 | JSP91010 | JR Sports | 4.8V 700mah NiCd battery |
| 1 | DX6i | Spektrum | 6-channel RC transmitter, 2.4 GHz |

Table C.1: Bill of Materials for Test Airframe

C.2 Avionics Package

Once the bare circuit boards have been divided, solder paste can be placed on all of the populated pads. This can be done either manually or by using a solder mask generated from the layout file. The relevant parts may then be placed manually or with standard automated fabrication tools. Care must be taken to observe the polarity of certain capacitors and active components.

The team recommends two solder reflow passes when using manual construction. Several of the larger inductors and capacitors take significant time to heat to the melting point, which may cause damage to the active components, and should be installed first. The remaining surface-mount components may be installed at once. Through-hole components, including the bus and debugging headers, should be installed separately.

Note that on the sensors board, there are several QFN packages that have no visible leads from the top. Extreme care must be taken with these components when soldering to avoid solder bridges. After construction, it is advisable to check for solder bridges both visually with the aid of a microscope, and electrically with a digital multimeter. Electrically reported shorts should be compared with the system schematic to establish whether connectivity is expected.

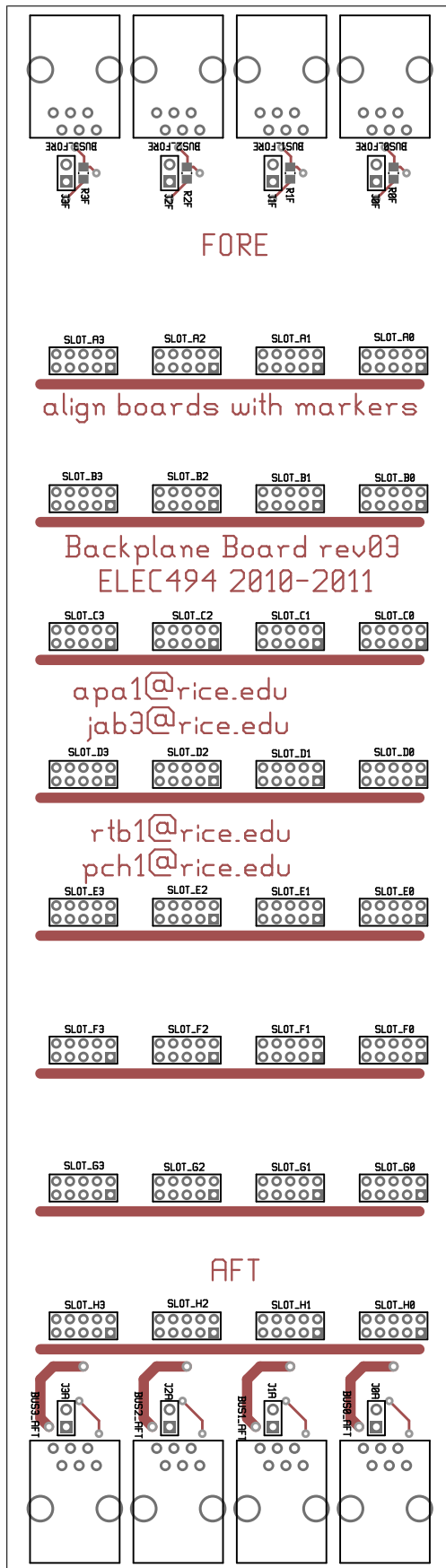


Figure C.1: Front assembly diagram for Backplane Rev 03, reproduced to scale. The silkscreen indicates the component reference designators for the corresponding pads. Part information for each reference designator is in Table C.2.

APPENDIX C. ASSEMBLY INSTRUCTIONS AND BILL OF MATERIALS

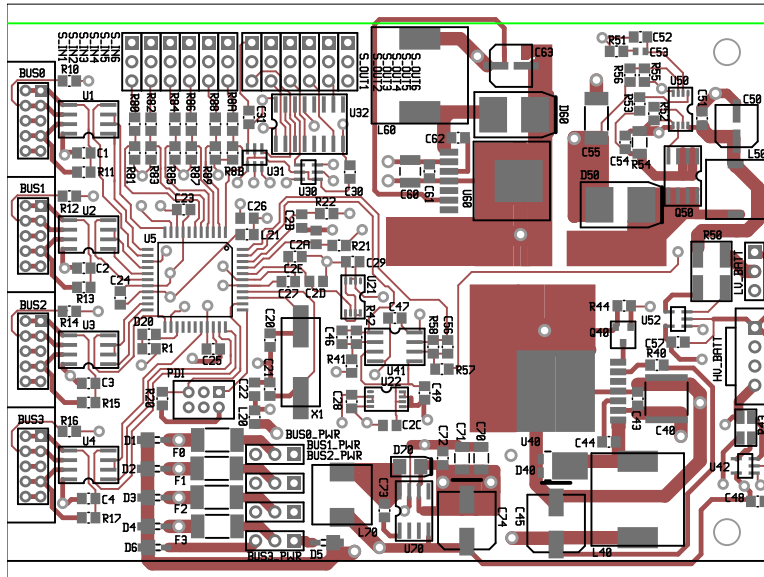


Figure C.2: Front assembly diagram for Servo Board Rev 03, reproduced to scale. The silkscreen indicates the component reference designators for the corresponding pads. Part information for each reference designator is in Table C.3.

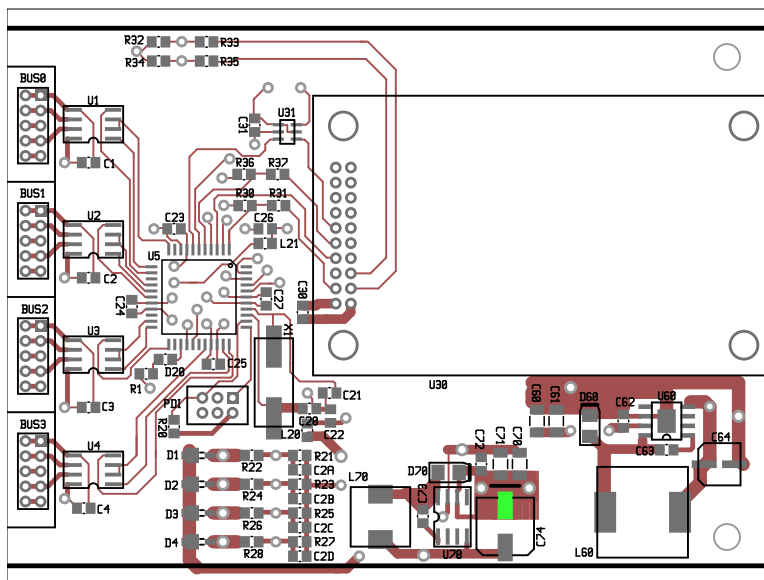


Figure C.3: Front assembly diagram for Radio Board Rev 03, reproduced to scale. The silkscreen indicates the component reference designators for the corresponding pads. Part information for each reference designator is in Table C.4.

APPENDIX C. ASSEMBLY INSTRUCTIONS AND BILL OF MATERIALS

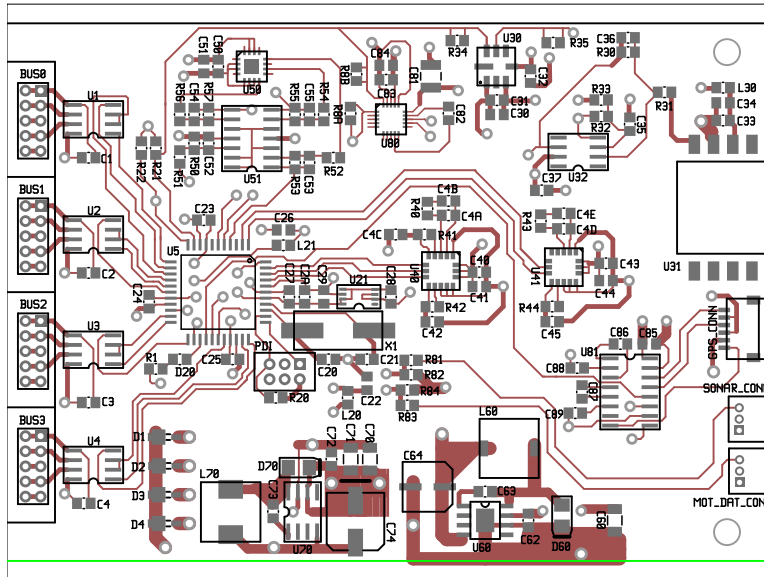


Figure C.4: Front assembly diagram for Sensors Board Rev 03, reproduced to scale. The silkscreen indicates the component reference designators for the corresponding pads. Part information for each reference designator is in Table C.5.

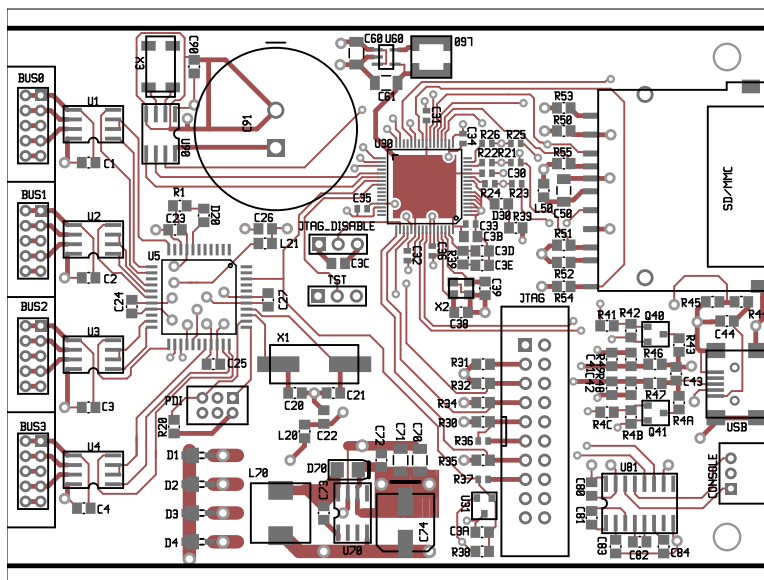


Figure C.5: Front assembly diagram for GPC Board Rev 02, reproduced to scale. The silkscreen indicates the component reference designators for the corresponding pads. Part information for each reference designator is in Table C.6.

C.2.1 Backplane, revision 03

Table C.2: Bill of Materials for Backplane Rev 03

| Qty | Refdes | Mfr | Mfr Part | Description |
|-----|------------------|-------|----------------|---------------------------------------|
| 32 | BUS_{A...G} | 3M | 950410-6102-AR | CONN SOCKET 10POS 2MM VERT T/H |
| | | FCI | 63453-110LF | 10P VERT RECEPT DR .76 MICROMETERS AU |
| 8 | R1,R2 | Rohm | MCR10EZPF1001 | RES 1.00K OHM 1/8W 1% 0805 SMD |
| 8 | J1,J2 | 3M | 961102-6404-AR | CONN HEADER VERT SGL 2POS GOLD |
| 8 | | Tyco | 881545-1 | SHUNT LP HANDLE 2POS |
| 4 | BUS_FORE,BUS_AFT | Molex | 43202-6101 | RA 6/6 PORT 1 low profile |
| 4 | BUS_FORE,BUS_AFT | Tyco | 216548-1 | 1X1 6/6 PCB RJ25 |

C.2.2 Servo Board, revision 03

Table C.3: Bill of Materials for Servo Board Rev 03

| Qty | Refdes | Mfr | Mfr Part | Description |
|-----|--|---------|--------------------|--------------------------------------|
| 4 | BUS{0,1,2,3} | 3M | 951210-7622-AR | 2x5pin 2.0mm right angle male header |
| 8 | R10, R11, R12, R13, R14, R15, R16, R17 | Rohm | MCR10EZPF2701 | RES 2.70K OHM 1/8W 1% 0805 SMD |
| 4 | C1, C2, C3, C4 | Murata | GRM219R71C104KA01D | CAP CER .1UF 16V 10% X7R 0805 |
| 4 | U1, U2, U3, U4 | TI | SN65HVD12D | IC TRANSCEIVER RS485 3.3V 8-SOIC |
| 6 | D1, D2, D3, D4, D5, D6 | STMicro | STPS1L40M | DIODE SCHOTTKY 40V 1A DO-216AA |
| 4 | BUS{0, 1, 2, 3}_PWR | 3M | 961103-6404-AR | CONN HEADER VERT SGL 3POS GOLD |

APPENDIX C. ASSEMBLY INSTRUCTIONS AND BILL OF MATERIALS

Table C.3: Bill of Materials for Servo Board Rev 03

| Qty | Refdes | Mfr | Mfr Part | Description |
|------------|-----------------------------------|---------------------|------------------------|----------------------------------|
| 4 | (none) | Tyco | 881545-2 | SHUNT LP W/HANDLE 2 POS 30AU |
| 4 | F0, F1, F2, F3 | Littelfuse | 1812L125DR | PTC 1.25A 15VDC RESETTABLE 1812L |
| 1 | U5 | Atmel | ATxmega32A4-AU | AVR MCU 32K flash 1.6V 44-TQFP |
| 1 | X1 | Abracon | ABLS2-7.3728MHZ-D4Y-T | CRYSTAL 7.3728 MHZ 18PF SMD |
| 2 | C20, C21 | AVX | 08055A120JAT2A | CAP CERM 12PF 5% 50V NP0 0805 |
| 1 | PDI | Hirose | DF11-6DS-2DSA(05) | CONN RECEPT 6POS 2MM PCB TIN |
| 1 | R20 | Rohm | MCR10EZPF1002 | RES 10.0K OHM 1/8W 1% 0805 SMD |
| 1 | L20 | TDK | MLZ2012E100MT | INDUCTOR MULTILAYER 10UH 0805 |
| 1 | L21 | Laird | LF0805A252R-10 | FERRITE CHIP 1267OHMS 100MA 0805 |
| 6 | C22, C26, C2A, C2B, C2C, C2D | Rohm | TCPOJ106M8R | CAP TANT 10UF 6.3V 20% SMD |
| 7 | C23, C24, C25, C27, C28, C29, C2E | Murata | GRM219R71C104KA01D | CAP CER .1UF 16V 10% X7R 0805 |
| 1 | R1 | Rohm | MCR10EZPF4700 | RES 470 OHM 1/8W 1% 0805 SMD |
| 1 | D20 | Stanley Electric Co | FR1112H-TR | LED RED 0805 SMD |
| 1 | U21 | Linear | LTC6652BHMS8-2.5#PBF | IC REF PREC LN 8-MSOP |
| 1 | U22 | Linear | LTC6652BHMS8-2.048#PBF | IC REF PREC LN 8-MSOP |
| 2 | R21, R22 | Rohm | MCR10EZPF1001 | RES 1.00K OHM 1/8W 1% 0805 SMD |
| 2 | U30, U31 | TI | TXB0101DBVR | IC VOLT-LVL TRANSL 1BIT SOT23-6 |
| 2 | C30, C31 | Murata | GRM219R71C104KA01D | CAP CER .1UF 16V 10% X7R 0805 |
| 1 | U32 | TI | CD4017BM96 | IC 10-OUT DECADE COUNTER 16-SOIC |
| 6 | S_OUT{1,2,3,4,5,6} | 3M | 961103-6404-AR | CONN HEADER VERT SGL 3POS GOLD |

APPENDIX C. ASSEMBLY INSTRUCTIONS AND BILL OF MATERIALS

Table C.3: Bill of Materials for Servo Board Rev 03

| Qty | Refdes | Mfr | Mfr Part | Description |
|------------|---------------|------------------|--------------------|--|
| 1 | HV_BATT | Molex | 70543-0003 | CONN HEADER 4POS .100 VERT GOLD |
| 1 | U40 | National | LM2676S-12/NOPB | IC REG SIMPLE SWITCHER TO-263-7 |
| 1 | C40 | TDK | C5750X7R1H106M | MLCC - SMD/SMT 2220 10uF 50volts X7R 20% |
| 1 | C43 | Kemet | C0805C104K5RACTU | CAP .10UF 50V CERAMIC X7R 0805 |
| 1 | C44 | Yageo | CC0805KRX7R9BB103 | CAP 10000PF 50V CERAMIC X7R 0805 |
| 1 | D40 | Diodes Inc | PDS360-13 | DIODE SCHOTTKY 3A 60V PWRDI5 |
| 1 | L40 | Bourns | SRR1210-560M | Power Inductors 56uH |
| 1 | C45 | Nippon Chemi-Con | APXA160ARA390MF60G | CAP 39UF 16V ELECT POLY SMD |
| 1 | R40 | Susumu | RR1220P-2051-D-M | RES 2.05K OHM 1/10W .5% 0805 SMD |
| 1 | U41 | TI | OPA2336U | IC OPAMP GP R-R 100KHZ 8SOIC |
| 1 | R41 | Panasonic ECG | ERA-6AEB105V | RES 1M OHM 1/8W .1% 0805 SMD |
| 1 | R42 | Panasonic ECG | ERA-6AEB513V | RES 51K OHM 1/8W .1% 0805 SMD |
| 1 | C46 | TDK | C2012X7R1A105K | CAP CER 1.0UF 10V X7R 10% 0805 |
| 1 | U42 | TI | INA195AIDBVR | IC CURRENT MONITOR 3% SOT23-5 |
| 1 | R43 | Ohmite | LVK12R010FER | RES .01 OHM 1/2W 1% 4-TERM 1206 |
| 3 | C47, C48, C49 | Murata | GRM219R71C104KA01D | CAP CER .1UF 16V 10% X7R 0805 |
| 1 | R44 | Rohm | MCR10EZPF1002 | RES 10.0K OHM 1/8W 1% 0805 SMD |
| 1 | Q40 | Diodes/Zetex | BSS138TA | MOSFET N-CH 50V 200MA SOT23-3 |
| 1 | LV_BATT | 3M | 961103-6404-AR | CONN HEADER VERT SGL 3POS GOLD |
| 1 | U52 | TI | INA195AIDBVR | IC CURRENT MONITOR 3% SOT23-5 |
| 1 | R50 | Ohmite | LVK25R002FER | RES .002 OHM 2W 1% 4-TERM 1224 |

APPENDIX C. ASSEMBLY INSTRUCTIONS AND BILL OF MATERIALS

Table C.3: Bill of Materials for Servo Board Rev 03

| Qty | Refdes | Mfr | Mfr Part | Description |
|-----|--------|------------------|---------------------|----------------------------------|
| 1 | C57 | Murata | GRM219R71C104KA01D | CAP CER .1UF 16V 10% X7R 0805 |
| 1 | C50 | Nippon Chemi-Con | APXE160ARA330ME61G | CAP 33UF 16V ELECT POLY SMD |
| 1 | C51 | Murata | GRM219R71C104KA01D | CAP CER .1UF 16V 10% X7R 0805 |
| 1 | U50 | National | LM3478MM/NOPB | IC CTRLR SW REG N-CH 8MSOP |
| 1 | C52 | Yageo | CC0805KRX7R9BB332 | CAP 3300PF 50V CERAMIC X7R 0805 |
| 1 | C53 | Murata | GRM188R71E683KA01D | CAP CER 68000PF 25V 10% X7R 0603 |
| 1 | R51 | Susumu | RR1220P-751-D | RES 750 OHM 1/10W .5% 0805 SMD |
| 1 | R52 | Rohm | MCR10EZHF3012 | RES 30.1K OHM 1/8W 1% 0805 SMD |
| 1 | R53 | Susumu | RR1220P-751-D | RES 750 OHM 1/10W .5% 0805 SMD |
| 1 | C54 | Yageo | CC0805KRX7R9BB103 | CAP 10000PF 50V CERAMIC X7R 0805 |
| 1 | R54 | Stackpole | CSR 1/2 0.015 1% I | RES 0.015 OHM 1/2W 1% 1206 SMD |
| 1 | L50 | Pulse | P1167.272NLT | INDUCTOR PWR SHIELDED 1.8UH SMD |
| 1 | Q50 | Fairchild | FDS6690A_Q | MOSFETs SO-8 SGL N-CH 30V |
| 1 | D50 | Diodes Inc | B530C-13-F | DIODE SCHOTTKY 30V 5A SMC |
| 1 | C55 | TDK | C4532X7R1E226M | MLCC - SMD/SMT 1812 22uF 25volts |
| 1 | R55 | Rohm | MCR10EZPF1001 | RES 1.00K OHM 1/8W 1% 0805 SMD |
| 1 | R56 | Rohm | MCR10EZPF8451 | RES 8.45K OHM 1/8W 1% 0805 SMD |
| 1 | R57 | Panasonic ECG | ERA-6AEB184V | RES 180K OHM 1/8W .1% 0805 SMD |
| 1 | R58 | Panasonic ECG | ERA-6AEB363V | RES 36K OHM 1/8W .1% 0805 SMD |
| 1 | C56 | TDK | C2012X7R1A105K | CAP CER 1.0UF 10V X7R 10% 0805 |
| 1 | U60 | National | LM22676TJE-5.0/NOPB | IC REG SWITCH BUCK 3A 5V TO263-7 |
| 1 | C60 | TDK | C3225X7R1E106M | CAP CER 10UF 25V X7R 20% 1210 |

APPENDIX C. ASSEMBLY INSTRUCTIONS AND BILL OF MATERIALS

Table C.3: Bill of Materials for Servo Board Rev 03

| Qty | Refdes | Mfr | Mfr Part | Description |
|------------|------------------------------|------------------|--------------------|--|
| 1 | C61 | Taiyo Yuden | TMK212BJ105KG-T | CAP CER 1.0UF 25V X5R 0805 |
| 1 | C62 | Kemet | C0805C103K5RACTU | CAP 10000PF 50V CERAMIC X7R 0805 |
| 1 | D60 | Vishay | SL43-E3/57T | DIODE SCHOTTKY 4A 30V SMC |
| 1 | L60 | Bourns | SRR1260-150M | INDUCTOR POWER 15UH 5.0A SMD |
| 1 | C63 | Nippon Chemi-Con | APXC100ARA560ME60G | CAP 56UF 10V ELECT POLY SMD |
| 1 | U70 | National | LM2674M-3.3 | IC REG SW 3.3V 500MA STPDN 8SOIC |
| 2 | C70, C71 | Kemet | C1206C105K3RACTU | CAP 1.0UF 25V CERAMIC X7R 1206 |
| 1 | C72 | AVX | 08053C104KAT2A | CAP CERM .10UF 10% 25V X7R 0805 |
| 1 | C73 | Yageo | CC0805KRX7R9BB103 | CAP 10000PF 50V CERAMIC X7R 0805 |
| 1 | D70 | Diodes Inc | B130LAW-7-F | DIODE SCHOTTKY 1A 30V SOD123 |
| 1 | L70 | Coiltronics | DR74-101-R | INDUCTOR SHIELD PWR 100UH SMD |
| 1 | C74 | Nippon Chemi-Con | APXA160ARA390MF60G | CAP 39UF 16V ELECT POLY SMD |
| 6 | S_IN{1,2,3,4,5,6} | | | JR servo extension cable 12" male-female |
| 6 | R80, R82, R84, R86, R88, R8A | Rohm | MCR10EZPF1002 | RES 10.0K OHM 1/8W 1% 0805 SMD |
| 6 | R81, R83, R85, R87, R89, R8B | Rohm | MCR10EZPF2002 | RES 20.0K OHM 1/8W 1% 0805 SMD |

C.2.3 Radio Board, revision 03

Table C.4: Bill of Materials for Radio Board Rev 03

| Qty | Refdes | Mfr | Mfr Part | Description |
|-----|--|---------------------|-----------------------|--------------------------------------|
| 4 | BUS{0,1,2,3} | 3M | 951210-7622-AR | 2x5pin 2.0mm right angle male header |
| 4 | C1,C2,C3,C4 | Murata | GRM219R71C104KA01D | CAP CER .1UF 16V 10% X7R 0805 |
| 4 | U1,U2,U3,U4 | TI | SN65HVD12D | IC TRANSCEIVER RS485 3.3V 8-SOIC |
| 4 | D1,D2,D3,D4 | STMicro | STPS1L40M | DIODE SCHOTTKY 40V 1A DO-216AA |
| 1 | U5 | Atmel | ATxmega32A4-AU | AVR MCU 32K flash 1.6V 44-TQFP |
| 1 | X1 | Abracon | ABLS2-7.3728MHZ-D4Y-T | CRYSTAL 7.3728 MHZ 18PF SMD |
| 2 | C20,C21 | AVX | 08055A120JAT2A | CAP CER 12PF 5% 50V NP0 0805 |
| 1 | PDI | Hirose | DF11-6DS-2DSA(05) | CONN RECEPT 6POS 2MM PCB TIN |
| 1 | R20 | Rohm | MCR10EZPF1002 | RES 10.0K OHM 1/8W 1% 0805 SMD |
| 1 | L20 | TDK | MLZ2012E100MT | INDUCTOR MULTILAYER 10UH 0805 |
| 1 | L21 | Laird | LF0805A252R-10 | FERRITE CHIP 12670HMS 100MA 0805 |
| 2 | C22,C26 | Rohm | TCPOJ106M8R | CAP TANT 10UF 6.3V 20% SMD |
| 8 | C23, C24, C25, C27, C2A, C2B, C2C, C2D | Murata | GRM219R71C104KA01D | CAP CER .1UF 16V 10% X7R 0805 |
| 1 | R1 | Rohm | MCR10EZPF4700 | RES 470 OHM 1/8W 1% 0805 SMD |
| 1 | D20 | Stanley Electric Co | FR1112H-TR | LED RED 0805 SMD |
| 4 | R21,R23,R25,R27 | Rohm | MCR10EZPF6801 | RES 6.80K OHM 1/8W 1% 0805 SMD |
| 4 | R22,R24,R26,R28 | Rohm | MCR10EZPF1003 | RES 100K OHM 1/8W 1% 0805 SMD |
| 1 | U30 | Digi | XTend900-OEM | XTend 900 1W RPSMA - 40 Mile Range |
| 1 | U31 | TI | TXB0101DBVR | IC VOLT-LVL TRANSL 1BIT SOT23-6 |
| 2 | C30,C31 | Murata | GRM219R71C104KA01D | CAP CER .1UF 16V 10% X7R 0805 |

APPENDIX C. ASSEMBLY INSTRUCTIONS AND BILL OF MATERIALS

Table C.4: Bill of Materials for Radio Board Rev 03

| Qty | Refdes | Mfr | Mfr Part | Description |
|------------|--------------------|------------------|---------------------|----------------------------------|
| 4 | R31, R33, R35, R37 | Rohm | MCR10EZPF1002 | RES 10.0K OHM 1/8W 1% 0805 SMD |
| 4 | R30, R32, R34, R36 | Rohm | MCR10EZPF2002 | RES 20.0K OHM 1/8W 1% 0805 SMD |
| 1 | U60 | National | LM22675MRE-5.0/NOPB | IC REG SWITCH BUCK 1A 5V 8PSOP |
| 2 | C60, C61 | Kemet | C1206C105K3RACTU | CAP 1.0UF 25V CERAMIC X7R 1206 |
| 1 | C62 | Taiyo Yuden | TMK212BJ105KG-T | CAP CER 1.0UF 25V X5R 0805 |
| 1 | C63 | Kemet | C0805C103K5RACTU | CAP 10000PF 50V CERAMIC X7R 0805 |
| 1 | D60 | Diodes Inc | B30LAW-7-F | DIODE SCHOTTKY 1A 30V SOD123 |
| 1 | L60 | Wurth | 744771118 | INDUCTOR POWER 18UH 3.48A SMD |
| 1 | C64 | Nippon Chemi-Con | APXC100ARA560ME60G | CAP 56UF 10V ELECT POLY SMD |
| 1 | U70 | National | LM2674M-3.3 | IC REG SW 3.3V 500MA STPDN 8SOIC |
| 2 | C70, C71 | Kemet | C1206C105K3RACTU | CAP 1.0UF 25V CERAMIC X7R 1206 |
| 1 | C72 | AVX | 08053C104KAT2A | CAP CERM .10UF 10% 25V X7R 0805 |
| 1 | C73 | Yageo | CC0805KRX7R9BB103 | CAP 10000PF 50V CERAMIC X7R 0805 |
| 1 | D70 | Diodes Inc | B130LAW-7-F | DIODE SCHOTTKY 1A 30V SOD123 |
| 1 | L70 | Coiltronics | DR74-101-R | INDUCTOR SHIELD PWR 100UH SMD |
| 1 | C74 | Nippon Chemi-Con | APXA160ARA390MF60G | CAP 39UF 16V ELECT POLY SMD |

C.2.4 Sensors Board, revision 03

Table C.5: Bill of Materials for Sensors Board Rev 03

| Qty | Refdes | Mfr | Mfr Part | Description |
|-----|------------------------------|---------------------|-----------------------|--------------------------------------|
| 4 | BUS0, BUS1, BUS2, BUS3 | 3M | 951210-7622-AR | 2x5pin 2.0mm right angle male header |
| 4 | C1, C2, C3, C4 | Murata | GRM219R71C104KA01D | CAP CER .1UF 16V 10% X7R 0805 |
| 4 | U1, U2, U3, U4 | TI | SN65HVD12D | IC TRANSCEIVER RS485 3.3V 8-SOIC |
| 4 | D1, D2, D3, D4 | STMicro | STPS1L40M | DIODE SCHOTTKY 40V 1A DO-216AA |
| 1 | U5 | Atmel | ATxmega32A4-AU | AVR MCU 32K flash 1.6V 44-TQFP |
| 1 | X1 | Abrakon | ABLS2-7.3728MHZ-D4Y-T | CRYSTAL 7.3728 MHZ 18PF SMD |
| 2 | C20, C21 | AVX | 08055A120JAT2A | CAP CERM 12PF 5% 50V NP0 0805 |
| 1 | PDI | Hirose | DF11-6DS-2DSA(05) | CONN RECEPT 6POS 2MM PCB TIN |
| 3 | R20, R21, R22 | Rohm | MCR10EZPF1002 | RES 10.0K OHM 1/8W 1% 0805 SMD |
| 1 | L20 | TDK | MLZ2012E100MT | INDUCTOR MULTILAYER 10UH 0805 |
| 1 | L21 | Laird | LF0805A252R-10 | FERRITE CHIP 1267OHMS 100MA 0805 |
| 3 | C22, C26, C29 | Rohm | TCPOJ106M8R | CAP TANT 10UF 6.3V 20% SMD |
| 6 | C23, C24, C25, C27, C28, C2A | Murata | GRM219R71C104KA01D | CAP CER .1UF 16V 10% X7R 0805 |
| 1 | R1 | Rohm | MCR10EZPF4700 | RES 470 OHM 1/8W 1% 0805 SMD |
| 1 | D20 | Stanley Electric Co | FR1112H-TR | LED RED 0805 SMD |
| 1 | U21 | Linear | LTC6652BHMS8-2.5#PBF | IC REF PREC LN 8-MSOP |
| 1 | | Freescale | MPXM2102AS | SENS PRESSURE 14.5 PSI MAX MPAK |
| 1 | U30 | Bosch | BMP085 | DIGITAL BAROMETRIC PRESSURE SNSR |

APPENDIX C. ASSEMBLY INSTRUCTIONS AND BILL OF MATERIALS

Table C.5: Bill of Materials for Sensors Board Rev 03

| Qty | Refdes | Mfr | Mfr Part | Description |
|------------|-------------------------|--------------------|--------------------|--|
| 2 | C30, C34 | Rohm | TCP0J106M8R | CAP TANT 10UF 6.3V 20% SMD |
| 5 | C31, C32, C33, C35, C37 | Murata | GRM219R71C104KA01D | CAP CER .1UF 16V 10% X7R 0805 |
| 1 | U31 | Freescale | MPXV7002DP | Board Mount Pressure Sensors SOP DUAL 2KPA |
| 1 | L30 | TDK | MLZ2012E100MT | INDUCTOR MULTILAYER 10UH 0805 |
| 1 | U32 | TI | OPA335AID | 0.05uV/C max, Single-Supply CMOS Operational Amplifier |
| 1 | R33 | Rohm | MCR10EZPF1002 | RES 10.0K OHM 1/8W 1% 0805 SMD |
| 2 | R30, R31 | Rohm | MCR10EZPF2002 | RES 20.0K OHM 1/8W 1% 0805 SMD |
| 1 | R32 | Rohm | MCR10EZPF2702 | RES 27.0K OHM 1/8W 1% 0805 SMD |
| 1 | C36 | Murata | GRM21BR71E154KA01L | CAP CER .15UF 25V 10% X7R 0805 |
| 2 | C41, C44 | Rohm | TCP0J106M8R | CAP TANT 10UF 6.3V 20% SMD |
| 2 | C40, C43 | Murata | GRM219R71C104KA01D | CAP CER .1UF 16V 10% X7R 0805 |
| 1 | U40 | STMicroelectronics | LPR530AL | GYROSCOPE MEMS DUAL AXIS 16-LGA |
| 3 | R41, R42, R44 | Rohm | MCR10EZPF3302 | RES 33.0K OHM 1/8W 1% 0805 SMD |
| 3 | C42, C4C, C45 | AVX | 08055C124KAT2A | CAP CERM .12UF 10% 50V X7R 0805 |
| 2 | R40, R43 | Rohm | MCR10EZPF1002 | RES 10.0K OHM 1/8W 1% 0805 SMD |
| 2 | C4A, C4D | Yageo | CC0805KRX7R9BB103 | CAP 10000PF 50V CERAMIC X7R 0805 |
| 2 | C4B, C4E | Taiyo Yuden | EMK212B7474KD-T | CAP CER .47UF 16V X7R 0805 |
| 1 | U41 | STMicroelectronics | LY530ALH | GYROSCOPE MEMS SGL AXIS 16-LGA |
| 1 | U50 | Analog Devices | ADXL335 | Triple Axis Accelerometer +- 3G |

APPENDIX C. ASSEMBLY INSTRUCTIONS AND BILL OF MATERIALS

Table C.5: Bill of Materials for Sensors Board Rev 03

| Qty | Refdes | Mfr | Mfr Part | Description |
|------------|------------------------------|------------------|--------------------|--|
| 1 | U51 | TI | OPA4330AIDR | 1.8V, 35ÅµA, microPower, Precision, Zero Drift CMOS Op Amp |
| 1 | C51 | Rohm | TCPOJ106M8R | CAP TANT 10UF 6.3V 20% SMD |
| 2 | C50, C52 | Murata | GRM219R71C104KA01D | CAP CER .1UF 16V 10% X7R 0805 |
| 1 | R50 | Rohm | MCR10EZPF1502 | RES 15.0K OHM 1/8W 1% 0805 SMD |
| 1 | R51 | Rohm | MCR10EZPF1002 | RES 10.0K OHM 1/8W 1% 0805 SMD |
| 6 | R52, R53, R54, R55, R56, R57 | Rohm | MCR10EZPF2002 | RES 20.0K OHM 1/8W 1% 0805 SMD |
| 3 | C53, C54, C55 | Murata | GRM21BR71E154KA01L | CAP CER .15UF 25V 10% X7R 0805 |
| 1 | U60 | National | LM22675MR-5.0/NOPB | IC REG SWITCH BUCK 1A 5V 8PSOP |
| 1 | C60 | Kemet | C1206C105K3RACTU | CAP 1.0UF 25V CERAMIC X7R 1206 |
| 1 | C62 | Taiyo Yuden | TMK212BJ105KG-T | CAP CER 1.0UF 25V X5R 0805 |
| 1 | C63 | Yageo | CC0805KRX7R9BB103 | CAP 10000PF 50V CERAMIC X7R 0805 |
| 1 | D60 | Diodes Inc | B30LAW-7-F | DIODE SCHOTTKY 1A 30V SOD123 |
| 1 | L60 | Pulse | P1167.154NLT | INDUCTOR PWR SHIELDED 113UH SMD |
| 1 | C64 | Panasonic ECG | EEE-FK1E330P | CAP ELECT 33UF 25V FK SMD |
| 1 | U70 | National | LM2674M-3.3 | IC REG SW 3.3V 500MA STPDN 8SOIC |
| 2 | C70, C71 | Kemet | C1206C105K3RACTU | CAP 1.0UF 25V CERAMIC X7R 1206 |
| 1 | C72 | AVX | 08053C104KAT2A | CAP CERM .10UF 10% 25V X7R 0805 |
| 1 | C73 | Yageo | CC0805KRX7R9BB103 | CAP 10000PF 50V CERAMIC X7R 0805 |
| 1 | D70 | Diodes Inc | B130LAW-7-F | DIODE SCHOTTKY 1A 30V SOD123 |
| 1 | L70 | Coiltronics | DR74-101-R | INDUCTOR SHIELD PWR 100UH SMD |
| 1 | C74 | Nippon Chemi-Con | APXA160ARA390MF60G | CAP 39UF 16V ELECT POLY SMD |

APPENDIX C. ASSEMBLY INSTRUCTIONS AND BILL OF MATERIALS

Table C.5: Bill of Materials for Sensors Board Rev 03

| Qty | Refdes | Mfr | Mfr Part | Description |
|-----|-------------------------|-------------|-----------------------|--------------------------------------|
| 1 | U80 | Honeywell | HMC5843 | SENSOR MAGNETIC 3 AXIS 20-LCC |
| 1 | C81 | TDK | C3225X7R1E106M | CAP CER 10UF 25V X7R 20% 1210 |
| 1 | C82 | Taiyo Yuden | UMK212B7224KG-T | CAP CER .22UF 50V X7R 0805 |
| 1 | offboard | Garmin | GPS 18x LVC | Sensitive WAAS GPS receiver PPS puck |
| 1 | GPS_CONN | JST | SM06B-SRSS-TB(LF)(SN) | CONN HEADER SH 6POS SIDE 1MM TIN |
| 1 | U81 | TI | MAX3232EIDR | IC RS3232 LINE DVR/RCVR 16-SOIC |
| 5 | C83, C86, C87, C88, C89 | Murata | GRM219R71C104KA01D | CAP CER .1UF 16V 10% X7R 0805 |
| 2 | C84, C85 | Rohm | TCP0J106M8R | CAP TANT 10UF 6.3V 20% SMD |
| 1 | MOT_DAT_CONN | JST | S3B-ZR(LF)(SN) | CONN HEADER ZH SIDE 3POS 1.5MM |
| 1 | SONAR_CONN | JST | S3B-ZR(LF)(SN) | CONN HEADER ZH SIDE 3POS 1.5MM |
| 2 | R81, R83 | Rohm | MCR10EZPF1002 | RES 10.0K OHM 1/8W 1% 0805 SMD |
| 2 | R82, R84 | Rohm | MCR10EZPF2002 | RES 20.0K OHM 1/8W 1% 0805 SMD |

C.2.5 GPC Board, revision 02

Table C.6: Bill of Materials for GPC Board Rev 02

| Qty | Refdes | Mfr | Mfr Part | Description |
|-----|------------------------------|---------------------|-----------------------|--------------------------------------|
| 4 | BUS0, BUS1, BUS2, BUS3 | 3M | 951210-7622-AR | 2x5pin 2.0mm right angle male header |
| 4 | C1,C2,C3,C4 | Murata | GRM219R71C104KA01D | CAP CER .1UF 16V 10% X7R 0805 |
| 4 | U1,U2,U3,U4 | TI | SN65HVD12D | IC TRANSCEIVER RS485 3.3V 8-SOIC |
| 4 | D1,D2,D3,D4 | STMicro | STPS1L40M | DIODE SCHOTTKY 40V 1A DO-216AA |
| 1 | U5 | Atmel | ATxmega32A4-AU | AVR MCU 32K flash 1.6V 44-TQFP |
| 1 | X1 | Abrakon | ABLS2-7.3728MHZ-D4Y-T | CRYSTAL 7.3728 MHZ 18PF SMD |
| 2 | C20,C21 | AVX | 08055A120JAT2A | CAP CERM 12PF 5% 50V NP0 0805 |
| 1 | PDI | Hirose | DF11-6DS-2DSA(05) | CONN RECEPT 6POS 2MM PCB TIN |
| 1 | R20 | Rohm | MCR10EZPF1002 | RES 10.0K OHM 1/8W 1% 0805 SMD |
| 1 | L20 | TDK | MLZ2012E100MT | INDUCTOR MULTILAYER 10UH 0805 |
| 1 | L21 | Laird | LF0805A252R-10 | FERRITE CHIP 1267OHMS 100MA 0805 |
| 2 | C22,C26 | Rohm | TCPOJ106M8R | CAP TANT 10UF 6.3V 20% SMD |
| 4 | C23,C24,C25,C27 | Murata | GRM219R71C104KA01D | CAP CER .1UF 16V 10% X7R 0805 |
| 1 | R1 | Rohm | MCR10EZPF4700 | RES 470 OHM 1/8W 1% 0805 SMD |
| 1 | D20 | Stanley Electric Co | FR1112H-TR | LED RED 0805 SMD |
| 6 | R21, R22, R23, R24, R25, R26 | Stackpole | RMCF 1/16 0 R | RES 0.0 OHM 1/10W 0603 SMD |
| 1 | U30 | Atmel | AT91SAM7S256-AU-001 | IC ARM7 MCU 32BIT 256K 64LQFP |
| 2 | C3B,C3C | Rohm | TCPOJ106M8R | CAP TANT 10UF 6.3V 20% SMD |

APPENDIX C. ASSEMBLY INSTRUCTIONS AND BILL OF MATERIALS

Table C.6: Bill of Materials for GPC Board Rev 02

| Qty | Refdes | Mfr | Mfr Part | Description |
|------------|-----------------------------------|---------------------|--------------------------|----------------------------------|
| 7 | C30, C31, C32, C33, C34, C35, C36 | AVX Corporation | 0603YC104KAT2A | CAP CERM .1UF 10% 16V X7R 0603 |
| 1 | X2 | Abracon | ABM8G-18.432MHZ-18-D2Y-T | CRYSTAL 18.432 MHZ 18 PF SMD |
| 2 | C38,C39 | FIXME | | |
| 1 | R39 | Rohm | MCR10EZPF1501 | RES 1.50K OHM 1/8W 1% 0805 SMD |
| 1 | C3D | Panasonic - ECG | PCC102BNCT-ND | CAP 1000PF 50V CERM CHIP 0805 |
| 1 | C3E | Murata | GRM216R71H103KA01D | CAP CER 10000PF 50V 10% X7R 0805 |
| 1 | R33 | Rohm | MCR10EZPF4700 | RES 470 OHM 1/8W 1% 0805 SMD |
| 1 | D30 | Stanley Electric Co | PY1112H-TR | LED YELLOW-GREEN 0805 SMD |
| 1 | U31 | Microchip | MCP130T-300I/TT | IC SUPERVISOR 3.00V LOW SOT23 |
| 1 | R38 | Rohm | MCR10EZPF1002 | RES 10.0K OHM 1/8W 1% 0805 SMD |
| 1 | C3A | FIXME | | |
| 5 | R30, R31, R32, R34, R35 | Rohm | MCR10EZPF4702 | RES 47.0K OHM 1/8W 1% 0805 SMD |
| 2 | R36,R37 | Stackpole | RMCF 1/16 0 R | RES 0.0 OHM 1/10W 0603 SMD |
| 1 | JTAG | Sullins | SBH11-PBPC-D10-ST-BK | CONN HEADER 2.54MM 20POS GOLD |
| 2 | JTAG_DISABLE,TST | 3M | 961103-6404-AR | CONN HEADER VERT SGL 3POS GOLD |
| 2 | (none) | Tyco | 881545-2 | SHUNT LP W/HANDLE 2 POS 30AU |
| 1 | USB | Mill-Max | 897-43-005-00-100001 | CONN RECEIPT MINI-USB TYPE B SMT |
| 2 | R41,R4C | Rohm | MCR10EZPF1000 | RES 100 OHM 1/8W 1% 0805 SMD |
| 3 | R42,R4B,R45 | Rohm | MCR10EZPF4702 | RES 47.0K OHM 1/8W 1% 0805 SMD |
| 1 | R44 | Rohm | MCR10EZPF2702 | RES 27.0K OHM 1/8W 1% 0805 SMD |

APPENDIX C. ASSEMBLY INSTRUCTIONS AND BILL OF MATERIALS

Table C.6: Bill of Materials for GPC Board Rev 02

| Qty | Refdes | Mfr | Mfr Part | Description |
|------------|------------------------------|--------------|--------------------|----------------------------------|
| 2 | R46,R47 | Rohm | MCR10EZPF27R0 | RES 27.0 OHM 1/8W 1% 0805 SMD |
| 2 | R48,R49 | Rohm | MCR10EZPF3303 | RES 330K OHM 1/8W 1% 0805 SMD |
| 2 | R43,R4A | Rohm | MCR10EZPF1501 | RES 1.50K OHM 1/8W 1% 0805 SMD |
| 2 | Q40,Q41 | Diodes, Inc. | BSS84-7-F | MOSFET P-CH 50V 130MA SOT23-3 |
| 2 | C41,C42 | AVX | 08055A150JAT2A | CAP CERM 15PF 5% 50V NP0 0805 |
| 1 | C43 | AVX | 08051A330JAT2A | CAP CERM 33PF 5% 100V NP0 0805 |
| 1 | C44 | Murata | GRM219R71C104KA01D | CAP CER .1UF 16V 10% X7R 0805 |
| 1 | SD/MMC | AVX | 145638009211859+ | CONN MEMORY CARD NORMAL TOP PCB |
| 1 | L50 | TDK | MLF2012DR47K | INDUCTOR MULTILAYER 0.47UH 2012 |
| 1 | C50 | Rohm | TCA0J476M8R | CAP TANT 47UF 6.3V 20% SMD6.3V |
| 6 | R50, R51, R52, R53, R54, R55 | Rohm | MCR10EZPF4702 | RES 47.0K OHM 1/8W 1% 0805 SMD |
| 1 | U60 | National | LM3670MF-1.8 | IC CONV DC/DC STEP-DOWN SOT23-5 |
| 1 | L60 | Bourns | SRR4028-470Y | INDUCTOR POWER 47UH 0.75A 4028 |
| 1 | C60 | TDK | C3216X7R1C475K | CAP CER 4.7UF 16V X7R 10% 1206 |
| 1 | C61 | TDK | C3216X5R1A106M | CAP CER 10UF 10V X5R 20% 1206 |
| 1 | U70 | National | LM2674M-3.3 | IC REG SW 3.3V 500MA STPDN 8SOIC |
| 2 | C70,C71 | Kemet | C1206C105K3RACTU | CAP 1.0UF 25V CERAMIC X7R 1206 |
| 1 | C72 | AVX | 08053C104KAT2A | CAP CERM .10UF 10% 25V X7R 0805 |
| 1 | C73 | Yageo | CC0805KRX7R9BB103 | CAP 10000PF 50V CERAMIC X7R 0805 |
| 1 | D70 | Diodes Inc | B130LAW-7-F | DIODE SCHOTTKY 1A 30V SOD123 |
| 1 | L70 | Coiltronics | DR74-101-R | INDUCTOR SHIELD PWR 100UH SMD |

APPENDIX C. ASSEMBLY INSTRUCTIONS AND BILL OF MATERIALS

Table C.6: Bill of Materials for GPC Board Rev 02

| Qty | Refdes | Mfr | Mfr Part | Description |
|------------|-----------------|------------------|-----------------------|----------------------------------|
| 1 | C74 | Nippon Chemi-Con | APXA160ARA390MF60G | CAP 39UF 16V ELECT POLY SMD |
| 1 | CONSOLE | Hirose | DF3-3P-2DS(01) | CONN HEADER 3POS 2MM R/A GOLD |
| 1 | U81 | TI | MAX3232EIDR | IC RS3232 LINE DVR/RCVR 16-SOIC |
| 1 | C80 | Rohm | TCP0J106M8R | CAP TANT 10UF 6.3V 20% SMD |
| 4 | C81,C82,C83,C84 | Murata | GRM219R71C104KA01D | CAP CER .1UF 16V 10% X7R 0805 |
| 1 | U90 | Maxim | DS1302ZN+ | IC TIMEKEEPER T-CHARGE IND 8SOIC |
| 1 | C90 | Murata | GRM219R71C104KA01D | CAP CER .1UF 16V 10% X7R 0805 |
| 1 | X3 | Abracon | ABS25-32.768KHZ-6-1-T | CRYSTAL 32.768 KHZ 6.0 PF SMD |
| 1 | C91 | Elna America | DB-5R5D105T | CAP DOUBLE LAYER 1.0F 5.5V RAD |

C.3 Additional Tools

C.3.1 Airframe Construction

Although the *Senior Telemaster* kit comes largely pre-built, some essential tools are still needed for final assembly and for modifications needed to mount the avionics. All of these tools can be obtained from any reputable hobby store selling R/C aircraft.

Attachment of balsa and plywood components requires gap-filling cyanoacrylate glue in most cases. Attaching the tail assembly should be done with 5-minute epoxy. A set of X-acto knives is needed for removing damaged covering material and cutting balsa. A hacksaw is sufficient for cutting thick balsa and plywood, in combination with coarse-grained sandpaper to remove unevenness. Most of the additional wood needed for modifying the airframe consists of pieces fashioned from simple half-inch square balsa sticks.

As minor damage to the airframe is inevitable, the material covering it will need to be patched. This requires a supply of Mylar covering, ideally Super Monokote from TopFlite. A monokote sealing iron will also be needed. Scissors are necessary for cutting pieces of Monokote

Installing new pushrods will require strong wire cutters. Small and medium screwdrivers of both Phillips and flathead variety, as well as a complete hex wrench set, are used for a variety of tasks.

A specialized prop-boring tool is necessary for modifying propellers to fit on the drive shaft of the electric motor correctly.

C.3.2 Software Development

| Qty | Part # | Mfr | Description |
|------------|---------------|------------|---|
| 3 | ATAVRISP2 | Atmel | AVR INSystem mkII Programming Kit |
| 2 | PGM-07834 | Sparkfun | JTAG USB OCD Programmer/Debugger for ARM processors |
| 1 | DEV-00774 | Sparkfun | Atmel ARM SAM7-256 Development Board |
| 3 | [custom] | [custom] | Shore Power Supply made from standard 12V 800mA wall supply |
| 3 | BOB-09822 | Sparkfun | USB to RS-485 Converter |

Table C.7: List of development tools

C.3.3 Testing Supplies

| Qty | Part # | Mfr | Description |
|------------|---------------|------------|--|
| 1 | 213046 | SkyRC | iCharger iC6 LiPo / NiCd Battery Charger |
| 1 | 102989 | Saitek | Cyborg EVO PC USB Joystick |
| 1 | 58318 | Hitec | Hitec R/C Transmitter to USB interface |
| 3 | [std] | [various] | 6-plug power strip |
| 2 | 177 | Fluke | Digital Multimeter |
| 2 | [std] | [various] | Extra-Sharp multimeter Probes |

Table C.8: List of development tools

D Budget

D.1 Revenue

The team was allocated \$ 2,500 from the Rice Electrical and Computer Engineering department and \$ 2,025 from the Texas Space Grant Consortium for project development work during the 2010-2011 school year. Development work over the summer was funded by the team members directly.

D.2 Expenses

The expenses for the semester are detailed in Table D.1.

| Date | Description | Cost in USD |
|-------------|---|--------------------|
| October 30 | AVR Microcontroller Programmers | 68.00 |
| November 6 | RPSMA to SMA Connectors for Telemetry Radio Antenna | 17.79 |
| January 7 | AMA Memberships | 145.00 |
| January 10 | Spare Parts for Second Prototype Airframe | 345.95 |
| January 12 | Anemometer | 107.10 |
| January 20 | Panel 02 PCBs from Advanced Circuits | 643.90 |
| January 26 | Backplane Headers | 34.25 |
| January 28 | Components for Panel 02 | 455.83 |
| January 28 | Antennas for Telemetry Radio | 20.31 |
| January 29 | Servo Y-Connectors and Transmitter USB Interface | 90.85 |
| February 15 | Pitot-Static Tubes | 59.85 |
| March 26 | Connectors for Pitot-Static Lines | 26.79 |
| March 26 | 720p Video Camera for Second Prototype | 186.27 |
| | Total | 2201.89 |

Table D.1: Expenses for the 2010-2011 School Year